NASA
Contractor Report 180899
MTI 87TR56

AVSCOM
Technical Report 88-C-007

High Speed Balancing Applied to the T700 Engine

J. Walton, C. Lee, and M. Martin
Mechanical Technology Incorporated
Latham, New York

March 1989

Prepared for
Lewis Research Center
Under Contracts NAS3-23929 and NAS3-24633

National Aeronautics and
Space Administration

US ARMY
AVIATION
SYSTEMS COMMAND
AVIATION R&T ACTIVITY

TABLE OF CONTENTS

1.0 SUMMARY

This report presents results of T700 power turbine high-speed flexible rotor balancing evaluations and engine test cell diagnostic guidelines for the T53, T55, and T700 engines. The high-speed balancing evaluation was accomplished in two phases. The first phase used assembled T700 power turbine modules, while the final phase used a power turbine rotor assembly that permitted access to all four available balancing planes yet still incorporated engine bearing and damper assemblies. The initial tests demonstrated the feasibility of high-speed flexibile rotor balancing, while the second phase of testing evaluated the approach most likely to be used in an overhaul environment. To make the second phase as meaningful as possible, mounting hardware that simulated engine support structures and that would fit in an existing high-speed balancing facility at Corpus Christi Army Depot (CCAD) was designed and fabricated for the balancing study. In both test series, it was shown that high-speed, multiplane flexible rotor balancing of T700 power turbine rotors is feasible.

An analytical evaluation of the T700 compressor rotor was also completed. This analytical evaluation showed that multiplane, multispeed dynamic balancing techniques can be effective in reducing imbalance-induced vibrations in the compressor rotor. It was further shown that it may be possible to eliminate the low-speed component balancing and replace it with a single, multispeed, multiplane balancing process. The elimination of the low-speed component balancing was considered when it was seen that vibration levels at 30,000 rpm could be aggravated by the low-speed balancing process. Further confirmation of the T700 compressor rotor response, through experimental evaluation, is required before a multispeed, multiplane balancing process should be considered for implementation at the Army overhaul center.

Finally, a series of diagnostic guidelines has been established for the T700, T55, and T53 based on engine test cell data acquired at CCAD during acceptance testing of overhauled engines. These guidelines identify the major vibration components present in the engines and their relative magnitudes at several test points. They also present a strategy for identifying the most likely cause of an engine rejected for high vibrations.

2.0 INTRODUCTION

T700 turbine engines have recently been added to the inventory of engines, which includes the T53 and T55 turboshaft engines, that is overhauled at the CCAD facility. In preparation for this increased workload, the U.S. Army has embarked upon a program to investigate the feasibility of high-speed flexible rotor balancing of the T700 engine rotors and to establish procedures for diagnosing causes of engine test cell vibration rejects for T53, T55, and T700 power turbines.

This report covers the work performed by MTI under contracts NAS3-23929 and NAS3-24633. Under contract NAS3-23929, MTI evaluated both T700 power turbine and compressor rotor high-speed balancing feasibility and designed hardware to modify the existing CCAD T53/T55 high-speed balancing system (HSBS) for balancing of the T700 power turbine rotors. Prior to the feasibility tests, the Army/NASA drivetrain facility, located at MTI, was reactivated and modified under Tasks 1, 2, and 5 to permit the installation, operation, and evaluation of high-speed multiplane balancing of T700 power turbine modules at speeds to 20,000 rpm.

Under Task 3, high-speed balancing procedures for the T700 power turbine were developed. Development of these procedures involved testing of various combinations of balance planes and speeds in an effort to determine the most efficient balancing approach. Using the developed approach, five T700 rotors were high-speed balanced.

The design modifications necessary for high-speed balancing of the T700 power turbine rotors at CCAD using the current HSBS were completed under Task 4. The final task of contract NAS3-23929, Task 6, was a rotordynamic analytical study of the T700 gas generator rotor. This effort was included to evaluate the response of the T700 gas generator rotor to various levels of imbalance and thereby assess the potential effectiveness of high-speed multiplane balancing in controlling gas generator rotor imbalance-induced vibrations.

Contract NAS3-24633 was a follow-on, four-task effort that continued the activities that were begun under NAS3-23929. The first task of this follow-on effort was the fabrication and verification of the HSBS modification hardware using the Army/NASA drivetrain facility at MTI. Following checkout of the hardware, the Task 2 effort called for four T700 power turbine rotors to be installed into the modified facility for high-speed multiplane balancing evaluations. Of the four rotors, two followed normal assembly and low-speed balancing procedures, while two of the rotor assemblies were not low-speed balanced.

The second half of contract NAS3-24633 called for engine vibration data from six overhauled T700s (installed in a CCAD engine test cell) to be acquired for assessment of the vibration spectra. These data acquired under Task 3 were then used in Task 4 to develop vibration diagnostic procedures for T700 power turbines undergoing post overhaul acceptance testing at CCAD. In addition to the T700, vibration diagnostic procedures were established for the T53 and T55 engines based on vibration data previously acquired at CCAD.

3.0 T700 POWER TURBINE BALANCING EVALUATIONS

The objectives of this effort were to assess and verify high-speed multiplane balancing potential for the General Electric T700 turboshaft helicopter engine through a series of experimental evaluations. In the first series of balancing evaluations, five T700 power turbine modules were installed and balanced in the high-speed balancing facility at MTI. In the second series of balancing evaluations, a total of three power turbine rotors (with the hot section casing removed) were installed in a high-speed balancing chamber and were balanced for smooth operation at 20,000 rpm.

3.1 Description of T700 Turboshaft Engine

The General Electric T700 is an advanced, high-performance turboshaft engine developed by the U.S. Army for utility tactical transport aircraft system (UTTAS) and advanced attack helicopter (AAH) applications. Specifically selected to power helicopters, the T700 represents a modern, efficient, and relatively simple gas turbine in the 1500 shaft horsepower class. The T700 gas generator has five axial stages and one centrifugal compressor stage that are driven by two air-cooled turbine stages to a speed of 44,740 rpm. The low-speed power turbine module has two uncooled turbine stages operated at a constant 20,000 rpm.

To achieve its high power level and low specific fuel consumption at a light weight, the T700 engine design resulted in power turbine and gas generator rotors that both operate above bending critical speeds. As such, the application of high-speed multiplane balancing in the overhaul process may provide benefits through reduced vibrations.

3.2 Test Facility

All testing of both the T700 power turbine modules and rotors was completed in the Army/NASA drivetrain facility at MTI. This facility, shown in Figure 1, was developed under joint sponsorship of the U.S. Army, NASA Lewis Research Center, and MTI. The facility is used to study the dynamic behavior of advanced drivetrain systems and components of various types and sizes. It can accommodate entire structures for dynamic testing, including the tail booms of U.S. Army utility helicopters and drive components of surface effect ships. Components that can be studied include advanced shaft designs, including composite shafting, gas turbine engine rotors, novel speed reduction transmissions, dampers, high-misalignment couplings, etc. A 300-hp electric motor is used to drive rotors at speeds to 20,000 rpm. Through the use of a four-square gearbox arrangement, axial torques to 8000 in.-lb may be applied to test rotors. Finally, MTI's computerized laboratory data acquisition and balancing systems are used to balance from 1 to 20 planes simultaneously at up to five speeds.

A sketch of the setup used for the T700 power turbine module high-speed balancing evaluations is presented in Figure 2. As can be seen, the engine module is placed in a vacuum chamber and is driven by the drivetrain facility high speed gear box. The vacuum chamber was necessary to reduce windage losses and permit operation to 20,000 rpm without overloading the drivetrain motor and to provide safety shielding. Figure 3 shows the facility used for balancing the T700 power turbine rotors. Since the engine casing is removed, the

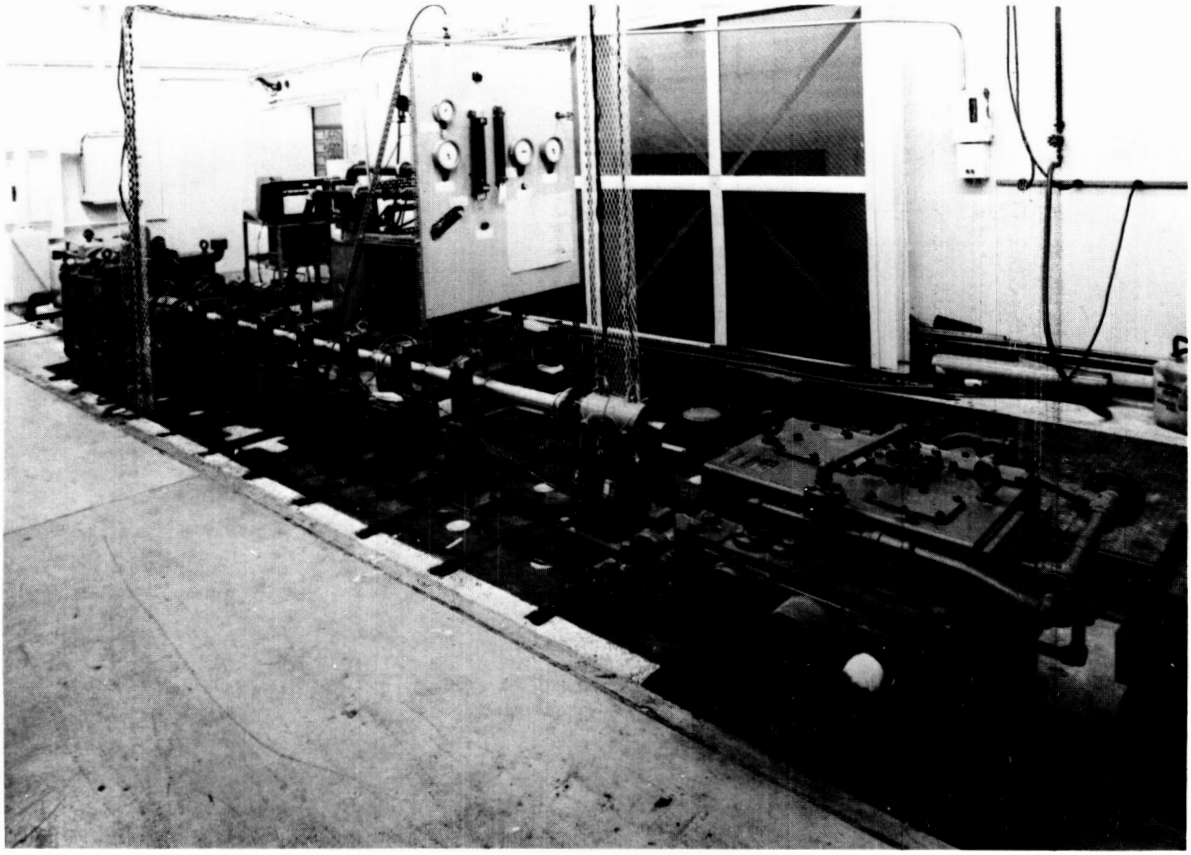

Figure 1 High-Speed Rotordynamics Test Facility

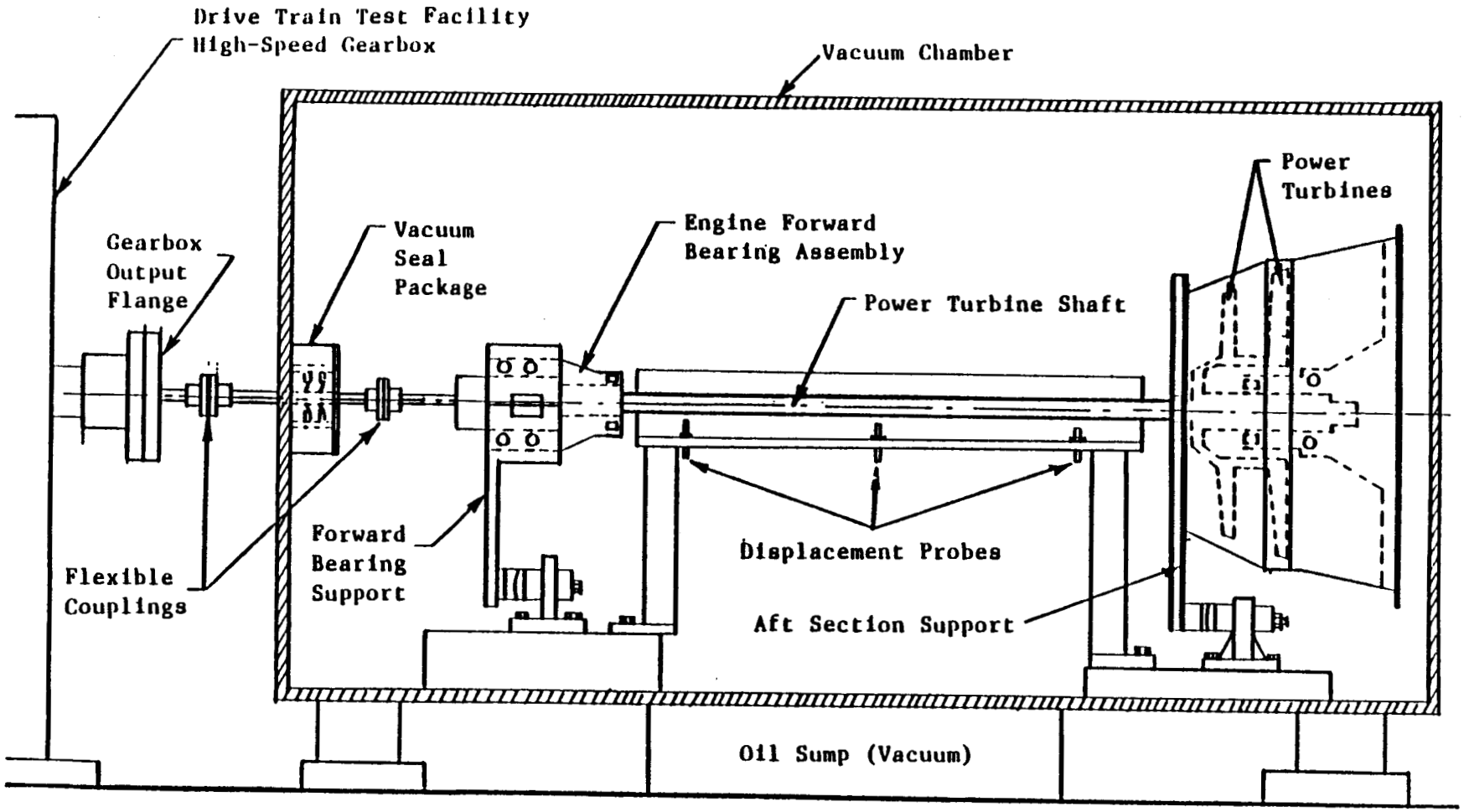

Figure 2 T700 Power Turbine Test Rig

rotor and its support structure differ from that used to evaluate the balancing results for the engine modules (see Figure 2). The structures were designed to closely resemble the engine support characteristics, fit into the existing CCAD HSBS, and interface to the T700 power turbine rotor subassembly.

Instrumentation used for both test series is seen in Figure 3. The primary instrumentation used for all testing included a tachometer for speed measurement, six proximity probes to measure shaft displacement orbits, and thermocouples to monitor the lubricant temperature. An accelerometer was used in several tests to monitor the vibrations on the forward bearing assembly. Signals from the instrumentation were fed into the laboratory computerized data acquisition system and recorded on tape for both on-line balancing analysis and monitoring, as well as post-test review.

3.3 Power Turbine Module Balancing

A total of six power turbine modules were balanced using a weighted least-squares-influence coefficient balancing approach. A three-speed, three-plane set of influence coefficients was calculated based on test runs of rotor serial number GE-L-007566. Trial weights were installed sequentially in balance planes 2, 3, and 6, as shown in Figure 4. Vibration data were then acquired at 8950, 14,250, and 20,000 rpm. The three balancing speeds were selected based on the rotor response shown in Figures 5a, 6a, and 7a. As can be seen from these figures, the vibrations recorded at 8,950 and 14,250 rpm became quite large. While the vibrations at these speeds are not at a maximum, the selected speeds were chosen to permit the easy acquisition of response data from the trial weight runs without encountering vibrations so large that the balancing speed could not be achieved.

Following development of the influence coefficients, six power turbine modules were balanced and evaluated for operation at 20,000 rpm. Table 1 presents the balancing results showing the as-received, or baseline condition, and the rotor vibrations after balancing. Additional data presented in Table 1 include the percent change in vibration amplitude and the orbit ratio before and after balancing at 20,000 rpm. In some instances, vibration amplitudes were increased at individual probes. This trade-off (increasing vibrations at one probe while reducing at another) was often necessary to provide for overall reductions along the length of the rotor or to improve the orbit circularity near the rotor bearings. The orbit ratio is the ratio of the vertical and horizontal probes and is presented for purposes of evaluating the balancing results. Ratios closer to 1.0 indicate more circular orbits and, thus, a reduction in the alternating load experienced by the rotor bearings. In some instances, orbit circularity was degraded. However, this degradation was often coupled with reduction in overall vibrations at the probe pairs or with very small orbits. Consequently, the overall bearing loads in both cases were reduced, indicating a successful balancing evaluation.

After the weighted least-squares balancing evaluations, power turbine serial number P7278 was installed in the T700 balancing facility. The as-installed vibration readings are summarized in Table 2. The runout corrected data were calculated by vectorially adding the measured data to the corresponding sensor data measured at approximately 400 rpm (rotor runout). Using the influence coefficients previously calculated, an alternative balancing plan, called

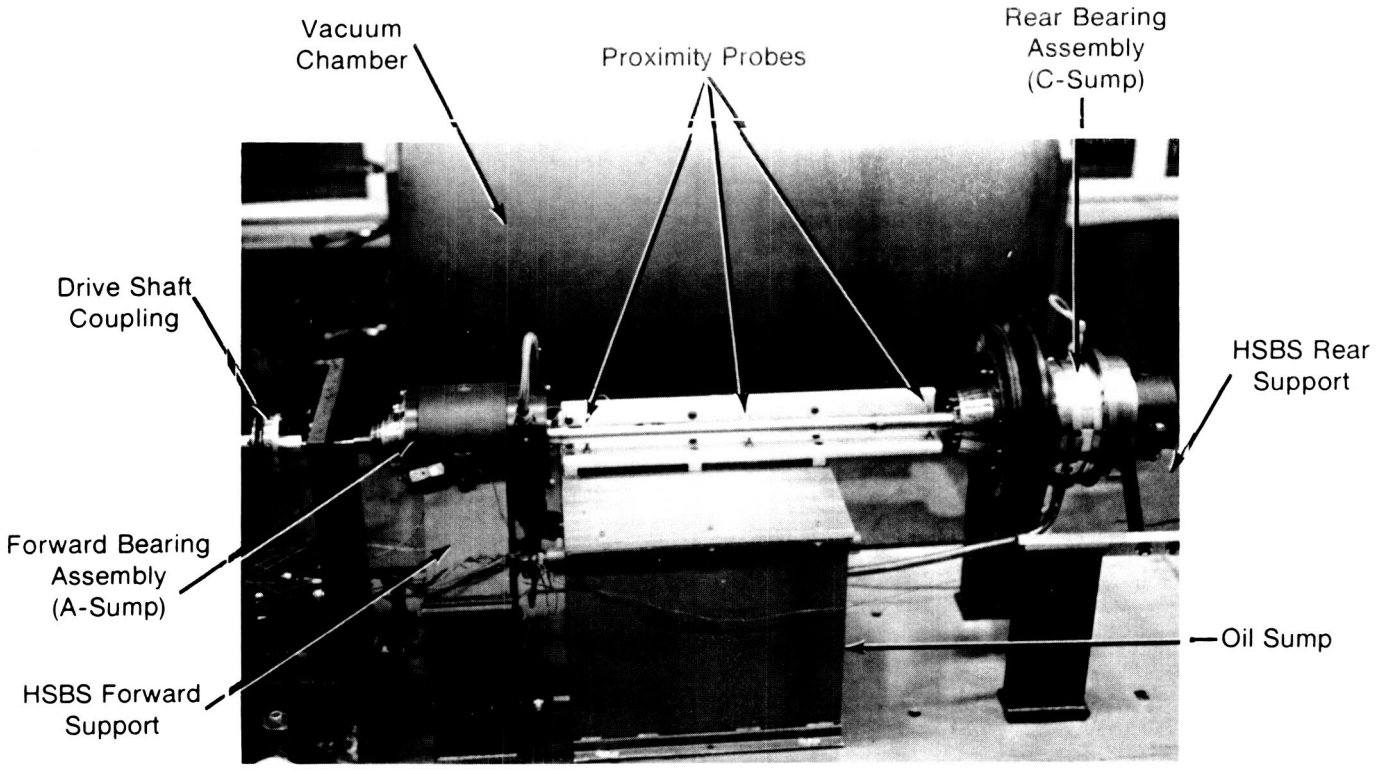

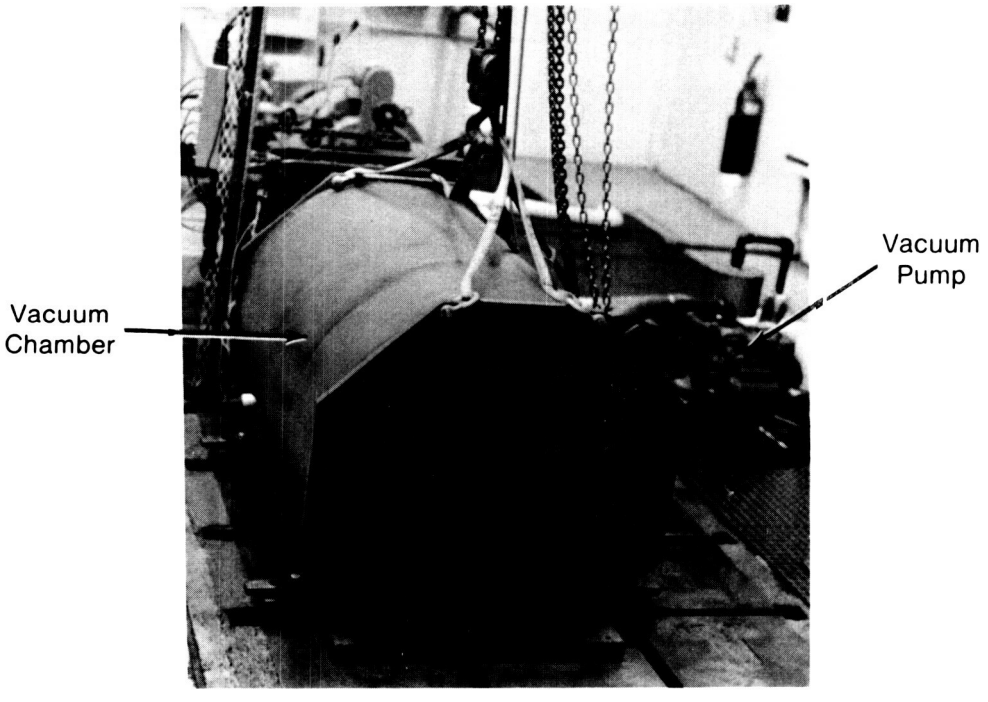

Figure 3 T700 Power Turbine Rotor Balancing Facility

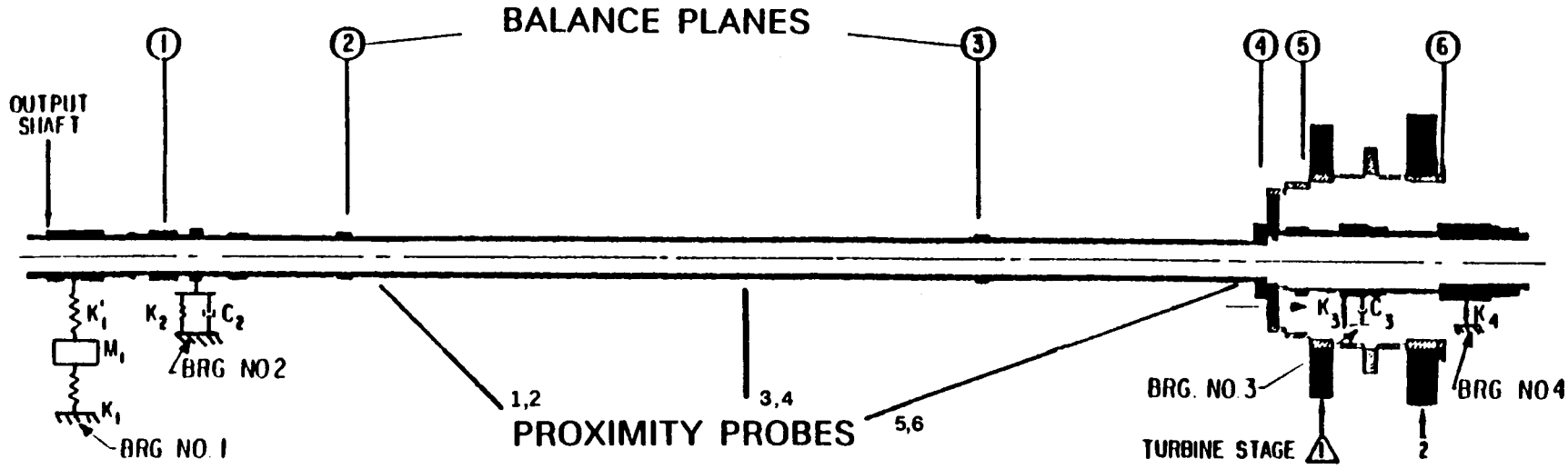

Figure 4 T700 Power Turbine Instrumentation Setup and Balance Plane Definition

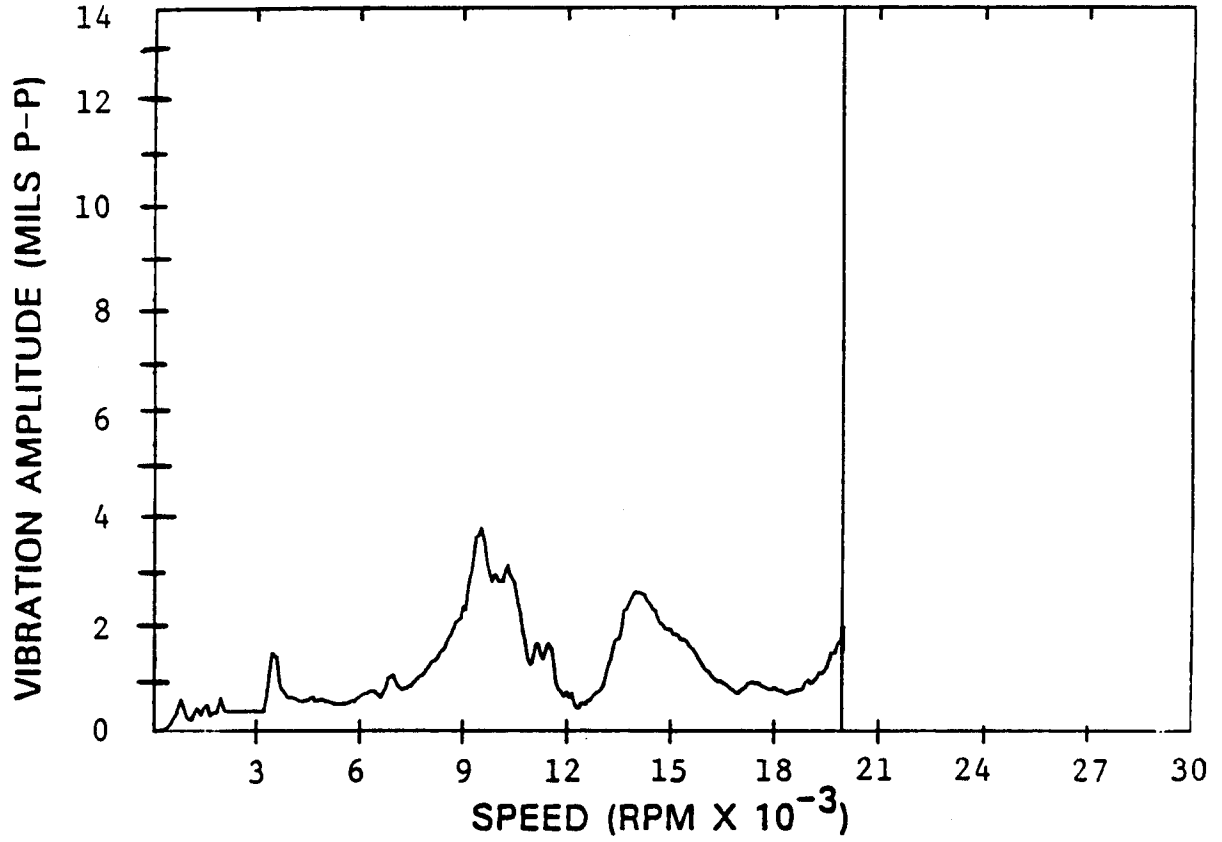

a) As-Received Condition

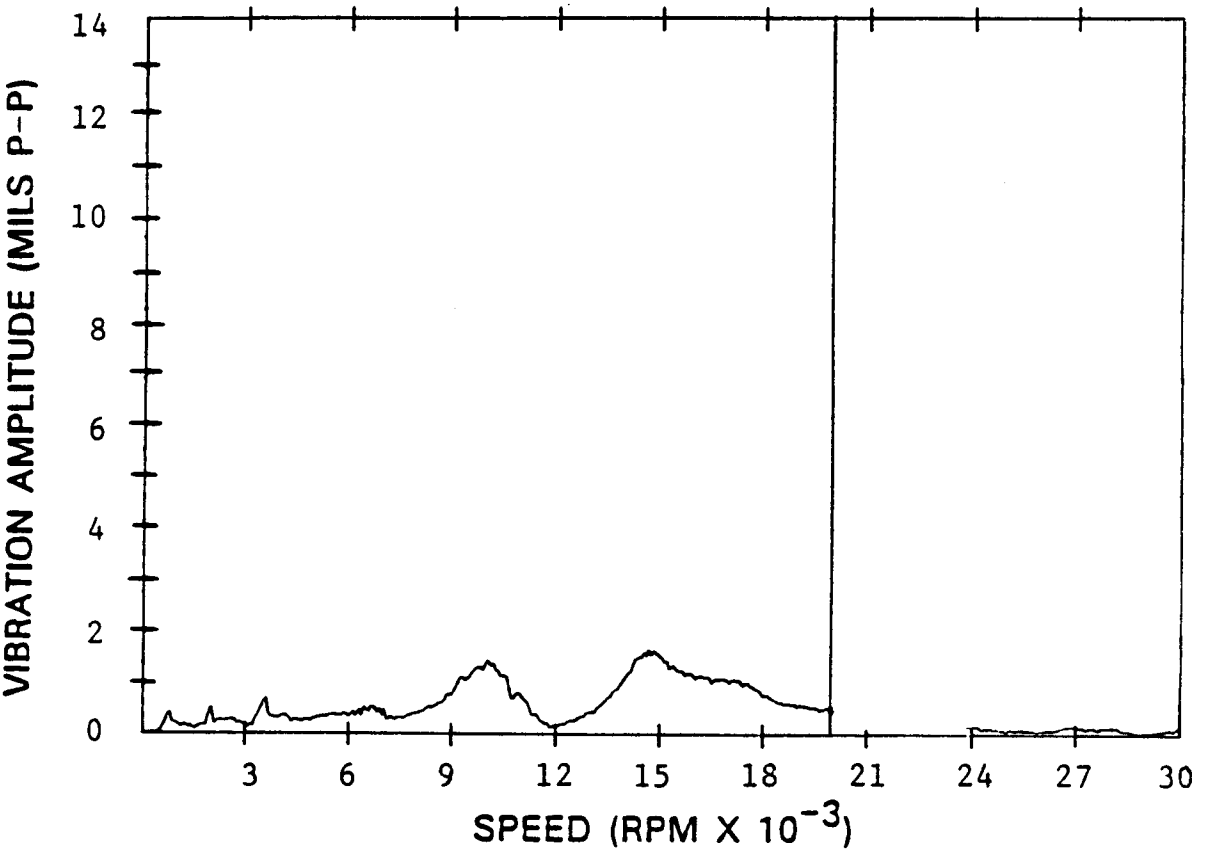

b) After High-Speed Balancing

Figure 5 Power Turbine (GE-L-007566) Vibration Levels, Forward Displacement Probe

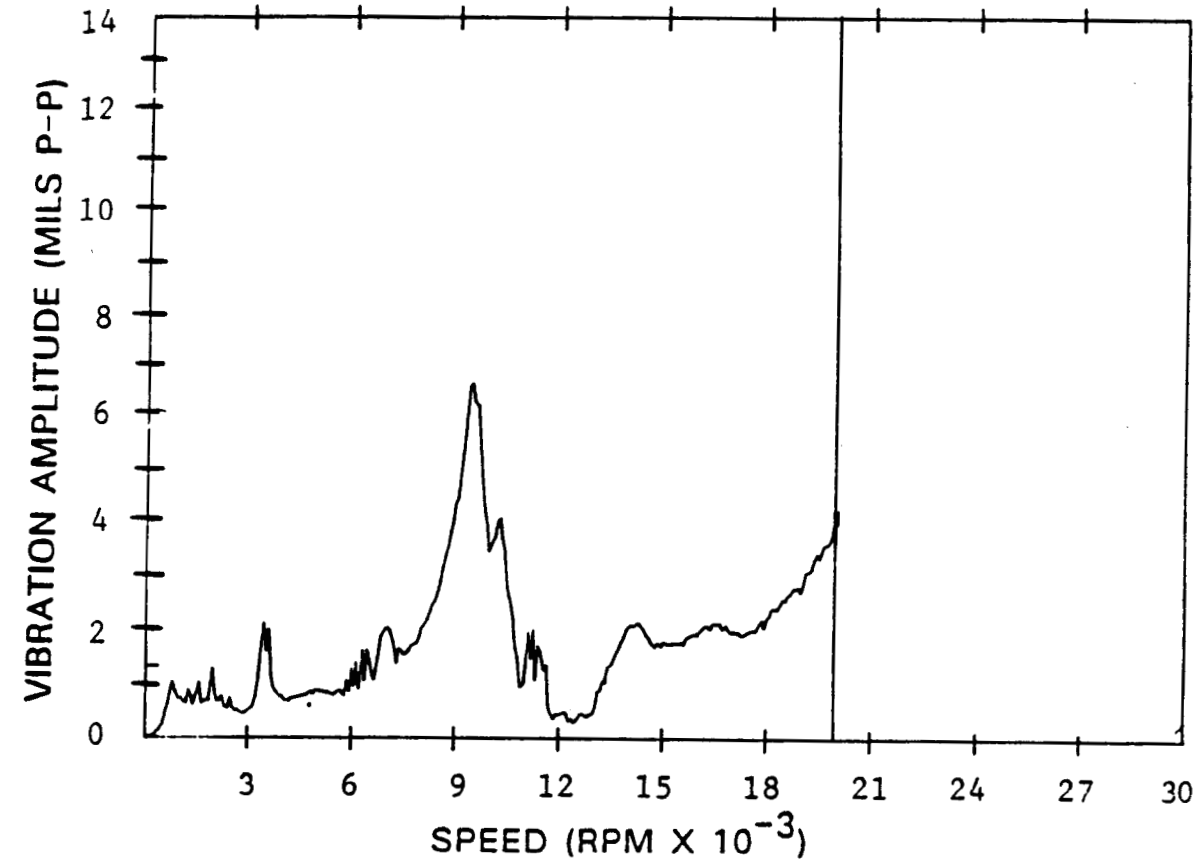

a) As-Received Condition

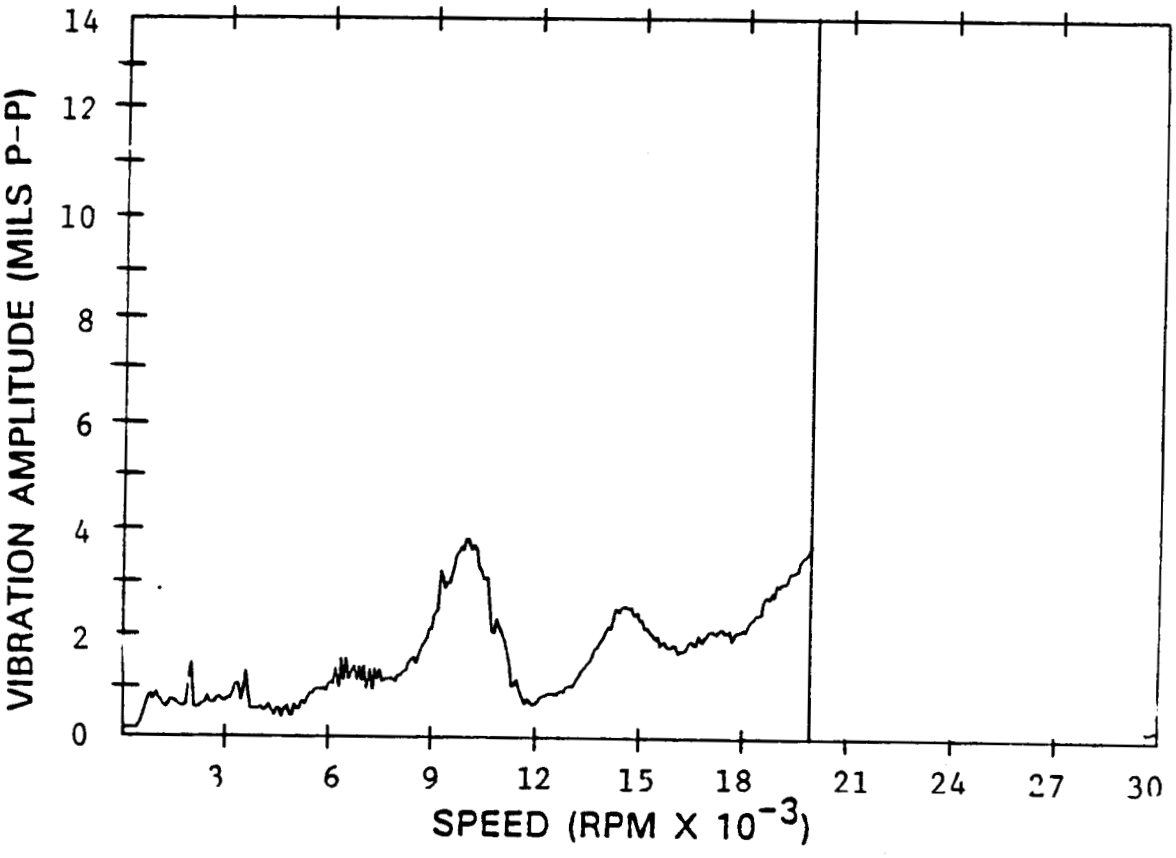

b) After High-Speed Balancing

Figure 6 Power Turbine (GE-L-007566) Vibration Levels, Shaft Midspan Displacement Probe

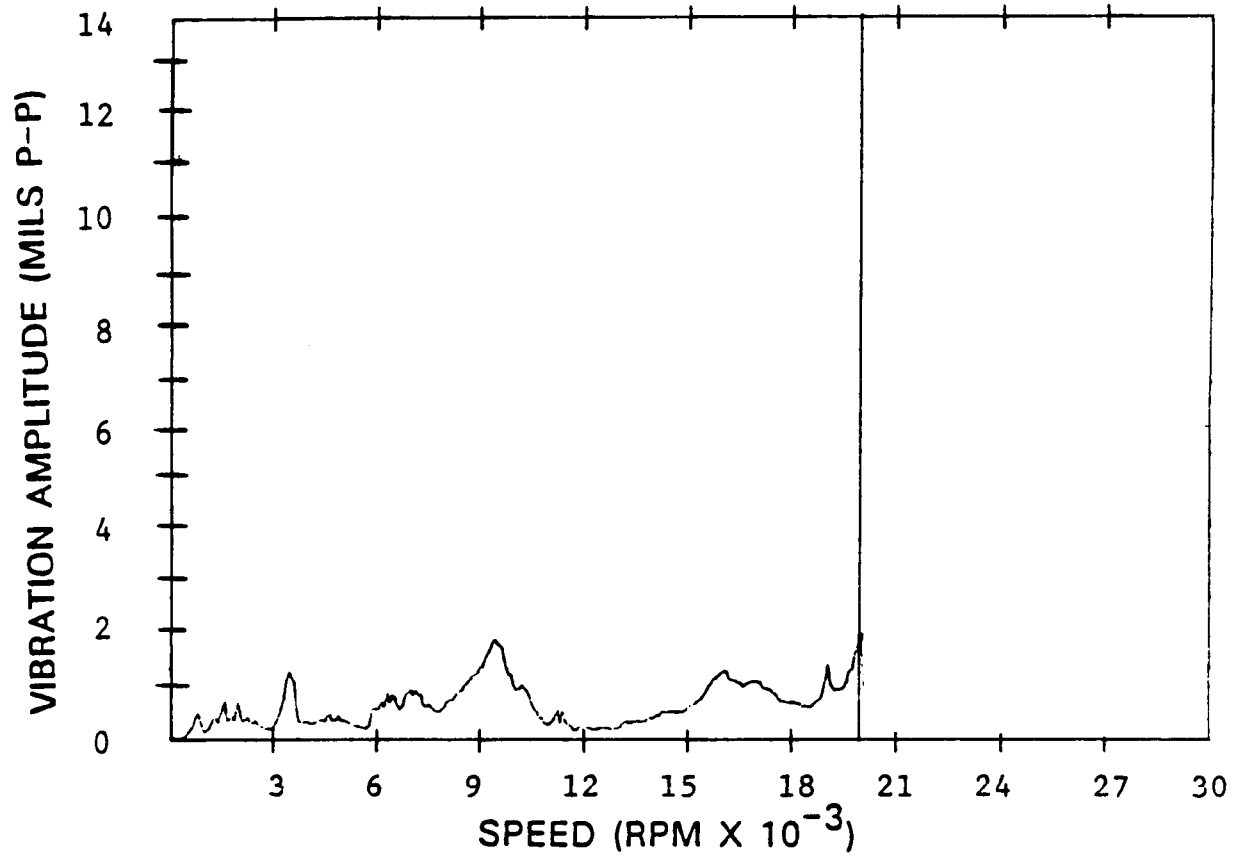

a) As-Received Condition

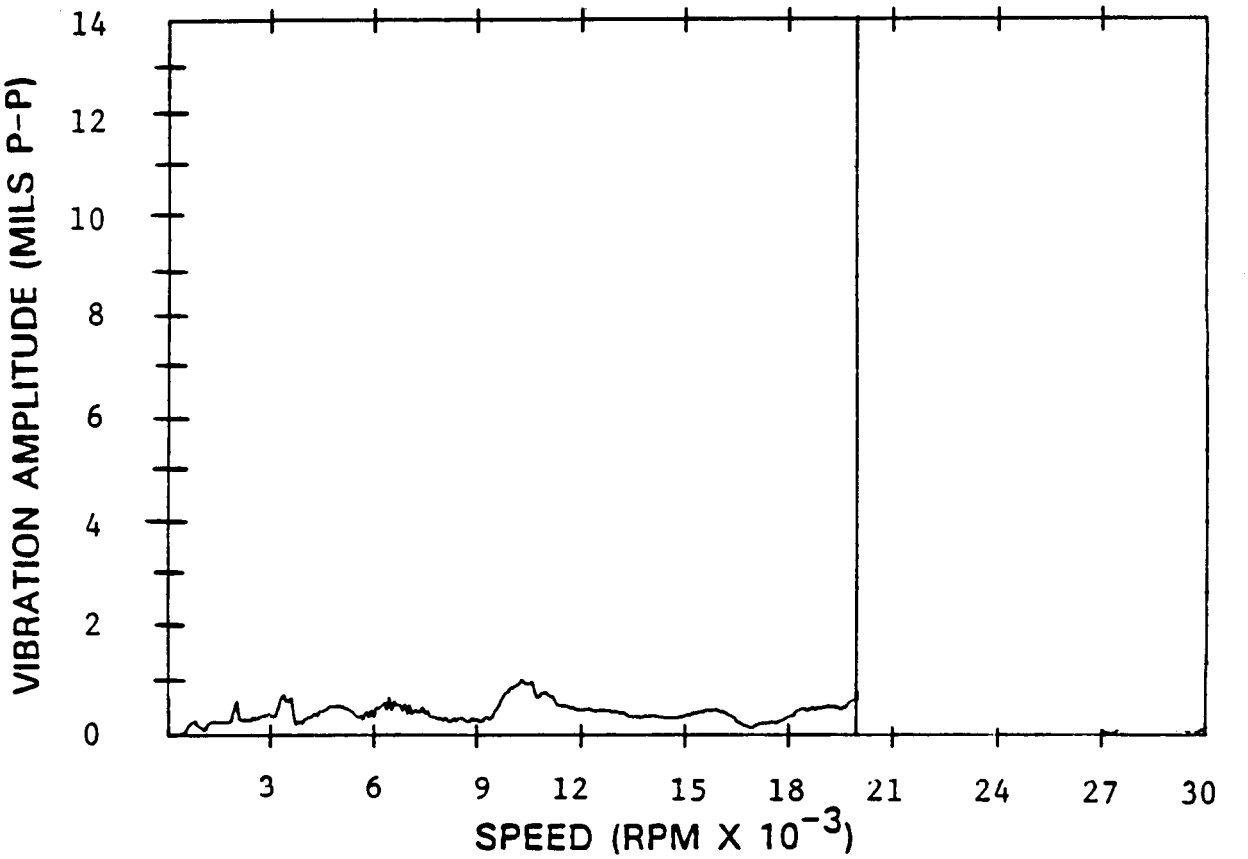

b) After High-Speed Balancing

Figure 7 Power Turbine (GE-L-007566) Vibration Levels, Turbine End Displacement Probe

TABLE 1

T700 POWER TURBINE MODULE BALANCING RESULTS
(20,000 rpm)

Probe	Baseline (Mils)	After Balancing (Mils)	% Reduction	Orbit Ratio	
				Baseline	After Balancing
Rotor 7245					
1	2.391	0.907	62		
2	3.140	1.951	38	0.76	0.46
3	6.028	4.765	21		
4	0.344	1.310	-280	0.06	0.27
5	0.639	1.118	-75		
6	2.008	0.144	93	0.32	0.13
Rotor 7239					
1	2.539	1.008	60		
2	4.111	2.530	38	0.62	0.40
3	6.070	4.081	33		
4	0.455	2.186	-380	0.07	0.54
5	0.314	0.934	-197		
6	2.850	1.485	48	0.11	0.63
Rotor 7948					
1	1.326	1.651	-25		
2	3.086	1.553	50	0.43	0.94
3	3.691	4.413	-20		
4	1.999	2.238	-12	0.54	0.51
5	2.976	3.107	-5		
6	2.202	2.344	-6	0.74	0.76
Rotor 7256					
1	2.539	0.326	87		
2	4.111	0.587	86	0.62	0.56
3	6.070	3.956	35		
4	0.455	0.935	-105	0.07	0.24
5	0.314	4.175	-1230		
6	2.850	1.678	41	0.11	0.40

Table 1 continued

Probe	Baseline (Mils)	After Balancing (Mils)	% Reduction	Orbit Ratio	
				Baseline	After Balancing
Rotor 7972					
1	1.365	0.460	66		
2	0.551	0.678	-23	0.40	0.68
3	5.862	3.017	49		
4	2.692	2.250	16	0.46	0.75
5	2.866	2.063	28		
6	3.074	2.822	8	0.93	0.73
Rotor 7925					
1	1.291	0.619	52		
2	2.344	1.093	53	0.55	0.57
3	4.595	4.486	2		
4	1.026	0.469	54	0.22	0.10
5	1.362	1.581	-19		
6	2.464	1.371	44	0.55	0.87

TABLE 2

T700 POWER TURBINE MODULE P7278, AS INSTALLED

		Baseline Data			
		Measured		Runout Corrected	
Speed	Sensor	Amplitude (Mils)	Phase	Amplitude (Mils)	Phase
8,950	1	1.211	52.3	1.521	77.5
8,950	2	0.792	64.7	0.882	77.8
8,950	3	1.905	43.4	2.367	82.7
8,950	4	0.987	77.3	1.369	117.2
8,950	5	0.122	312.4	0.468	107.3
8,950	6	0.758	227.1	0.942	195.1
20,000	1	1.740	341.7	1.242	359.1
20,000	2	0.595	46.5	0.633	66.0
20,000	3	8.514	284.0	7.288	277.7
20,000	4	3.401	331.1	2.547	326.9
20,000	5	1.472	213.0	1.480	190.3
20,000	6	1.482	267.9	1.255	249.1

constrained balancing, was evaluated. Constrained balancing permits the introduction of various constraints on the balance calculation. Examples of possible constraints are either a prescribed orbit at a particular speed or a prescribed maximum weight addition in a given plane. In this case, the constraint used was probes 1 and 5 constrained to zero amplitude at 20,000 rpm. The calculated balance weights listed below were installed.

- Plane 1 - 1.53 at 259°
- Plane 2 - 0.63 at 347°
- Plane 3 - 0.652 at 228°

The vibration data acquired after installation of the correction set are presented in Table 3. Probes 1 and 5 changed from 1.74 and 1.48 to 0.12 and 0.3 mils at 20,000 rpm. Plots of vibration amplitude versus speed for the as-installed and high-speed balanced conditions are presented in Figures 8 through 10 for probes 1, 3, and 5, respectively.

3.4 Power Turbine Rotor Balancing

A total of three power turbine rotors were balanced for this evaluation. Whereas the previous six rotors were installed in the balancing vacuum chamber with the turbine housing in place, the final three rotors did not have the turbine housing installed (see Figure 3). Removal of the power turbine casing was necessary to fully evaluate high-speed balancing procedures as they would be implemented in the overhaul process. With the casing installed, access to balance plane No. 6 (see Figure 4) is not possible.

Hardware was fabricated that permitted installation of T700 power turbines in the vacuum chamber without the turbine casing in place. The rear bearing support structure was designed to permit access to all balance planes on the rotor and to be dynamically similar to the engine casing support structure. Thus, these tests were intended to further evaluate high-speed balancing feasibility in a realistic engine configuration.

This balancing evaluation was conducted in two steps. First, the two sets of influence coefficients were established with the turbine casing installed. Second, high-speed balancing of the power turbine rotors was completed. The comparison of influence coefficients was not possible since rotor response resulted in different balance speeds for each of the two test configurations. The three balance speeds for the power turbine modules, reported on in Section 3.3, were 8,950, 14,250, and 20,000 rpm. The power turbine rotor balance speeds, determined through evaluation of rotor response characteristics, were 13,000, 17,000, and 20,000 rpm. The difference in the balance speeds most likely resulted from the fact that the rear bearing support assembly characteristics were not as expected. This was due, in part, to the need for an additional adapter extension required to interface to the power turbine rotors. The original test rig design anticipated full access to the rear bearings. The rotors, however, were delivered with the complete C-sump assembly installed, requiring modifications to the support structure.

However, since both the power turbine modules (case installed) and the power turbine rotor were balanced at 20,000 rpm, the influence coefficients were compared and found to differ significantly. In reviewing the influence coefficients, it was found that balance planes 4, 2, 3, and 6 ranked from most to

TABLE 3

T700 POWER TURBINE MODULE P7278 VIBRATION DATA
AFTER HIGH-SPEED BALANCING

		Measured Vibration		Net Vibration (Runout Subtracted)	
Sensor No.	Average Speed (rpm)	Amplitude (Units)	Phase (Deg)	Amplitude (Units)	Phase (Deg)
1	594.0	0.6119	307.9	0.0000	0.0
2	593.8	0.1566	316.1	0.0000	0.0
3	593.8	1.3835	315.5	0.0000	0.0
4	593.9	0.8090	341.3	0.0000	0.0
5	593.8	0.5527	289.3	0.0000	0.0
6	593.8	0.4815	318.3	0.0000	0.0
1	8953.8	1.2907	299.6	0.6910	292.3
2	8953.1	1.2430	295.1	1.0981	292.2
3	8953.5	2.8666	320.0	1.4912	324.1
4	8953.6	3.2877	324.6	2.5240	319.3
5	8954.2	1.1010	334.5	0.8124	3.3
6	8954.0	0.9423	355.4	0.6289	22.8
1	14248.4	1.4645	86.8	1.9670	98.6
2	14247.1	2.9538	242.5	2.9133	239.6
3	14247.7	3.7621	55.1	4.2184	73.9
4	14247.4	4.0976	250.0	4.1959	238.8
5	14246.4	1.7161	315.8	1.2464	327.3
6	14247.7	1.2273	4.4	0.9584	25.6
1	20002.7	0.1241	21.5	0.5890	116.3
2	20002.0	0.9876	133.1	1.1440	133.5
3	20005.3	6.9671	287.9	5.7770	281.5
4	20005.3	3.2659	3.4	2.5346	10.3
5	20006.0	0.3054	189.2	0.6767	135.7
6	20006.0	1.7011	277.5	1.3734	264.2

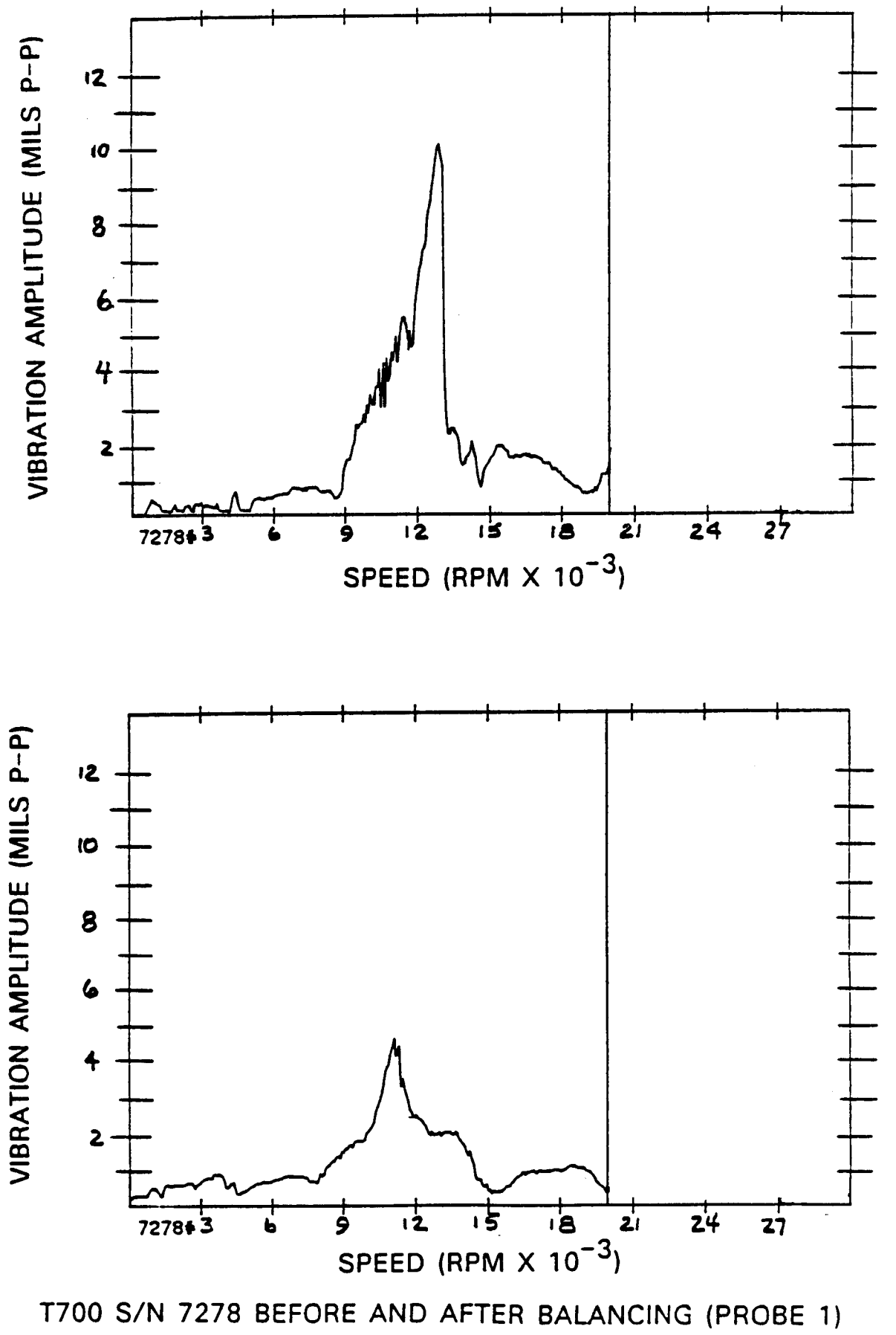

Figure 8 Constrained Balancing Results - Probe 1

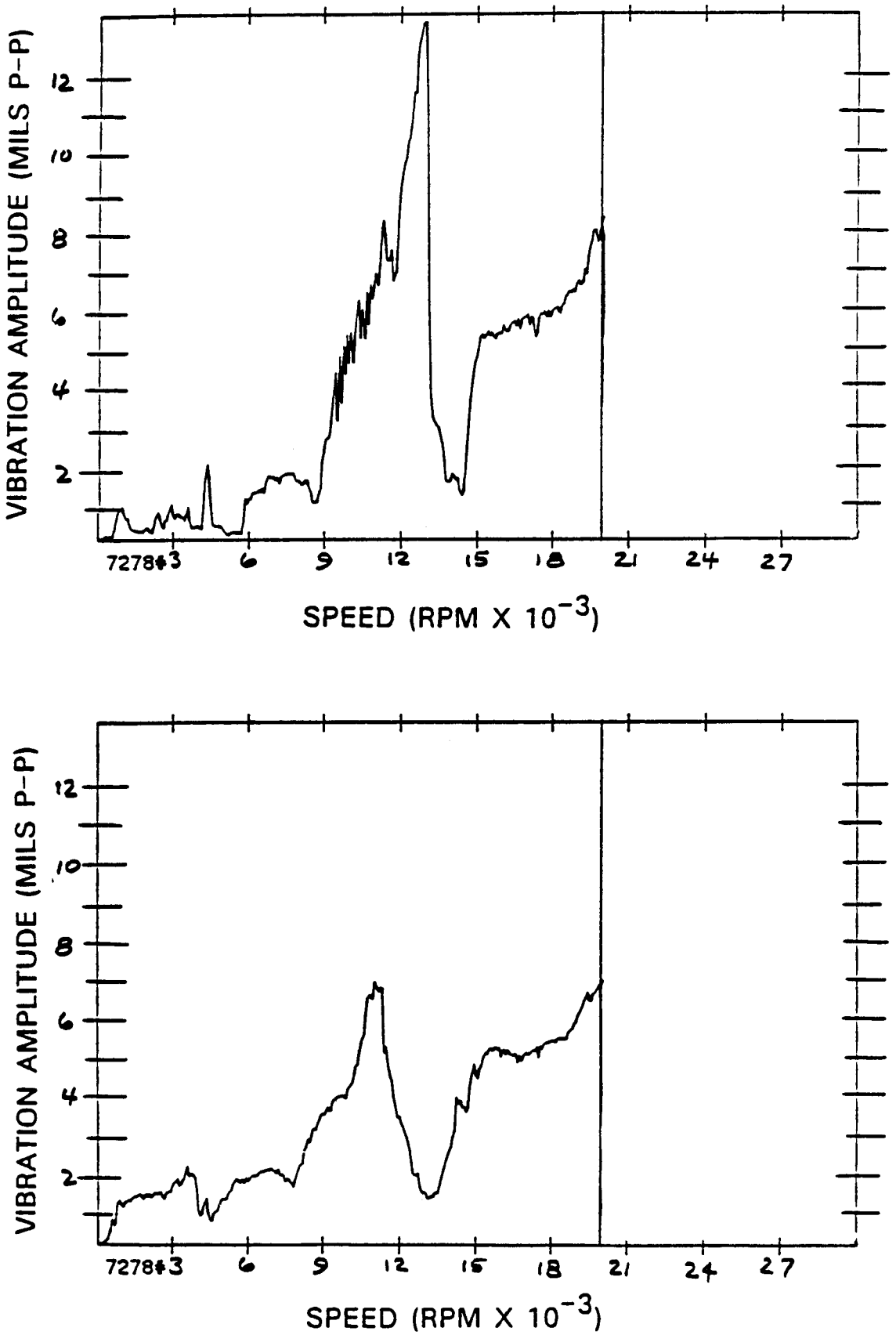

Figure 9 Constrained Balancing Results - Probe 3

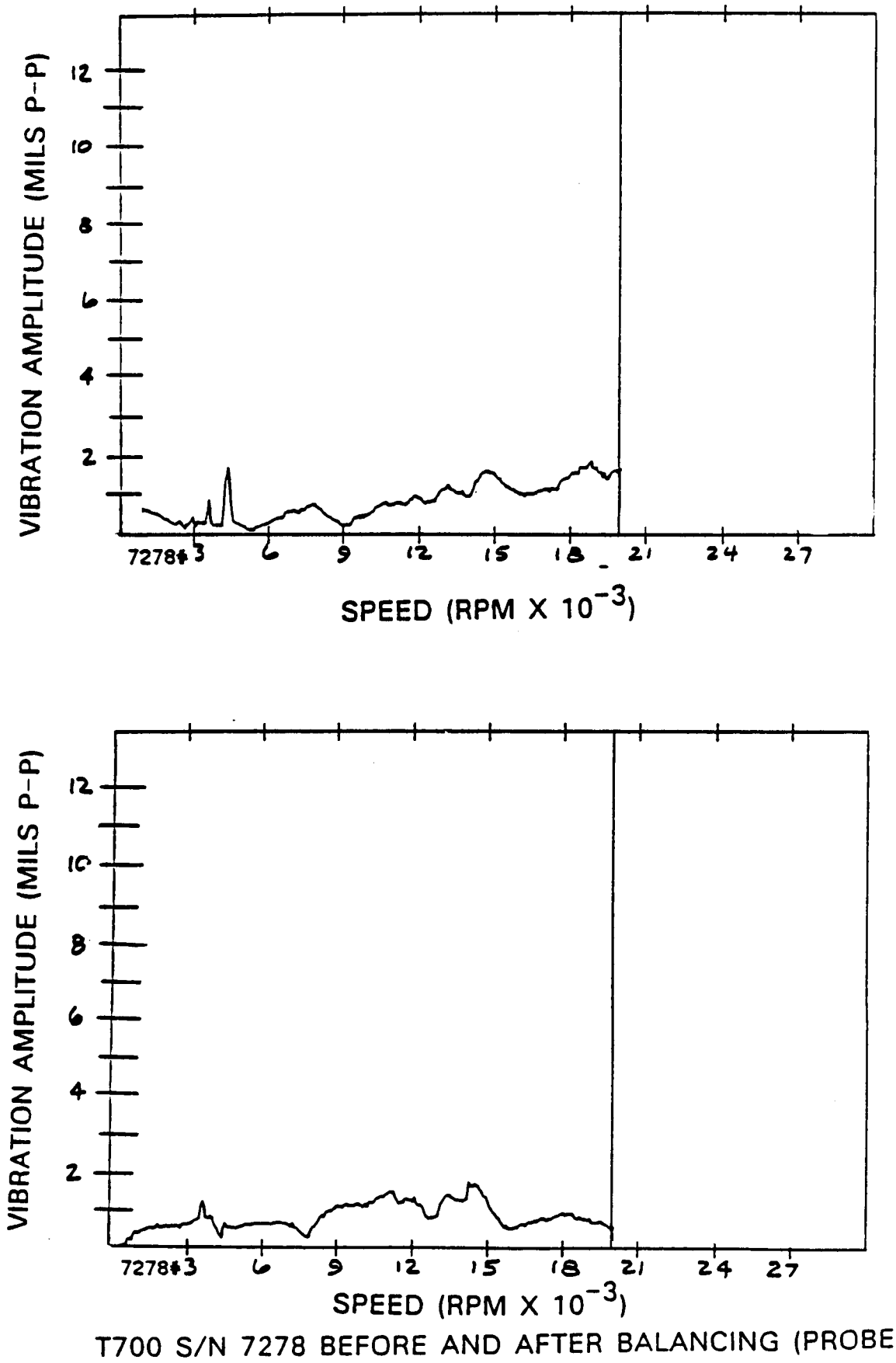

Figure 10 Constrained Balancing Results - Probe 5

least influential for the power turbine modules. On the other hand, the most ranking of balance planes for the power turbine rotors was 6, 2, 3, and 4.

Once the influence coefficient comparison was completed, the three available power turbine rotors were balanced. As with the power turbine modules, each of the rotors was successfully balanced, as shown in Table 4. Again, trade-offs between vibration reductions and orbit circularity were made. It should be noted that the results shown in Table 4 represent a single attempt at balancing each rotor. The procedure followed was to operate the rotor at each of the three balance speeds and acquire the vibration data all in one test run of the rotor. Using the established influence coefficients, correction weights were predicted and installed in planes 2, 3, and 6 on the rotor. With the installed correction weight set, the rotor was again operated at each of the three balance speeds and vibration data were taken. As seen in Figures 11, 12, and 13, vibrations at 20,000 rpm are generally improved over the unbalanced/baseline state. For example, vibrations recorded by probe 2 at 20,000 are all at 2 mils or above before balancing and below 2 mils after balancing. Similar trends are noted for probes 4 and 6 as well.

TABLE 4

T700 POWER TURBINE ROTOR BALANCING RESULTS
(20,000 rpm)

Probe	Baseline (Mils)	After Balancing (Mils)	% Reduction	Orbit Ratio	
				Baseline	After Balancing
Rotor 7239					
1	1.257	1.051	17		
2	1.719	0.233	86	0.73	0.22
3	0.484	2.824	-484		
4	4.892	3.398	30	0.10	0.83
5	1.292	1.053	19		
6	0.696	0.946	-36	0.54	0.90
Rotor 7256					
1	0.283	0.851	-200		
2	2.769	1.983	28	0.10	0.43
3	1.412	2.417	-71		
4	6.246	3.016	52	0.23	0.80
5	0.914	1.490	-63		
6	0.994	1.324	-33	0.92	0.89
Rotor 7278					
1	6.213	5.343	14		
2	1.917	0.859	55	0.31	0.16
3	9.932	6.159	38		
4	7.148	4.453	38	0.72	0.73
5	1.759	1.175	33		
6	1.724	0.908	47	0.98	0.78

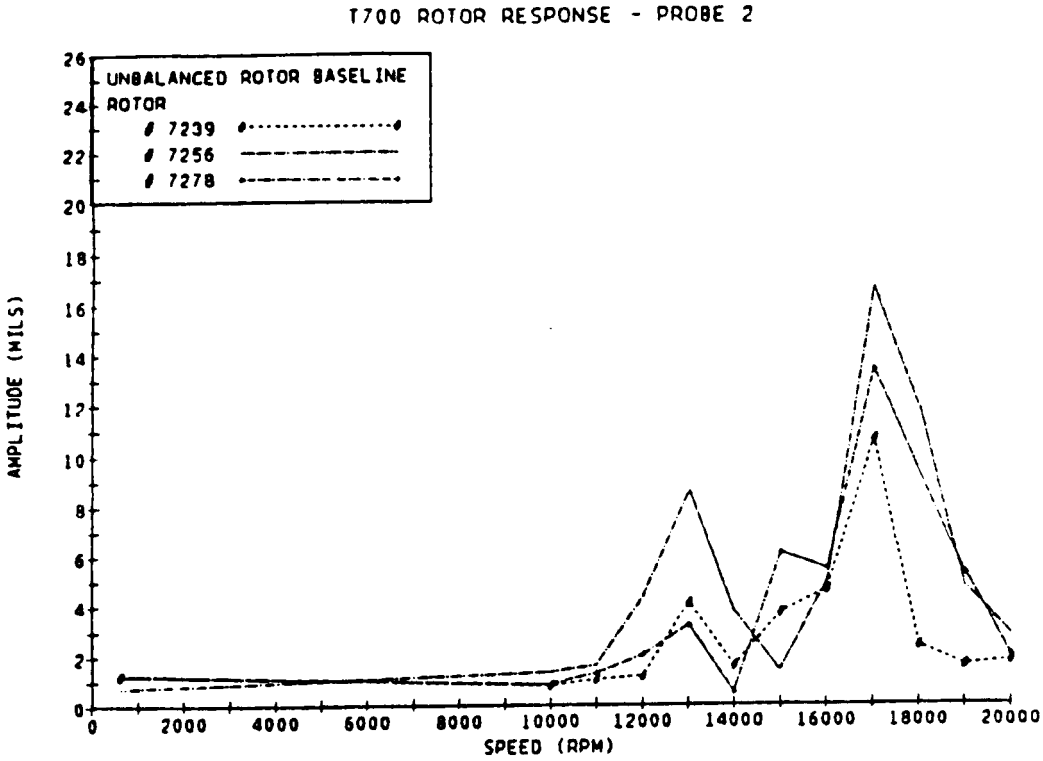

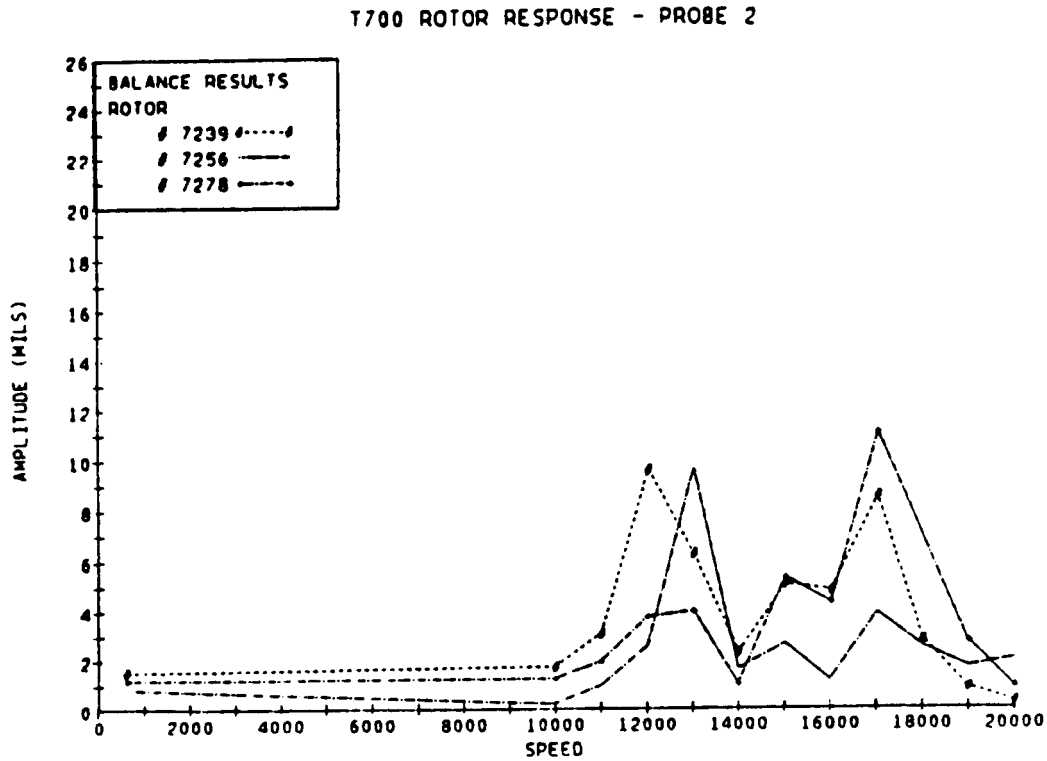

Figure 11 T700 Rotor Balancing Results - Probe 2

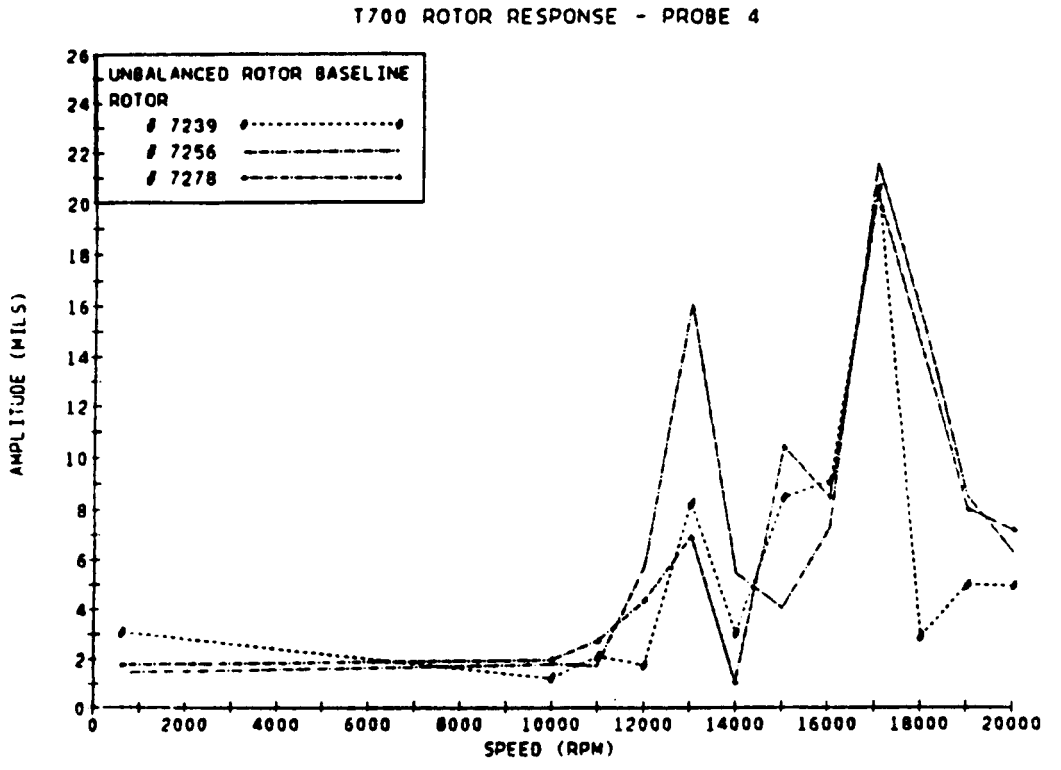

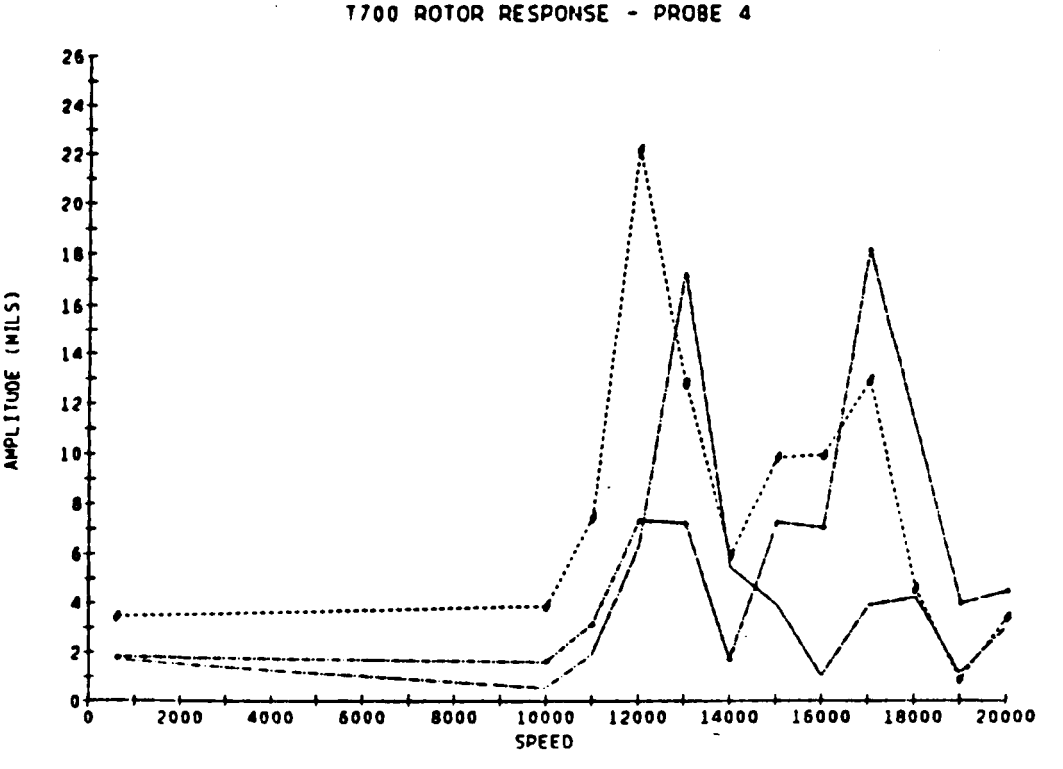

Figure 12 T700 Rotor Balancing Results - Probe 4

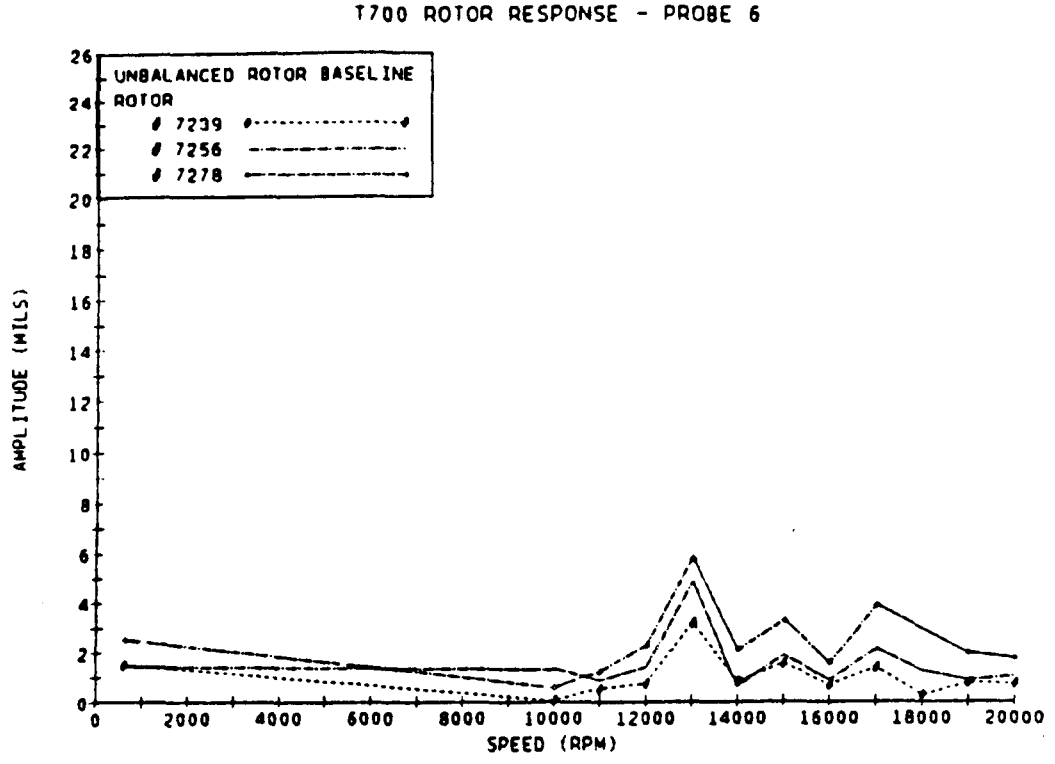

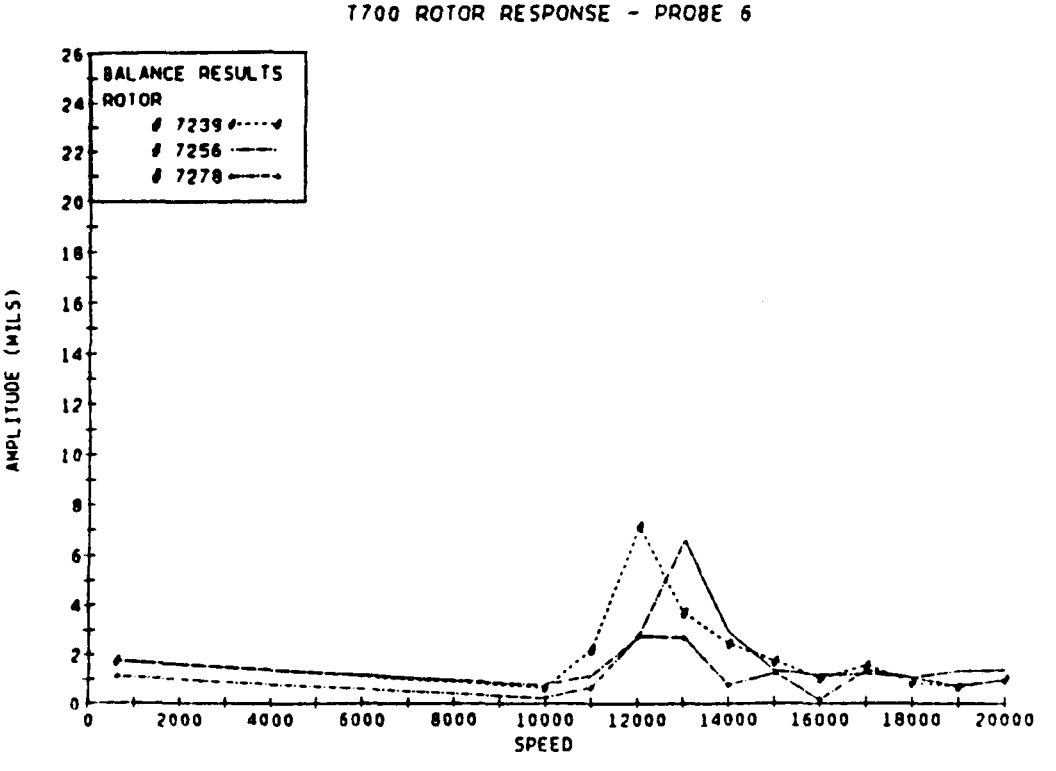

Figure 13 T700 Rotor Balancing Results - Probe 6

4.0 FORMULATION OF PROCEDURES FOR BALANCING T700 COMPRESSOR ROTOR

An analytical rotordynamic study has been conducted for the T700 engine gas generator for the purpose of obtaining a good understanding of its sensitivity to imbalance. Following the study of the rotor bearing system characteristics, typical imbalance amounts and distributions for T700 gas generators have been estimated from design drawings. For various levels of imbalance, a multiplane, multispeed balancing optimization study has been conducted to select the most effective balancing planes and speeds.

4.1 Construction of Analytical Model

For the rotordynamic analysis, a rotor bearing system must be represented by an analytical model. The complexity of the model often grows as the number of components, which make up the rotor, increases. A schematic of the T700 gas generator model is shown in Figure 14. The analytical model basically consists of a number of finite beam elements described by constant inner and outer diameters. The rigidity (or flexibility) of the shaft is represented by stiffness diameters. Inertia properties, such as mass and moments of inertia, are represented by mass diameters. Parts that do not contribute to or have little effect on the flexibility were modeled in the form of lumped inertias or increased mass diameters of relevant rotor sections.

For the T700 gas generator, stiffness diameters at each segment were digitized from the design drawing and mass diameters were used to account for additional mass. Some engineering judgement was used in determining the diameters of each rotor element. Lumped inertias are used to model compressor impellers and turbine disks. The rotor is mounted on two resilient squeeze-film damper bearings, which are located at stations 4 and 39 in this model.

4.2 Critical Speed Analysis

The critical speed analysis computes the undamped critical speeds of the system quickly and inexpensively for various bearing stiffnesses. This calculation is used mainly to investigate the effect of bearing (support) stiffness on the natural frequencies of the system. The supports, consisting of two rolling-element bearings that are, in turn, supported on fluid-film dampers, may have considerable variations in stiffness, depending on both damper design and bearing support structure. A critical speed map with nominal support stiffness varying from 10,000 to 200,000 lb/in. for both bearings is shown in Figure 15.

The T700 gas generator has a suspension system with unequal support stiffnesses, specifically 22,450 lb/in. at the compressor end and 33,250 lb/in. at the turbine end. When these values are applied to the mathematical rotor model, the resulting critical speeds are as follows:

- First mode at 5,852 rpm
- Second mode at 7,920 rpm
- Third mode at 27,580 rpm.

A plot of the mode shapes is given in Figure 16. Notice that the first two criticals are basically rigid body modes, while the third critical is a

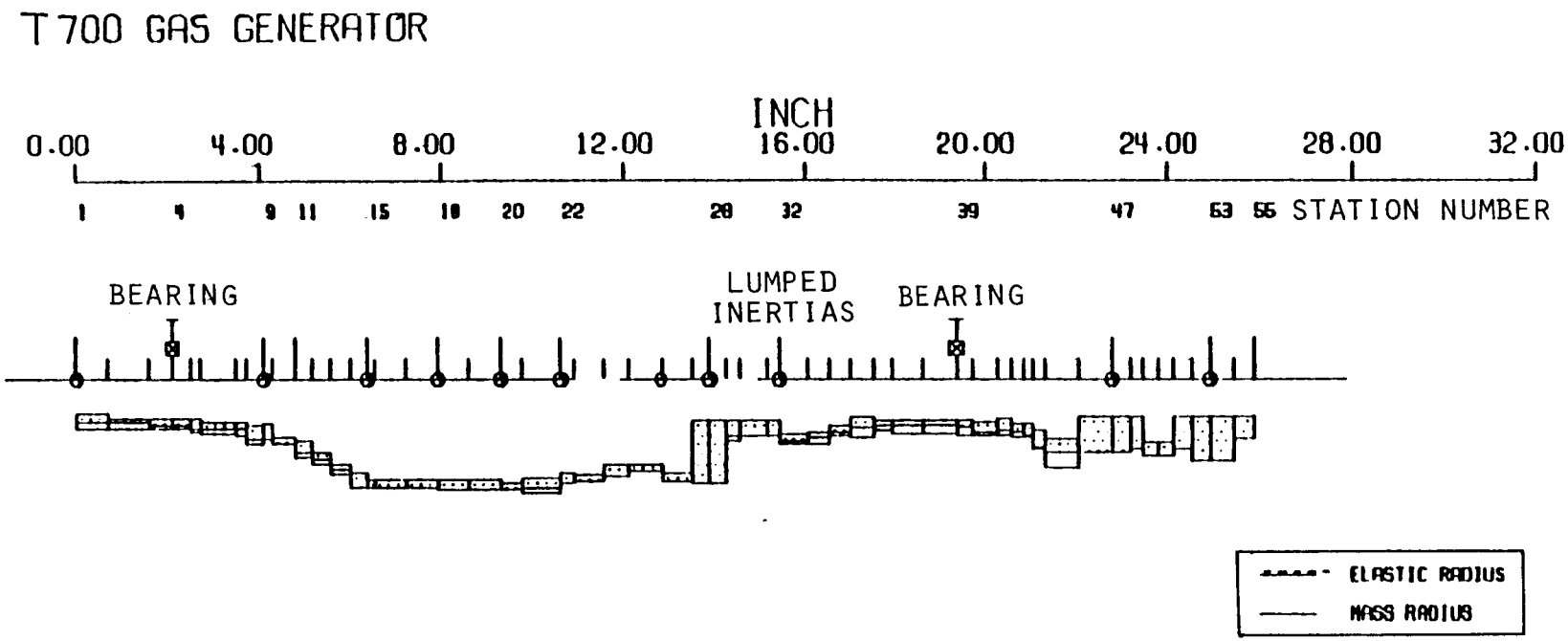

Figure 14 Analytical Model of the T700 Gas Generator

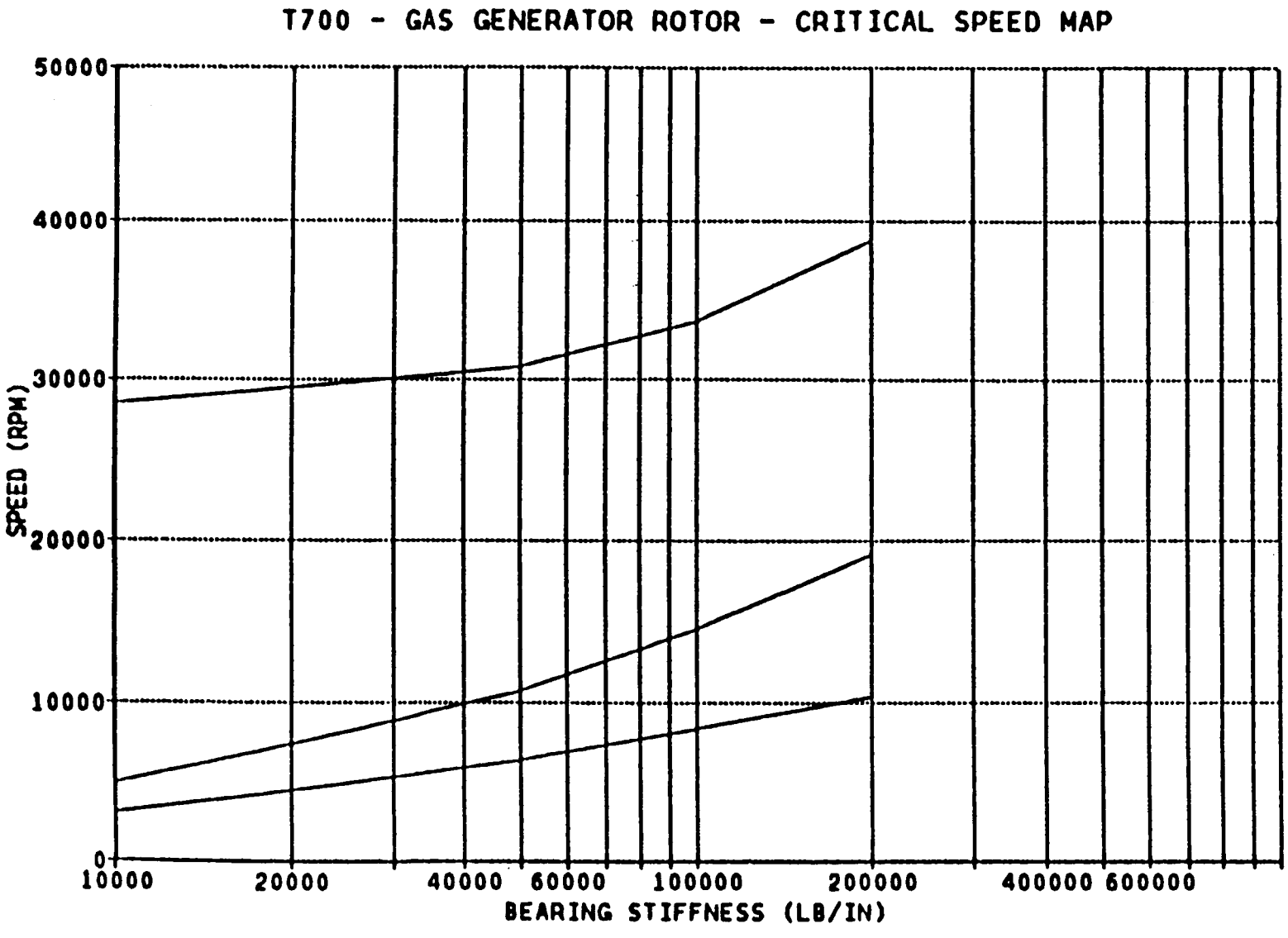

Figure 15 Critical Speed Map of the T700 Gas Generator

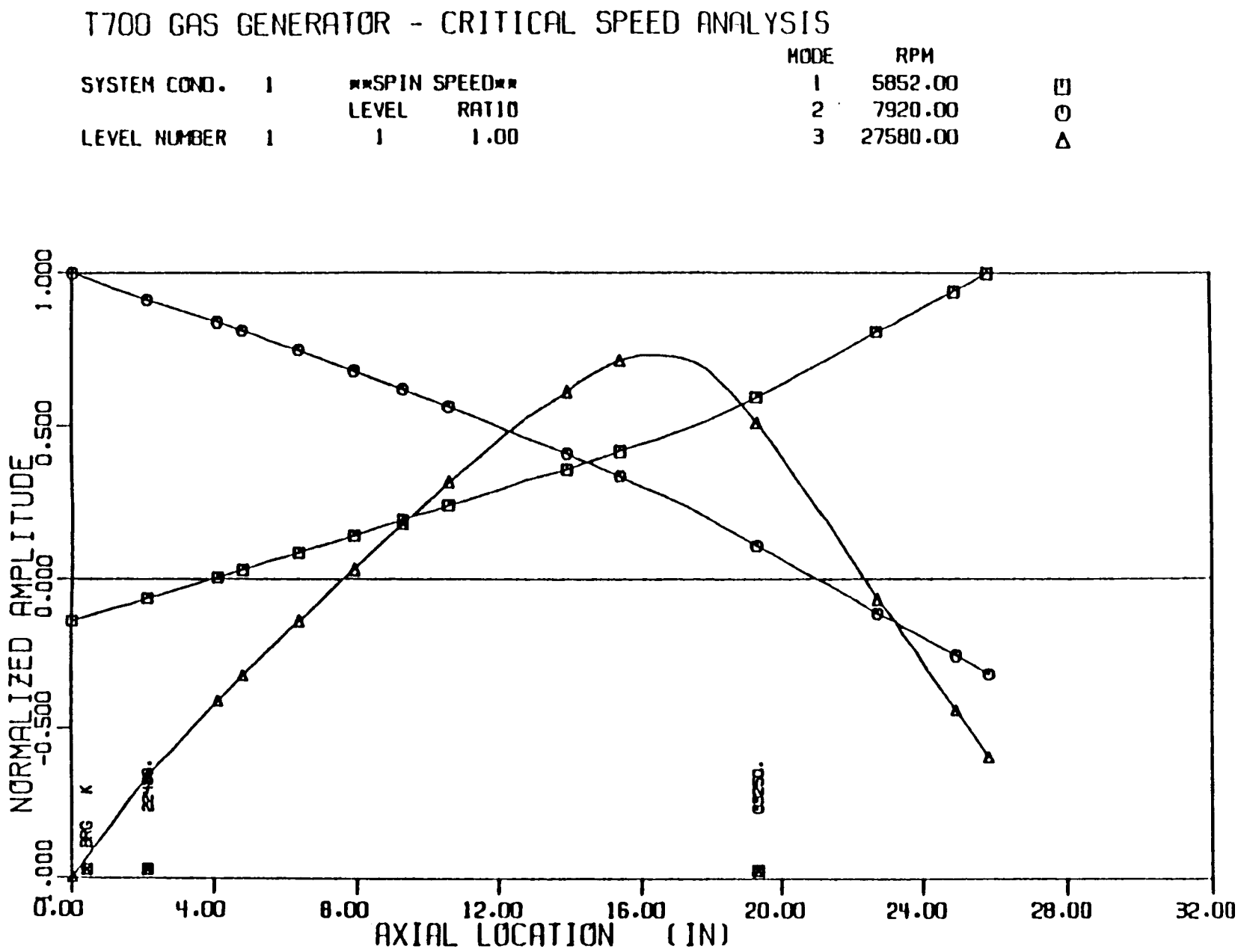

Figure 16 Natural Frequencies and Mode Shapes of the T700 Gas Generator

bending mode. All three modes fall below the desired operating speed range of 30,000 to 45,000 rpm.

4.3 Unbalance Response

Rotor response calculations require two additional inputs beyond those supplied for the undamped critical speed analysis. These are bearing damping and imbalance distribution.

4.3.1 Bearing Damping

Since rolling-element bearings are used in the system, little damping can be expected from the bearings. However, both bearings are supported on flexures and squeeze-film dampers. The nominal damping values of the two dampers are calculated based on the dimensions taken from the design drawings. Table 5 shows the bearing geometry and the nominal damping values.

4.3.2 Imbalance Distribution

In the absence of precise distributed imbalance measurements, the imbalance distributions used in the rotordynamic calculation are based on estimates. From manufacturing tolerances, a possible worst case imbalance may be determined for the rotor, but it must be kept in mind that significant additional imbalance may be present in the actual rotor due to unexpected material inhomogenities, worn (out-of-tolerance) parts, or other causes.

For the T700 gas generator, the rotor imbalance consists mainly of the following identifiable elements:

- Mass eccentricity due to the lack of concentricity between bearing surfaces and shaft outside diameter
- Mass eccentricity due to lack of concentricity between bearing surfaces and shaft inner diameter
- Mass eccentricity due to the lack of concentricity and perpendicularity between shaft and turbine component mounting surfaces
- Residual imbalance introduced to the rotor during assembly of the gas generator.

The magnitude of the mass eccentricity vectors of the above listed cases may be estimated from manufacturing drawings. However, the circumferential angular location of the mass eccentricity is, of course, unknown. Therefore, the total imbalance distribution of the rotor assembly can only be estimated from the available reference drawings. For purposes of this study, random angular distributions were assumed.

Runout limits at various locations on the shaft were taken from drawing No. 6035T77. In addition to the shaft runout, disks such as compressor and turbine wheels also have residual imbalance after a low-speed component balancing is conducted. A list of the total imbalance at each lumped mass station used in the dynamic rotor model is shown in Table 6.

Synchronous response calculation was employed to obtain the amplitudes for this standard baseline rotor. With randomly distributed imbalance along the shaft, amplitude versus speed at several selected stations is plotted, as

TABLE 5

DAMPER GEOMETRY AND NOMINAL DAMPING VALUES

	Bearing #3 Center Groove Fed (Unsealed)	Bearing #4 Center Groove Fed (Sealed)
Diameter (in.)	3.00	3.00
Length (in.)	0.78	0.587
Clearance (in.)	0.0035	0.0045
Viscosity (lb-sec/in.)	1.03×10^{-6}	1.03×10^{-6}
Damping Coefficient:		
Bxx = Byy (lb-sec/in.)	9.219	12.329

TABLE 6

IMBALANCE DISTRIBUTION OF LUMPED MASSES

Location	Station Number	Mass Eccentricity After Low-Speed Balancing (lb-in.)	Total Mass Eccentricity (lb-in.)	Angular Location (deg)
Thrust Pad	1		0.0026	90
Compressor 1	9	0.000656	0.0082	300
Compressor 2	15		0.0036	270
Compressor 3	18		0.0038	240
Compressor 4	20		0.0056	210
Compressor 5	22		0.0029	180
Impeller	28		0.0072	50
	32		0.0012	120
Turbine 1	47	0.001094	0.0048	90
Turbine 2	53	0.001094	0.0056	60

shown in Figure 17. Notice that the amplitude peaks are found at 5,900, 8,000, and 28,000 rpm. These speeds agree well with the previously calculated undamped critical speeds. The general damped deflected shapes are also included in Figure 18 for speeds of 8,000 and 26,000 rpm. Comparison of these deflected shapes indicates that the maximum amplitudes occur at the cold end of the rotor and shift toward the center as the rotor reaches its bending critical.

This baseline rotor model assumes that the low-speed component balancing of the disks has been performed. If the entire rotor is assembled without low-speed component balancing, additional imbalance of 1 g-in. (0.002 lb-in.) is added to each disk. The response of this worst baseline model was also calculated, as shown in Figure 19, at stations 1, 32, and 53.

4.4 Analytical Balancing

The major goal of this task was the evaluation of the effectiveness of multiplane, multispeed balancing in reducing the amplitude of the T700 gas generator to acceptable levels. The analytical means to conduct such a study are available in a computer program system, which calculates influence coefficients and required correction weights in sequence. The overall procedure of this approach can be summarized in the flow chart in Figure 20.

After the baseline rotor response was obtained from synchronous response calculations, analytical influence coefficients were calculated according to specified plane and probe locations. The balancing portion of the program then receives its input from the output of baseline response and influence coefficients calculations. The analytical process simulates the actual experimental operation performed during balancing of a rotor.

Previous sections described the process by which the rotor model was developed and which yielded baseline rotor response calculations. In this section, the considerations involved in the selection of balancing planes, probe locations, and balancing speeds are discussed. Following this, the results obtained from the simulated balancing operation are presented.

4.4.1 Sensitivity to Imbalance

In order to determine the balancing planes to be used in this analytical balancing procedure, a sensitivity study must be conducted to evaluate the influence of each plane. A unit imbalance was placed at each of the possible balance planes and the response calculated by synchronous imbalance response program. Responses at stations 1, 28, 32, and 53 (due to a unit imbalance at station 1) are plotted as functions of speed, as shown in Figure 21. Synchronous responses due to imbalance at other stations can be made to show the relative influence of each plane. This procedure is similar to acquiring influence coefficients in the laboratory. The influence coefficient matrix of the T700 rotor can be analytically calculated as described in the following section.

4.4.2 Calculation of Influence Coefficients

The T700 gas generator assembly is provided with eight balancing planes as shown by the design drawings. These are listed in Table 7. Seven plane and

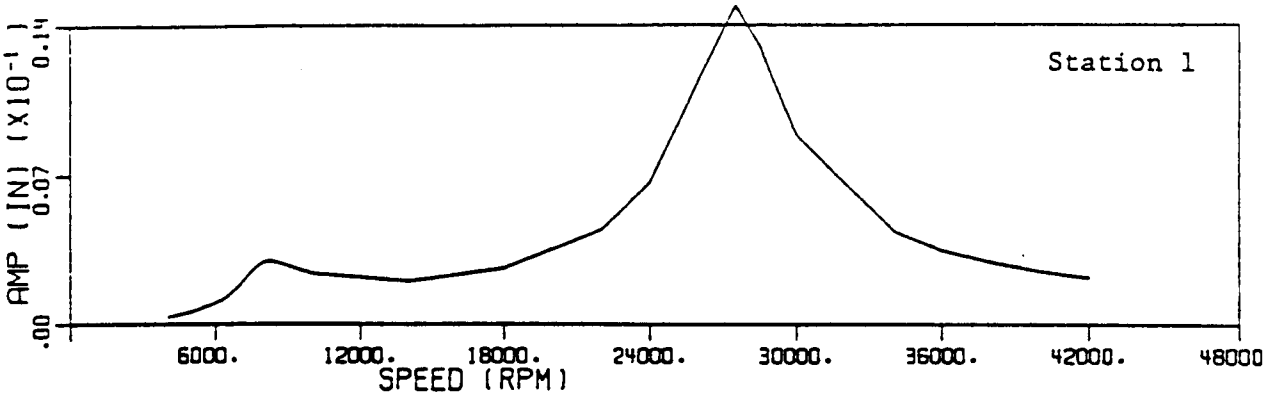

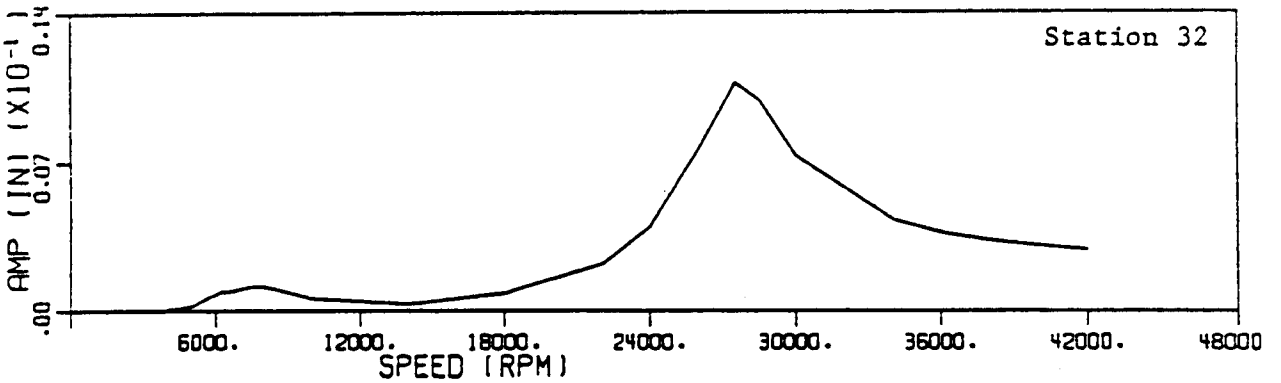

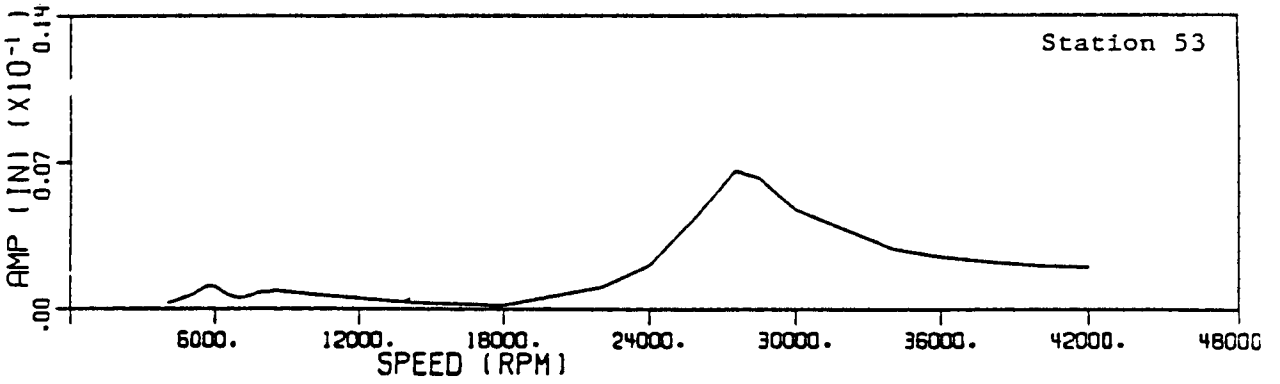

Figure 17 Balance Response with Standard Imbalance

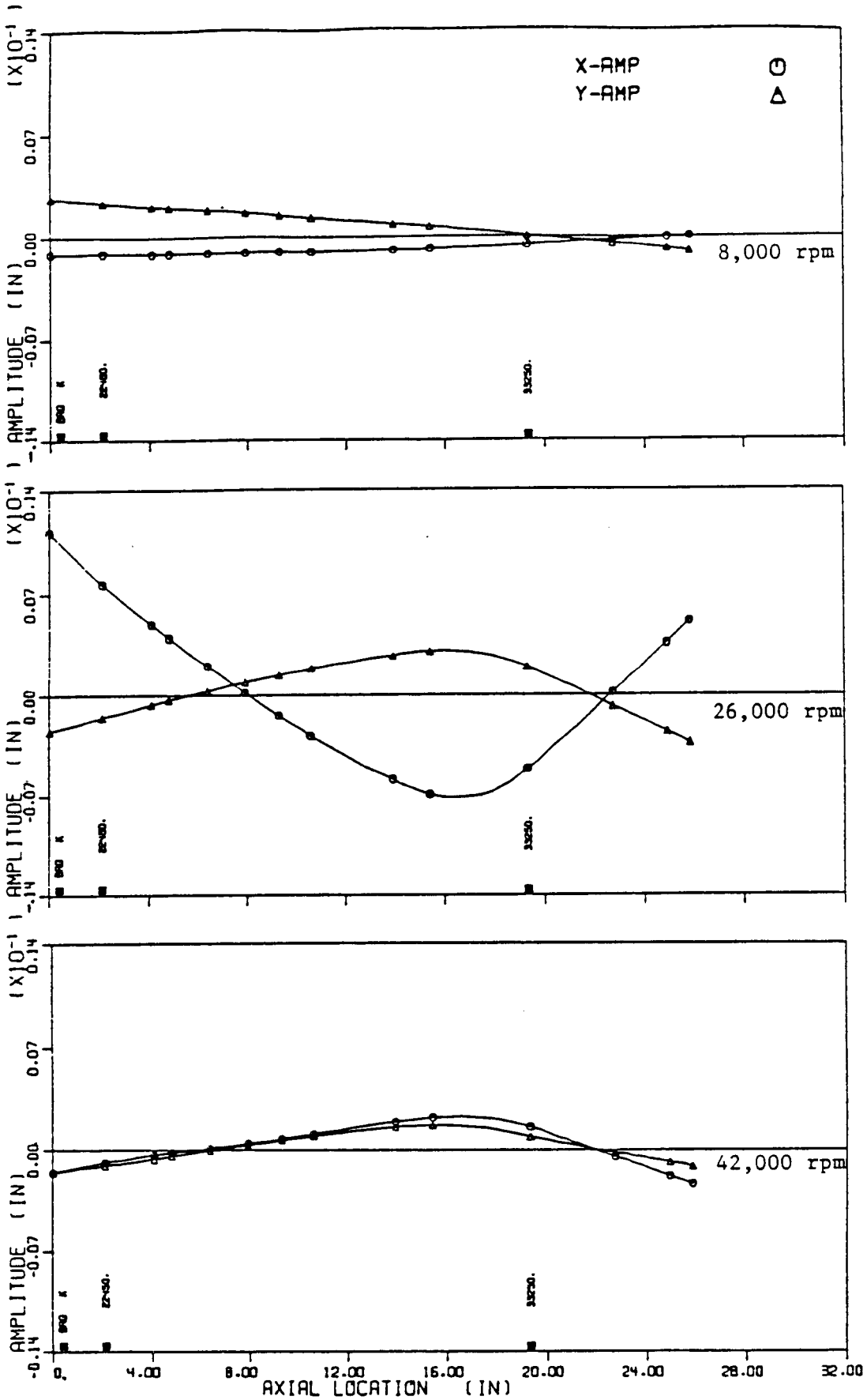

Figure 18 Deflected Rotor Shape at 8,000, 26,000 and 42,000 rpm with Baseline Imbalance

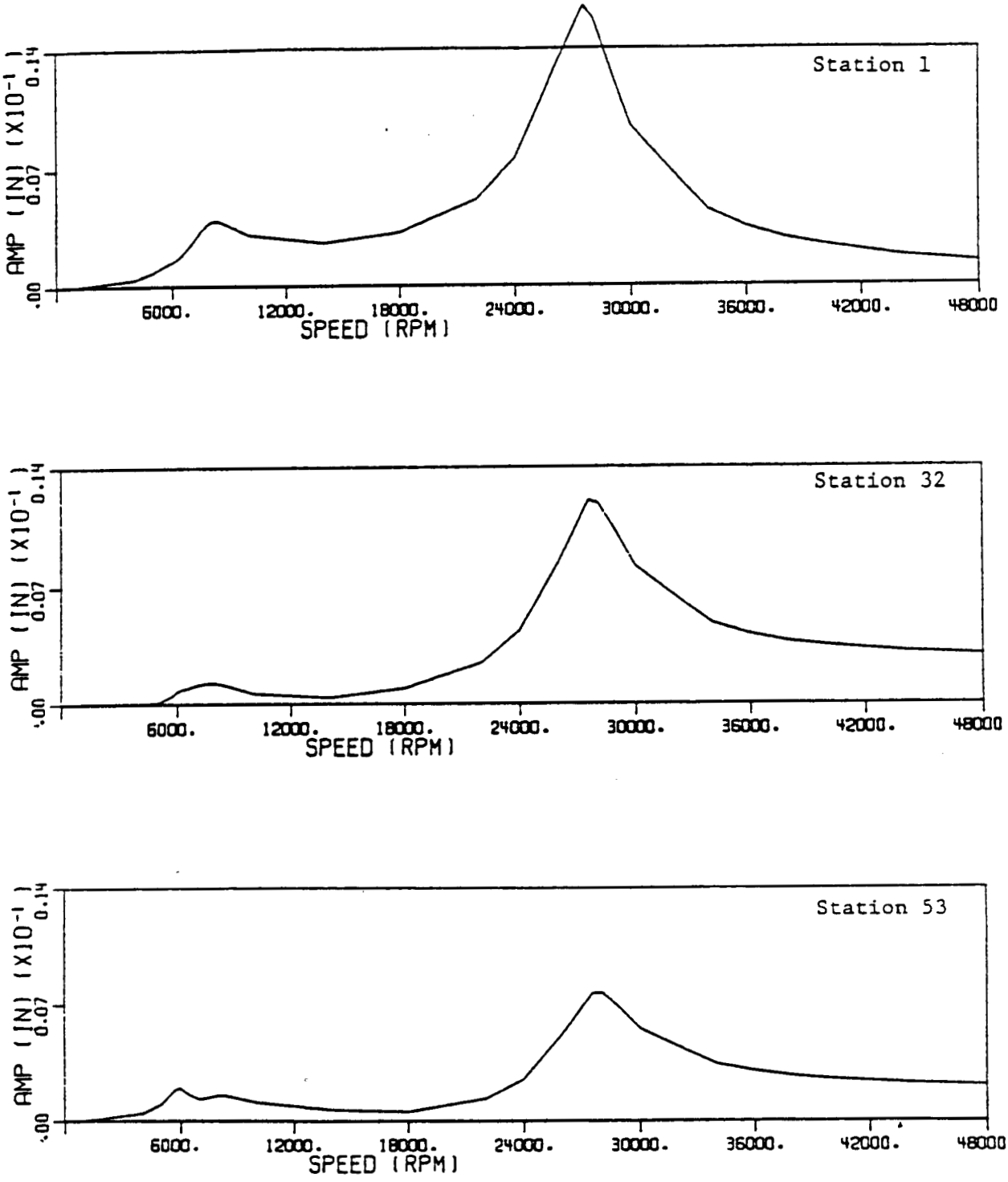

Figure 19 Baseline Response with Worst Imbalance

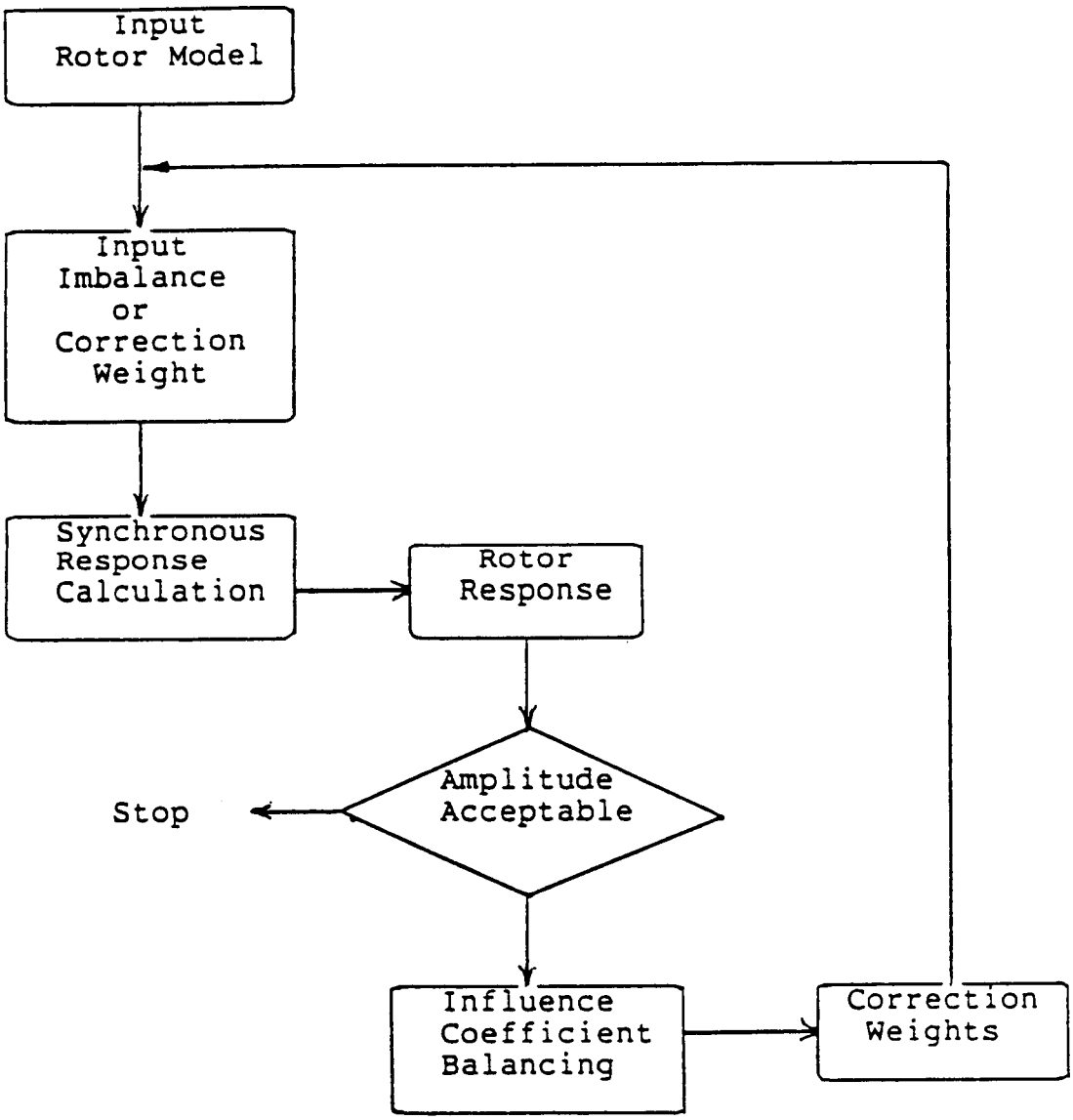

Figure 20 Flow Chart of Analytical Balancing Procedures

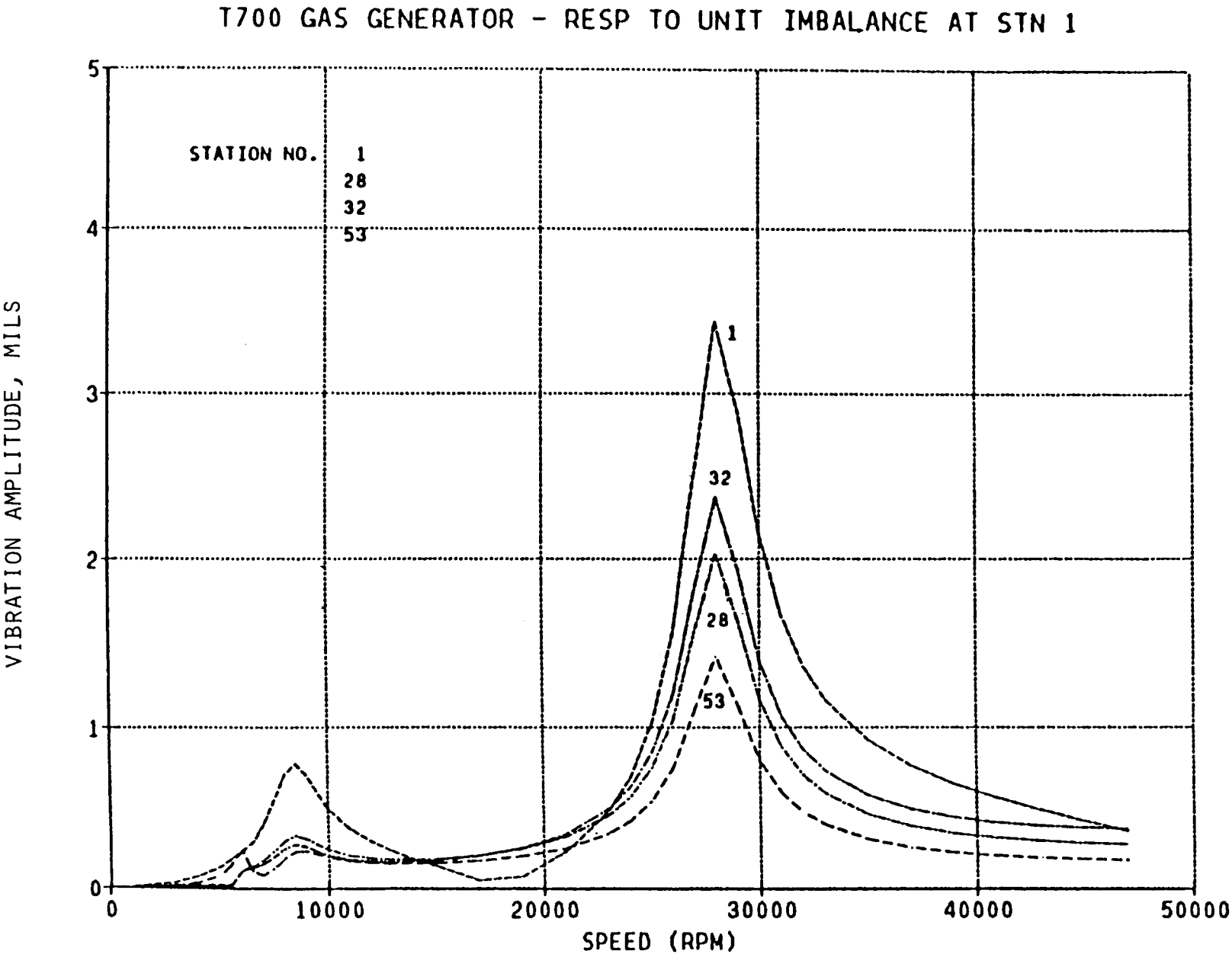

Figure 21 Response Due to Unit Imbalance at Station 1

TABLE 7

BALANCING PLANES OF T700 GAS GENERATOR

Drawing No.	Location	Station No.
6032T26	Compressor Stage 1	9
6032T27	Compressor Stage 2	15
6038T08	Compressor Stages 3 and 4	18, 20
6038T09	Compressor Stage 5	22
6038T74	Impeller, Centrifugal	28
6039T54	Turbine Stages 1 and 2	47, 53

probe locations were selected to evaluate the sensitivity of each plane and calculate the analytical influence coefficients. The plane locations are indicated in Figure 22. Note that even though seven planes were used to generate the influence coefficient matrix, it does not mean that all the planes must or will be used for balancing purposes. By applying engineering judgement, it was concluded that fewer than four planes are really required for multiplane, multispeed balancing of a flexible rotor such as the T700 gas generator. Consequently, a subset of the influence coefficient matrix was constructed to feed into the balancing software.

The analytical influence coefficient matrix was obtained from several runs of a synchronous response program. Response at probe locations was sifted from the output file to construct the influence coefficient matrix (α)

$$\alpha_{ij} = Q_i/u_j$$

where i and j indicate the row and column numbers, respectively; Q_i is the response at station i; and u_j is the unit imbalance at station j.

Not all of these balance planes are accessible when the engine is assembled. For the purpose of this multiplane, multispeed flexible rotor balancing study, the number of balancing planes must be kept small so that the complexity of the entire balancing process can be reduced to a minimum. The selection of the planes to be used in the final balancing can be based either on the mode shape of the rotor or on the 7 × 7 influence coefficient matrix obtained earlier.

At various speeds, each plane contributes differently to the total deflection of the rotor. In order to aid the judgement in selecting balancing planes, the sensitivity plots were used to identify the plane influence under different operating speeds. The relative magnitude of the response amplitude at various stations is the indication of the order of plane influence. The order of plane influence is shown for several rotor speeds, as shown in Table 8.

4.4.3 Selection of Balancing Planes and Speeds

Not all of the planes selected for influence coefficient matrix calculation are accessible when the engine is assembled. For the purpose of the multiplane, multispeed flexible rotor balancing study, three balancing planes will be utilized. These are planes 1, 5, and 7 or stations 1, 32, and 53, respectively.

The selection of these three planes is based on the sensitivity study of each balancing plane, as shown in Table 8. The first and the second critical speeds are basically rigid body modes so that a two-plane balance will be sufficient to reduce the amplitude. The third critical speed, however, is a flexible mode and requires multiplane balancing. Based on the mode shapes and analytically calculated influence coefficient matrix, the selected balance planes are adequate for balancing the rotor.

There are several criteria for the selection of balancing speeds:

1. Trial weight data must be obtained reasonably near the critical speeds, where rotor response is fairly high

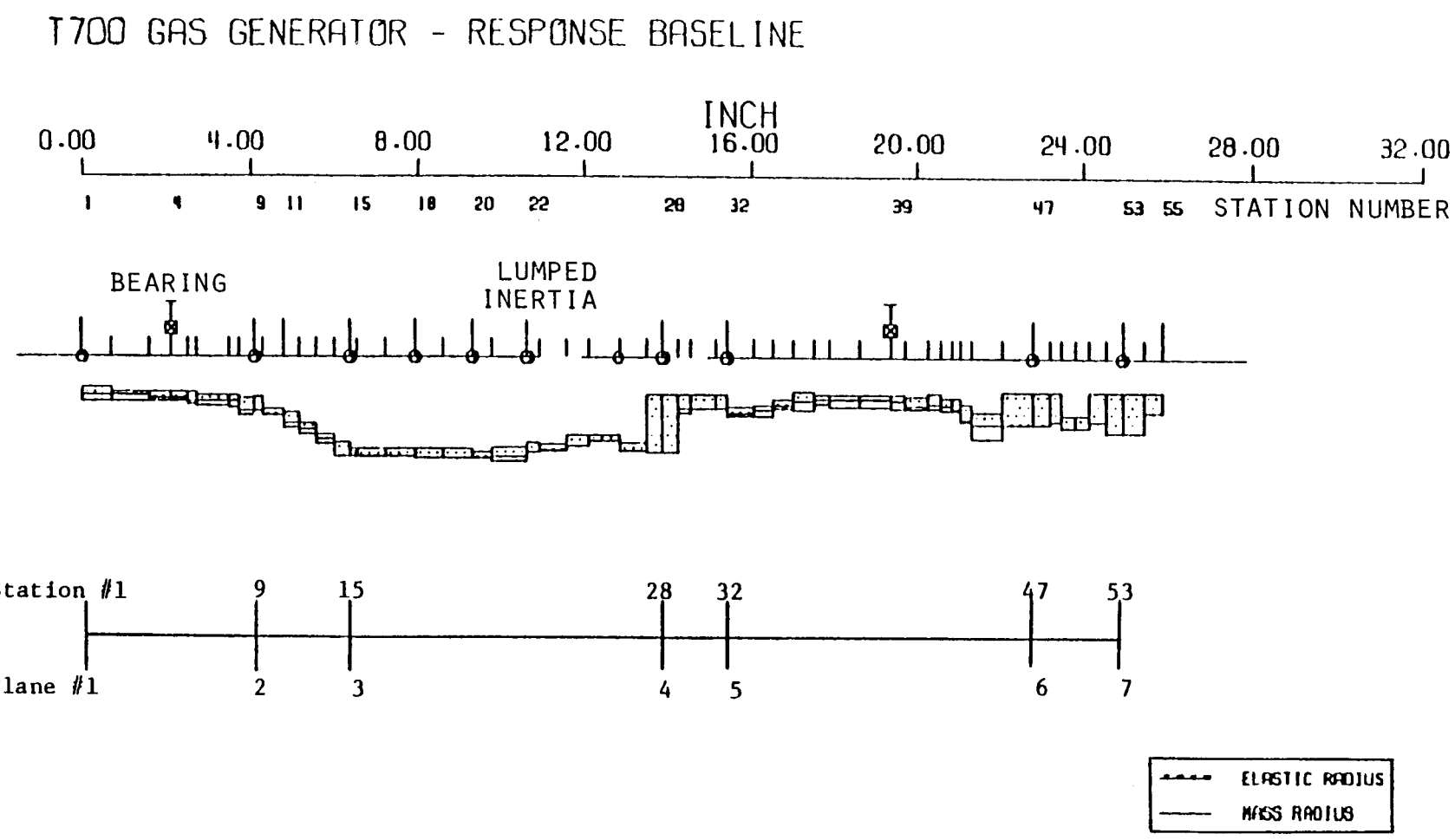

Figure 22 Selection of Balancing Planes

TABLE 8

ORDER OF PLANE INFLUENCE

Speed (rpm)	Order of Plane Influence (Plane Numbers) ← Most — Least →						
6,000	7	1	5	2	6	3	4
8,000	1	7	5	2	6	3	4
26,000	1	5	7	2	6	3	4
44,000	1	5	2	7	6	3	4

2. Rotor vibration amplitude must not exceed safe operating limits during either the baseline run or the trial weight run
3. Rotor amplitudes should be measured at speeds where the deflected rotor shapes are representative of the critical speeds to be traversed
4. Rotor amplitudes should also be measured at the operating speed.

These considerations lead to the selection of three balancing speeds at about 7,000, 22,000, and 42,000 rpm. Since it may not be possible to measure baseline response throughout the operating speed range due to excessive vibration levels, the procedure may require two or three balance runs.

The following balance speeds were used within the framework of the above discussion:

Run	Standard Baseline	Worst Baseline
First	7,000	6,000
Second	8,000 and 22,000	8,000 and 22,000
Third	8,000, 26,000, and 42,000	8,000, 26,000, and 42,000

The first balancing speed is lower for the worst baseline case due to increased initial rotor imbalance.

4.5 Balancing

The objective of this study is the evaluation of the effectiveness of multiplane, multispeed balancing in reducing the response amplitude of the T700 gas generator to acceptable operating levels. The approach allows rapid execution of the balancing operation. The balancing portion of the computer program receives its input from the amplitude calculated for the unbalanced rotor. The analytical process of calculating such rotor responses simulates the actual experimental operation, which is performed during balancing of a real rotor.

The standard baseline model was studied first. Since the first and second criticals are rigid body modes, two planes were used to balance at 7000 rpm. After correction weights are applied, the rotor cannot exceed 22,000 rpm due to excessive vibration, as shown in Figure 23. Notice that the amplitude became worse than the baseline response when the rotor reached the first bending critical around 22,000 rpm. This indicated that a rigid-body two-plane balancing cannot balance the rotor adequately. A three-plane balance was performed at 8,000 and 22,000 rpm. With this, the rotor can run to 45,000 rpm without excessive vibration after the second balancing run. Rotor response at station 1 is plotted in Figure 23. The deflected rotor shape near the bending critical (26,000 rpm), both before and after influence-coefficient-based, flexible rotor balancing, is shown in Figure 24. A similar plot is also included near the operating speed (45,000 rpm), as shown in Figure 25. Notice that the amplitude at the two bearing locations at both speeds is well below the clearance of the fluid-film damper. The dampers are operated at an eccentricity ratio of 0.5 or less. The bearing forces before and after balancing are also included, as shown in Figure 26.

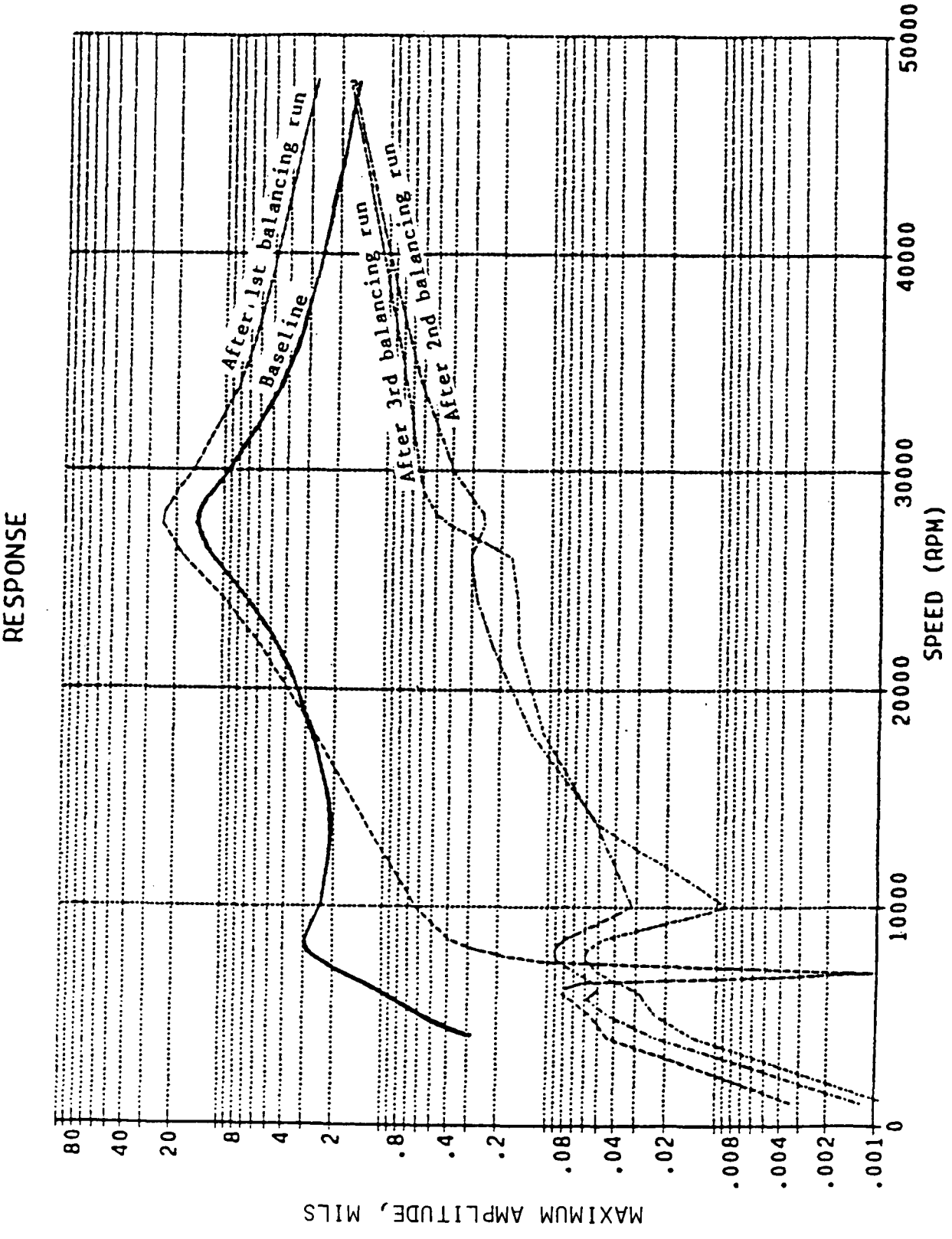

Figure 23 Calculated Maximum Amplitude at Station 1 with Initially Unbalanced Rotor and after Three Successive Balancing Runs (with Standard Imbalance)

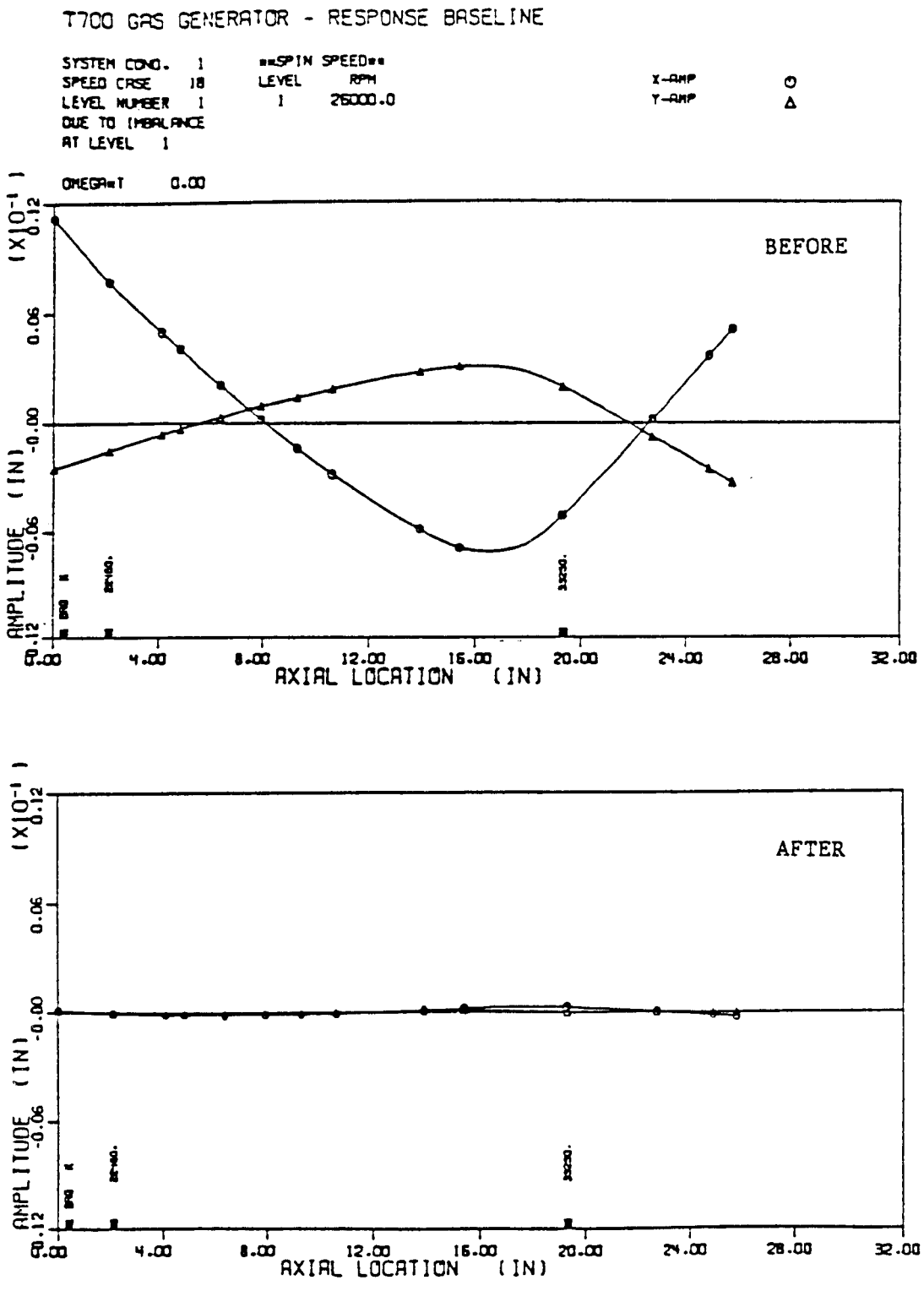

Figure 24 Deflected Rotor Shape at 26,000 rpm (before and after Balancing)

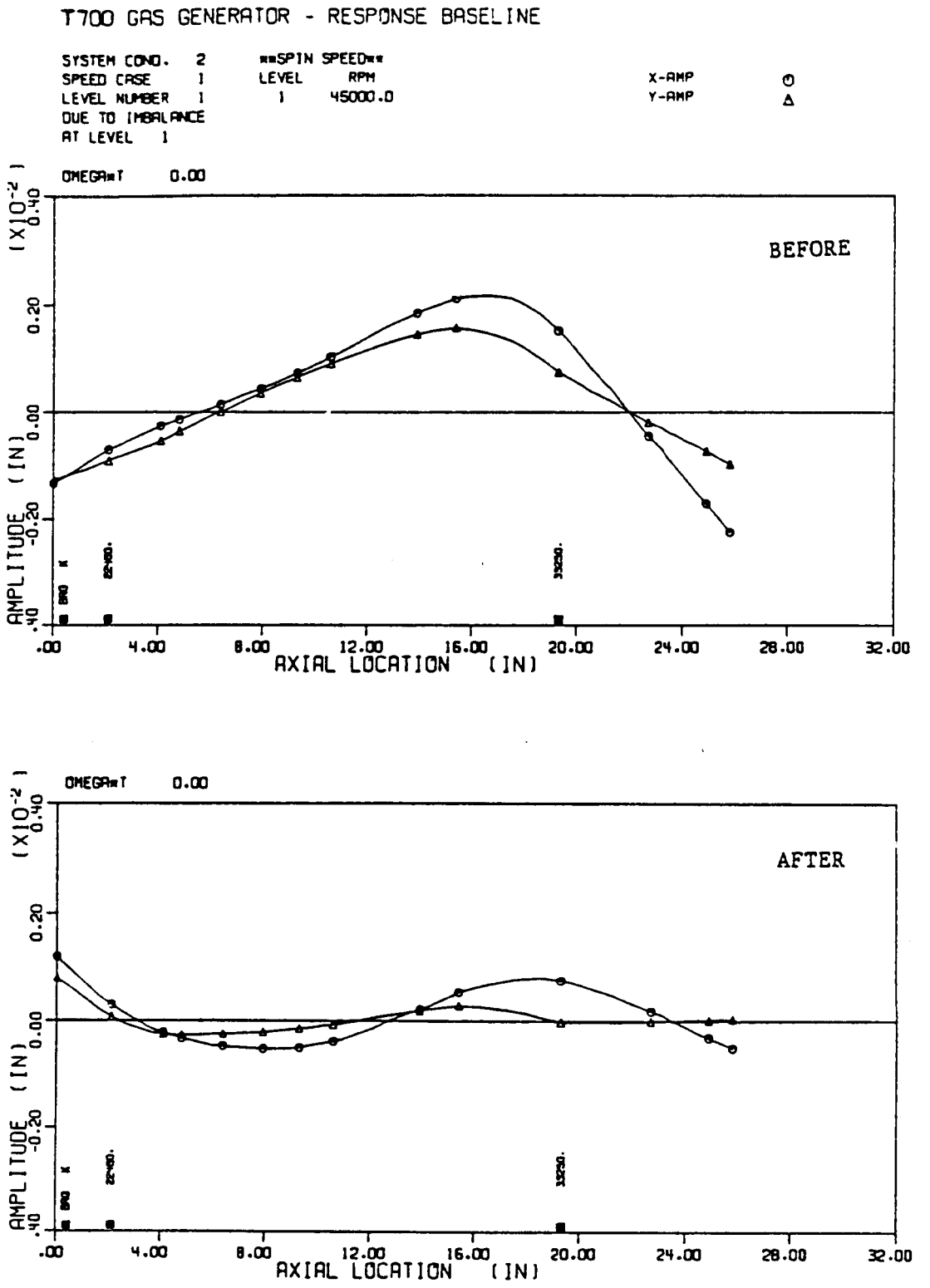

Figure 25 Deflected Rotor Shape at 45,000 rpm (before and after Balancing)

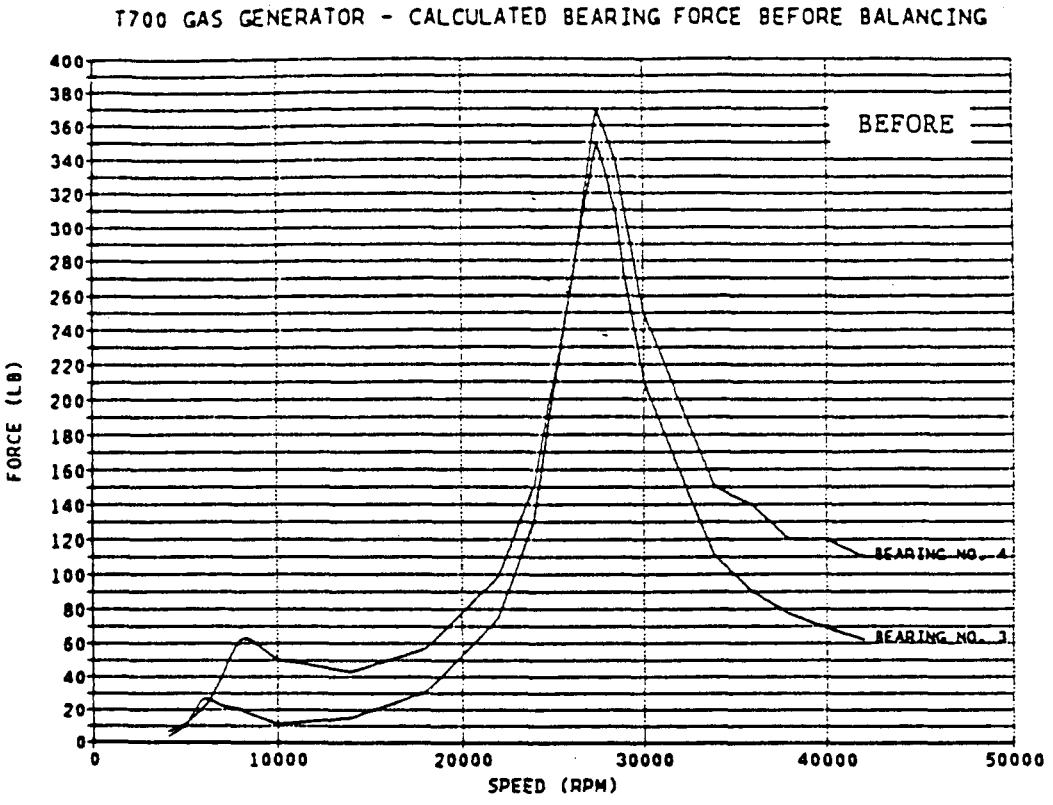

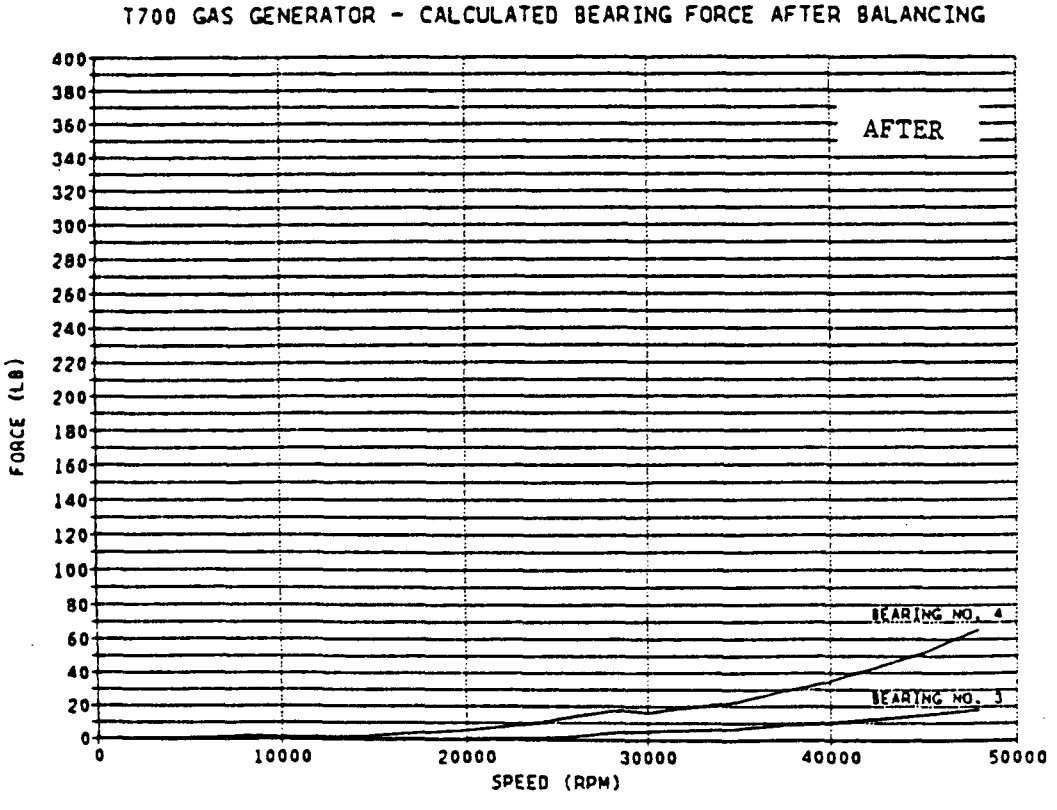

Figure 26 Bearing Forces before and after Balancing

The entire rotor was further balanced using all three planes at 8,000, 26,000, and 42,000 rpm. The same influence coefficient balancing technique was also used to reduce the amplitude at operating speed. The improvement, as shown in Figure 23, is not significant.

Similar to the procedures taken for the standard case, the worst baseline model is first balanced with the two end planes at 6000 rpm. The rotor is then further balanced with all three planes at 8,000 and 22,000 rpm. Third-step balancing was performed, but did not improve the overall performance significantly. The rotor amplitude at station 1 is plotted in Figure 27 to show the rotor response before and after each balancing run. Again, the response after the second balancing run is acceptable and the improvement after the third step is not significant.

4.6 Conclusions

The analytical balancing study has been conducted for the T700 gas generator. It was shown that multispeed, multiplane dynamic balancing techniques are effective in reducing the vibration level of the rotor. It is concluded that the rotor assembly, as presently manufactured, can be effectively high-speed balanced for low vibration throughout the entire speed range without low-speed component balancing, and that balancing at running speed results in minimal improvement in vibration levels.

Rigid body balancing increases amplitude at flexible criticals, which results in increased vibration in the gas generator operating speed range especially at the low end (30,000 rpm).

The analytical balancing procedure performed so far can qualitatively provide a general trend of the dynamic behavior of the rotor. A laboratory test is essential to confirm the results of this process.

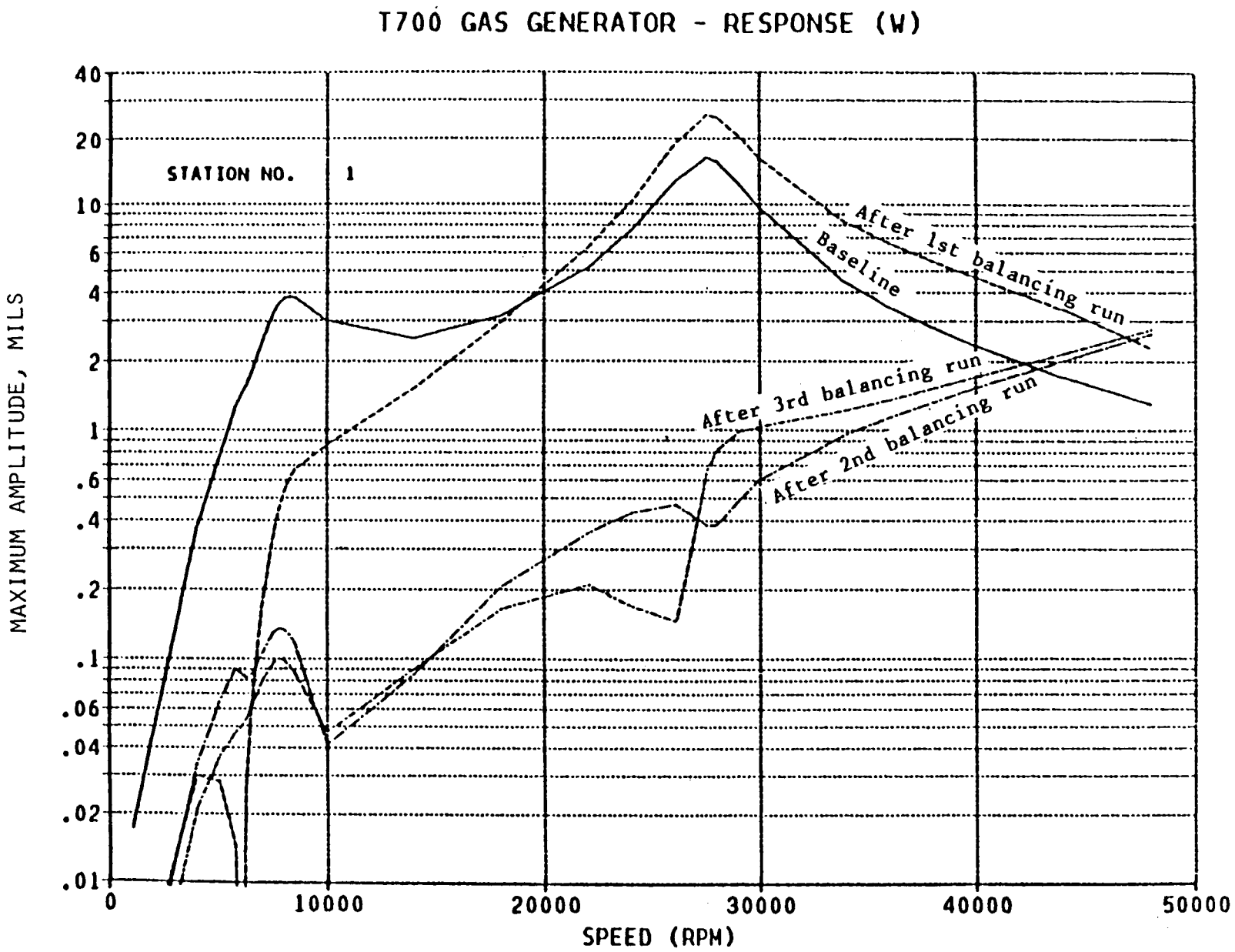

Figure 27 Calculated Maximum Amplitude with Initially Unbalanced Rotor and after Three Successive Balancing Runs (with Worst Imbalance)

5.0 ENGINE TEST CELL DATA

Current Army overhaul procedures require that engines undergo an acceptance test, during which critical performance and operating parameters are determined. Engines that experience vibrations that exceed allowable limits are returned to the rework area for corrective repairs. Currently, only minimal data are available to direct engine rework and interpretation of that data is subjective and dependent on the test cell operator's experience. These limitations, coupled with the requirement for rapid turnaround of overhauled engines, create a need for a capability that:

- Reduces time and cost of engine acceptance testing
- Provides direction for engine troubleshooting and location of engine vibration problems
- Increases availability of engines for flight operation.

Presently, only the overall vibration signal is available to CCAD personnel to diagnose a vibration problem. MTI's analysis was based on conversion of time data (overall vibration) to the frequency domain permitting determination of the discrete frequency and random frequency content of a complex vibration wave. This provides valuable information regarding the source and cause of vibration.

Under a past Army/NASA contract (NAS-20609), a portable real-time analyzer was used to perform FFT analysis of engine test cell data at CCAD for T53 and T55 engines. Samples of these frequency plots, highlighting some of the significant amplitudes, are shown in Figures 28 and 29. Similar plots for over twenty T53 and twenty T55 engines were obtained under NAS3-20609 and were available for further analysis under this program. Under Task 4, the T55 and T53 data were reviewed and used to develop criteria that can be used for identifying the cause of vibration problems during engine tests. T700 engine vibration data were tape recorded by CCAD personnel during this effort and provided to MTI for analysis and evaluation in developing diagnostic guidelines for CCAD personnel.

5.1 T700 Engine Data Review

Under Task 3 of the program, six different T700 engines underwent acceptance testing at CCAD and were monitored to obtain vibration frequency spectra. Analysis of the T700 engine test cell data provided an important indication of the relative significance of the power turbine and gas generator in terms of overall engine vibration levels. Tables 9 through 14 present a summary of all significant peaks observed for T700 engines for the maximum continuous power (MCP) and the intermediate rated power (IRP) test points. In each of these tables, the vibration data for each of the primary engine frequencies are presented in millivolts rms (mV_r). The data are for primary engine components such as the power turbine (N_p), gas generator (N_G), and accessory gearbox (AG). For the six engines, a total of 11 different sets of engine data were acquired. As seen in Tables 9 through 14, several of the engines had more than one power turbine module installed. The additional power turbine modules were installed and tested to provide spare/replacement power turbine modules and were not installed due to engine rejection.

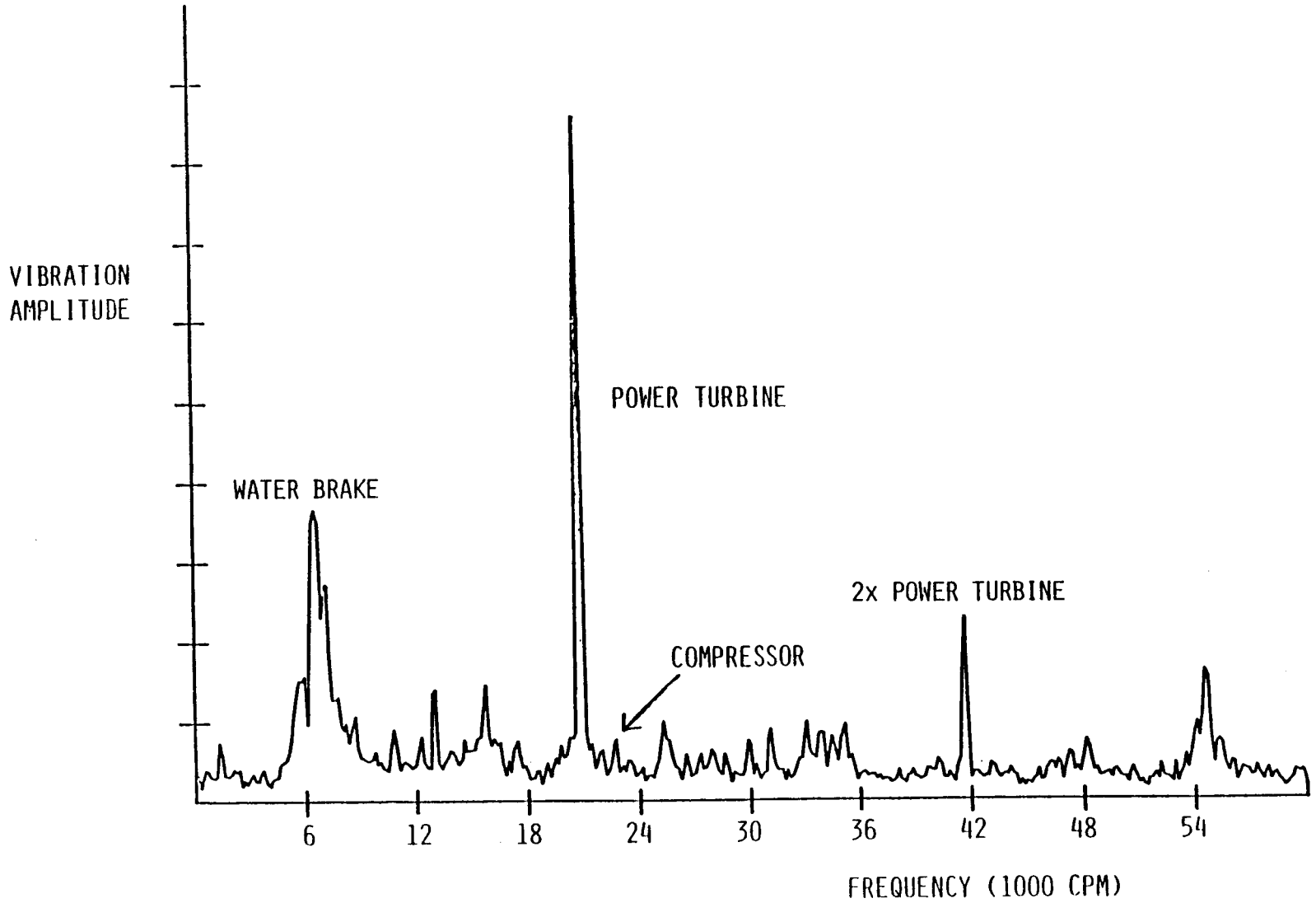

Figure 28 T53 Engine Test Frequency Plot

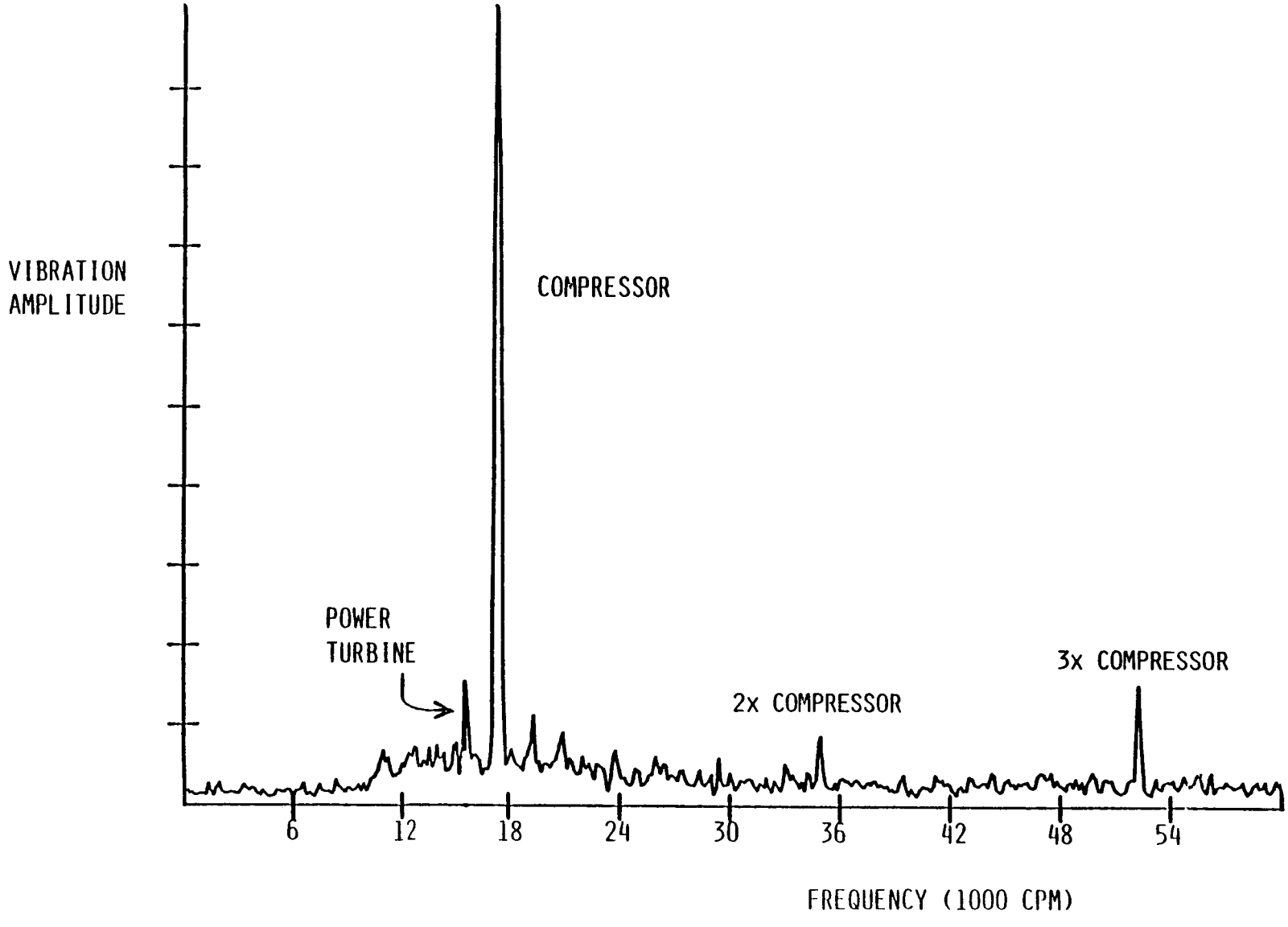

Figure 29 T55 Engine Test Frequency Plot

TABLE 9

T700 ENGINE TEST CELL DATA
Sensor 1, MCP Test Point

Engine Serial #	CCAD Overall Data	N_p	N_G	AG (mV)	2Np	$2N_G$	2AG	Additional Peak Frequencies & Amplitudes (Frequency - Amplitudes in mV)
207693(1)•		1.7	1.8	4.0				33.9 - 5, 34.8 - 3.3, 35.4 - 3.3, 32.7 - 2.5, 36 - 2.5, 84 - 1.9
207693(2)		1.7		2.3			1.8	34.5 - 3.2, 35.7 - 2.9, 33 - 2.5, 36.6 - 2.5, 96.3 - 1.6, 29.4 - 1.5, 75.3 - 1.4
207693(3)		2.4	1.5	1.7			2.1	76.5 - 2, 71.4 - 1.9, 67.2 - 1.5, 62.7 - 1.3, 66 - 1.3, 34.8 - 1.2
207693(4)		3.4	1.7	1.6			2.5	70.8 - 2.7, 75.9 - 2.5, 67 - 1.8, 62.7 - 1.4, 69.6 - 1.3, 61.5 - 1.3
306277(1)		1.0		2.8			8.5	37.8 - 4.6, 57 - 3.1, 54 - 2.1, 60.6 - 2.2, 53.4 - 1.7, 59.4 - 1.7, 58.2 - 1.6, 61.5 - 1.4
306277(2)		.7		3.0			8.3	38.1 - 5.2, 57.6 - 4.8, 59.7 - 2.2
306277(3)		1.0		3.2	1.2		9.1	37.8 - 5.5, 57.3 - 3.6, 61.2 - 2.4, 58.8 - 2.3, 60 - 1.9, 53.7 - 1.5
207971		1.1	1.8	2.3			3.5	37.8 - 2.2, 83.7 - 2.1, 69 - 2.0, 70.8 - 2.0, 66.9 - 1.7, 63 - 1.7, 5.4 - 1.65
307072	.3	1.8	7.8	2.9	1.1		2.8	23 - 1.3, 76.5 - 1.2, 41.7 - 1.1, 10.8 - 1.0, 31.8 - 1.0
306667	.4	4.3		2.2	1.3		6.1	38.1 - 11.4, 66.3 - 2.3, 10.8 - 1.5, 58.8 - 1.5, 41.7 - 1.3, 57.9 - 1.2
306148		3.7	2.2	3.7	2.6			38.4 - 7.75, 41.7 - 2.6, 52.5 - 2, 5.4 - 1.8, 63.6 - 1.4, 48.9 - 1.1, 10.8 - 1.1

*Numbers in parentheses indicate different power turbine module installed.

TABLE 10

T700 ENGINE TEST CELL DATA
Sensor 2, MCP Test Point

Engine Serial #	CCAD Overall Data	N_P	N_G	AG (mV)	$2N_P$	$2N_G$	2AG	Additional Peak Frequencies & Amplitudes (Frequency - Amplitude in mV)
207693(1)*		.4	1.9			4.3		48.3 - 2.1
207693(2)		1.0	4.5			.6		48 - 2.1, 31.5 - 1.2
207693(3)		2.0	2.2					48.3 - 1.3, 91.5 - 1.2, 62.7 - 1.1
207693(4)		3.7	2.3			1.4		41.7 - 1.1, 48 - 1.0, 63 - 9 (3NP), 37.8 - .8
306277(1)		1.5	1.4					30.6 - 1.1, 96 - .8
306277(2)		1.9	1.4		1.0			30.3 - .8
306277(3)		1.4	.7	1.1		2.1		63 (3xNP) - 2.9
207971		.3	6.3	.6				62.7 - 2.1, 48.3 - .9
307072	.3	5.9	5.3					39.9 - 1.8, 40.8 - 1.7, 41.7 - 1.2, 62.7 - 1.0, 37.8 - 9
306667	.3	.4	2.0					31.8 - 1.4, 38.1 - 1.0, 5.4 - .9, 30.9 - .9
306148		3.2	2.8	.7				41.7 - 2.1, 48.9 - 1.3, 5.4 - .8, 40.5 - .9

*Numbers in parentheses indicate different power turbine module installed.

TABLE 11

T700 ENGINE TEST CELL DATA
Sensor 3, MCP Test Point

Engine Serial #	CCAD Overall Data	N_p	N_G	AG (mV)	2Np	$2N_G$	2AG	Additional Peak Frequencies & Amplitudes (Frequency - Amplitude in mV)
207693(1)*		3.3	5.7	2.0	1.3	10.5		48.3 - 2.3, 53.7 - 1.4, 91.5 - 1.4, 41.7 - 1.3
207693(2)		2.8	8.3		1.0	6.2		90.6 - 1.6, 30.6 - 1.5, 31.5 - 1.4, 41.7 - 1.0
207693(3)		5.0	9.1			6.8		62.7 - 2.4, 81.3 - 1.7, 48.3 - 1.2, 28.8 - 1.1 70.8 - 1.1
207693(4)		6.3	6.5		1.3	4.9		63 - 2.1, 48 - 1.8, 37.8 - 1.7, 91.2 - 1.7, 65 - 1.5, 81 - 1.5, 42 - 1.3
306277(1)		1.7	1.4			4.4		31.5 - 1.6, 32.7 - 1.4, 48 - 1.2
306277(2)		2.8	4.1		2.2	5.4		41.7 - 2.2, 30.3 - 1.0
306277(3)		4.0	2.4	2.0	1.1	8.0		62.7 - 1.5, 96.3 - 1.3, 42 - 1.1, 48 - 1.1
207971		2.1	16.5			1.9		62.7 - 3.4, 37.5 - 1.7, 29.1 - 1.3, 80.4 - 1.2
307072	.3	7.4	3.9					39.9 - 6.7, 31.2 - 4.1, 37.8 - 1.8, 32 - 1.5, 42 - 1.5
306667	.3	1.6	7.8		2.5			31.5 - 2.5, 41.7 - 2.5, 39 - 2.0, 37.8 - 1.6 44.1 - 1.5, 35.1 - 1.4, 40.2 - 1.4
306148		7.1	6.5		6.6			31.2 - 2.4, 48.9 - 2.4, 30 - 1.9, 10.8 - 1.7, 32.7 - 1.7, 40.2 - 1.7

*Numbers in parentheses indicate different power turbine module installed.

TABLE 12

T700 ENGINE TEST CELL DATA
Sensor 1, IRP Test Point

Engine Serial #	CCAD Overall Data	N_P	N_G	AG (mV)	2Np	2NG	2AG	Additional Peak Frequencies & Amplitudes (Frequency - Amplitudes in mV)
207693(1)*		1.6	2.2	6.6			1.6	34.8 - 3.7, 33.6 - 3.4, 85.5 - 3, 35.7 2.6
207693(2)		1.6	1.6	4.2			1.4	34.5 - 3.4, 35.1 - 3.3, 33.9 - 2.9, 84.9 - 2.81, 33 - 2.5
207693(3)		2.3	1.1	3.3			2.6	67.5 - 1.9, 72.9 - 1.8, 78 - 1.5, 63.3 1.5, 69 - 1.5, 38 - .8
207693(4)		3.8	1.8	2.7			3.4	72 - 2.4, 62.7 - 1.8, 77.1 - 1.7, 70.2 1.5
306277(1)		.8	1.5	1.4			13.4	58.2 - 4.1, 38.4 - 3.5, 59.4 - 2.4, 62.4 - 2.2, 55.5 - 2.0
306277(2)		.8	2.3	2.0			11.5	58.5 - 4.9, 38.7 - 3.8, 59.7 - 1.8, 60.6 - 1.8, 55.5 - 1.7, 62.7 - 1.6
306277(3)		1.3	1.6	2.2			12.2	38.7 - 4.5, 58.5 - 4.2, 55.8 - 2.1, 62. - 2.1, 59.7 - 2.0
207555	.3	7.2	7.9	6.2	3.		5.8	38.8 - 7.9, 58.6 - 3.2, 41.7 - 3, 48.1 - 2.7, 45 - 2.5, 45.6 - 2.4
207971		1.0	.9	3.4			4.2	63 - 2.2, 68.4 - 2.2, 85.5 - 1.9, 72.3 - 1.8, 38.7 - 1.8, 64.8 - 1.8, 64.2 - 1.7, 5.4 - 1.5
307072	.3	3.8	7.2	3.3			3.4	39 - 2.4, 22.5 - 1.7, 49.2 - 1.3
306667	.4	3.9	1.3	2.6	1.2		5.7	38.7 - 10.3, 67.5 - 2., 37.5 - 1.8, 35.1 - 1.8, 49.2 - 1.8, 41.7 - 1.7, 10.8 - 1.5
306148		4.2	2.	4.	2.9		1.9	39 - 7.7, 42 - 2.9, 5.4 - 1.6, 53.4 - 1.6, 22.8 - 1.5, 50.1 - 1.5

*Numbers in parentheses indicate different power turbine module installed.

TABLE 13

T700 ENGINE TEST CELL DATA
Sensor 2, IRP Test Point

Engine Serial #	CCAD Overall Data	N_P	N_G	AG (mV)	2Np	$2N_G$	2AG	Additional Peak Frequencies & Amplitudes (Frequency - Amplitude in mV)
207693(1)*		.7	2.5	.8	.9	5.0		
207693(2)		1.5	5.8			1.1		48.9 - 1.6, 31.2 - 1.4
207693(3)		2.1	6.0			1.7		83.1 - 1.6
207693(4)		3.5	3.3					48.9 - 1.3
306277(1)		1.0	1.2			1.3		
306277(2)		1.5	1.3	.8		.8		
306277(3)		1.2	1.2			2.8		62.7 - 1.4, 63.3 - 1.3
207555	.3	5.6	5.3	4.2				38.5 - 4.4, 29.4 - 4.0, 30 - 2.9, 28.9 - 2.8, 28.2 - 2.6, .6 - 2.5, 5.7 - 2.5
207971		.2	5.2			.6		63 - 2.4, 38.4 - 1.6
307072	.3	4.8	4.1	.8				40.2 - 2.7, 39.3 - 2.1, 49.5 - 1.5
306667	.3	.6	2.2					39 - 1.3, 31.8 - 1.1
306148		3.1	1.3	1.0				49.5 - 1.9, 62.7 - 1.4

*Numbers in parentheses indicate different power turbine module installed.

TABLE 14

T700 ENGINE TEST CELL DATA
Sensor 3, IRP Test Point

Engine Serial #	CCAD Overall Data	N_p	N_G	AG (mV)	2Np	$2N_G$	2AG	Additional Peak Frequencies & Amplitudes (Frequency - Amplitude in mV)
207693(1)*		2.2	7.2		1.7	14.0	1.7	82.5 - 3.3
207693(2)		2.9	9.8		1.1	6.1		81.9 - 1.7
207693(3)		4.6	9.6			5.4		83.1 - 2.6, 63 - 2.5, 93.6 - 1.4
207693(4)		5.7	10.0			6.7		62.7 - 3.8, 48.9 - 2.2, 82.2 - 1.9, 64.5- 1.8, 38.4 - 1.7, 41.7 - 1.7, 69.9 - 1.7
306277(1)		.6	2.2			4.4		33.9 - 1.7, 32.7 - 1.7
306277(2)		2.6	4.3			2.1		
306277(3)		3.0	2.6	2.7		10.2		62.7 - 3.2, 38.4 - 1.5, 85.2 - 1.5
207555	.2	11.7	8.6	5.5				38.5 - 5.6, 38.1 - 3.8, 29.6 - 3.5, 28 - 3.0 29.1 - 2.9, 39.6 - 2.7, 14.4 - 2.2
207971		2.1	13.0			1.6		38.4 - 4.5, 62.4 - 3.7, 32.7 - 1.6, 49.2 - 1.6, 29.1 - 1.5
307072	.3	6.3	13.3		1.6	.2		40.2 - 4.4, 31.5 - 4.1, 38.4 - 3.1, 39.3 - 3.1, 42.9 - 2.1, 36.9 - 1.92
306667	.3	1.6	7.6			.1		39 - 2.94, 10.8 - 2.1, 41.7 - 2, 31.8 - 17, 39.6 - 1.6, 40.5 -1.4
306148		7.6	11.6			.2		42 - 2.7, 30 - 2.7, 30.9 - 2, 33.3 - 1.9, 38.4 - 1.8, 11.1 - 1.5

*Numbers in parentheses indicate different power turbine module installed.

Figures 30 through 32 are representative frequency domain, fast Fourier transform (FFT) plots acquired from the taped engine test cell data. These figures incorporate the FFT plot for each of the three vibration sensors located on the engine along with a list of the highest 10 vibration frequencies and their amplitudes in millivolts. The data presented in Figures 30 through 32 were taken with the T700 engine operating at intermediate rated power (IRP). At this test point, the power turbine, gas producer, and accessory gearbox operate at 20,700, 43,800, and 28,600 rpm, respectively. The significance of these particular figures is that the same gas producer was used for all three tests with different power turbines. On the third test (Figure 32), a rub was experienced on deceleration. The test cell operators reported that the overall vibration levels for this engine were well within acceptance limits and that they believed the rub to be in the power turbine. On disassembly, it was found that the gas producer, instead, had rubbed. A review of Figures 30 through 32 shows a high 2/rev vibration component for both the accessory gearbox and the gas producer. Specifically, the 2/rev of the gas producer is the dominant frequency on sensor number 3 for two of the three engine tests with a significant increase in amplitude being observed on test 3 (a value of 10.21 mV_r was measured). On the other hand, the 2/rev of the accessory gearbox (2 AG) was the dominant frequency measured on sensor 1 for each of the three test runs. Since sensor 1 is located on the accessory gearbox, the sensitivity to accessory gearbox vibrations was expected. A review of data for all engines showed that the 2-AG amplitudes measured on sensor 1 at IRP were significantly higher than the average measured value of 5.6 mV_r. This can be seen in Tables 12, 13, and 14.

The results of the overall data review indicated that sensor 1 is predominantly useful for monitoring accessory gearbox-related vibrations, while sensor 3 is best suited to monitoring and diagnosing gas producer and power turbine vibrations. Sensor 2 appears to present the same information as does sensor 3, only with a lower sensitivity. Consequently, it is expected that the largest portion of the T700 engine diagnostics could be performed with sensors 1 and 3. Once the data review was complete, the information was incorporated into the diagnostic manual presented as Appendix A.

5.2 T55 Engine Data

Previously recorded T55 engine test data were reviewed in a manner similar to that used for the T700. FFT plots of twenty T55 engines were reviewed and the dominant frequencies were identified at two engine test conditions, as shown in Tables 15 through 20. Figure 33 presents two representative FFT spectrum plots that, when reviewed in conjunction with Tables 15 through 20, show that the dominant frequencies observed for the T55 engine are at the power turbine (N_p) and gas generator (N_G) frequencies or multiples thereof. As seen in Figure 33 and confirmed in the data of Tables 15 through 20, the major sources of vibration for the T55 engines are related to the gas producer and power turbine 1/rev (imbalance-induced) vibrations. In addition, both 2 and 3/rev components of vibrations are frequently observed, which is indicative of misalignment and/or mechanical looseness. After being reviewed, the T55 data was incorporated into the diagnostic manual presented as Appendix A.

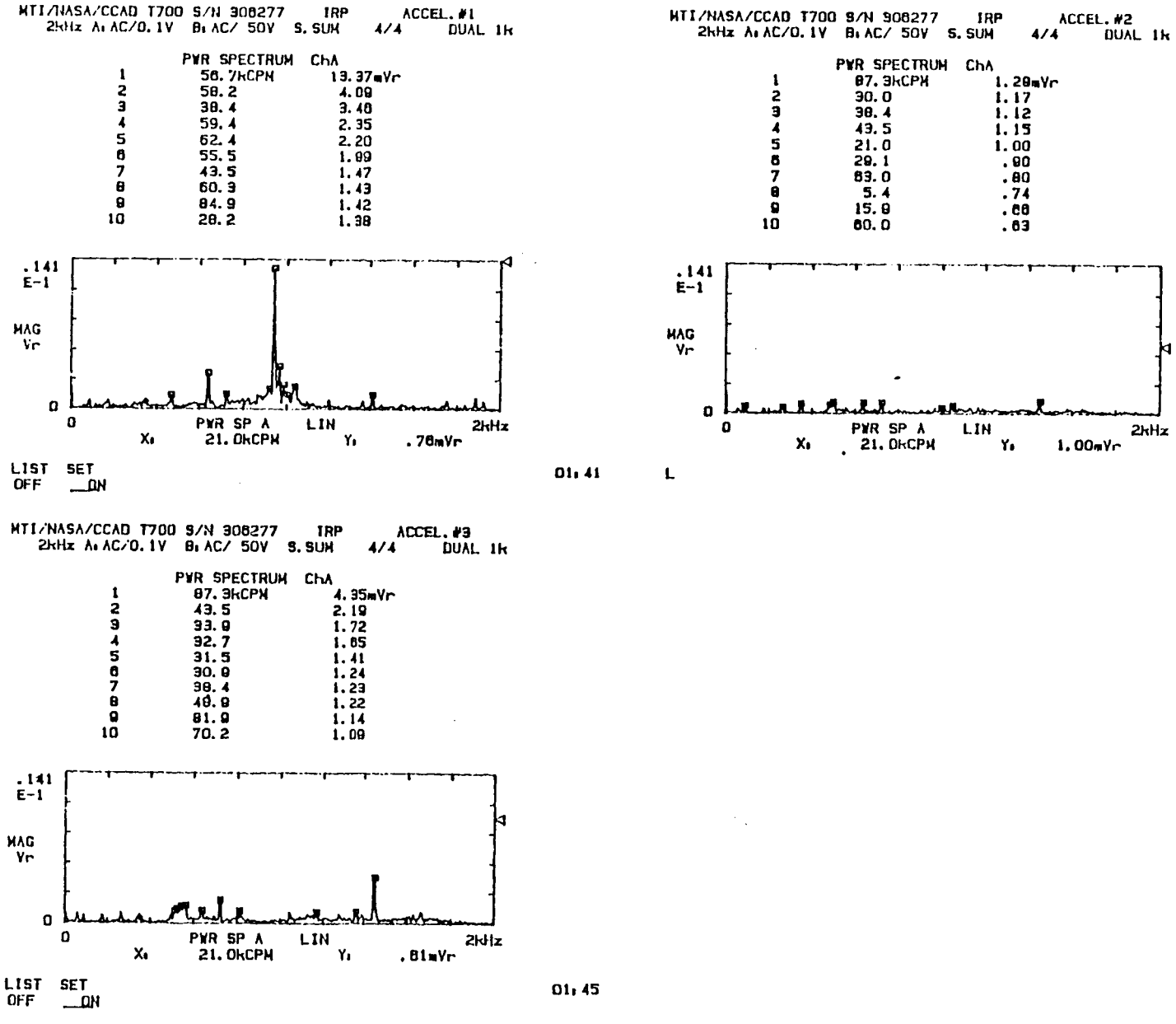

Figure 30 T700 Engine Serial No. 306277 Spectrum Plot at Intermediate Rated Power (IRP)

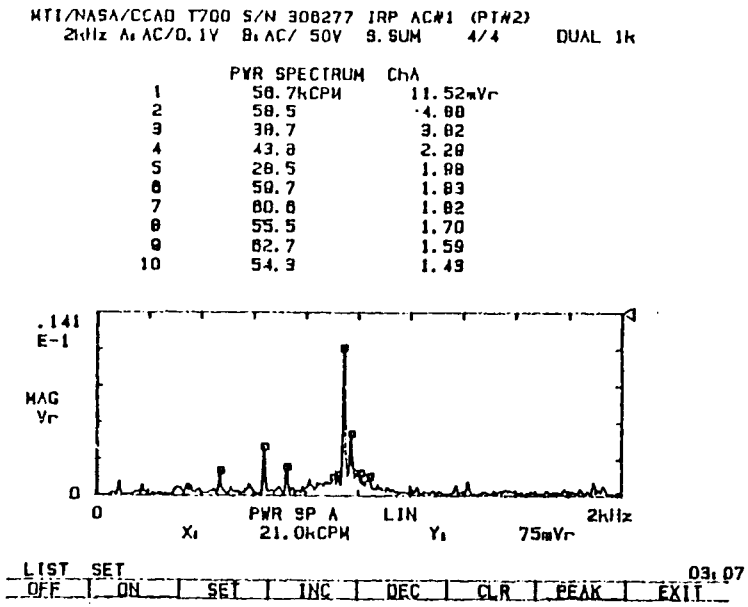

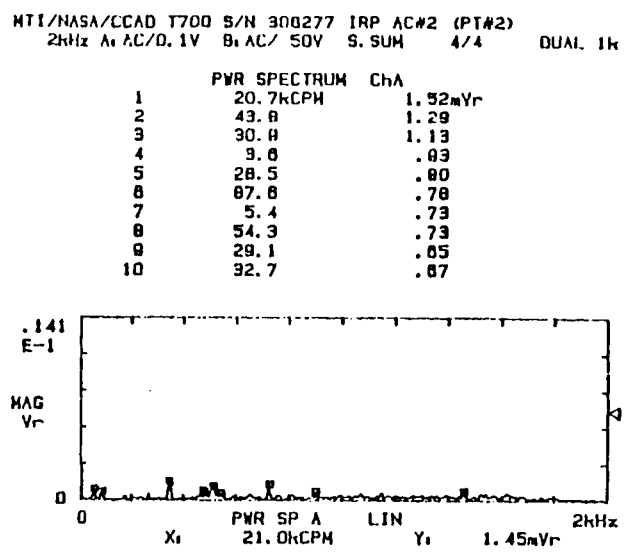

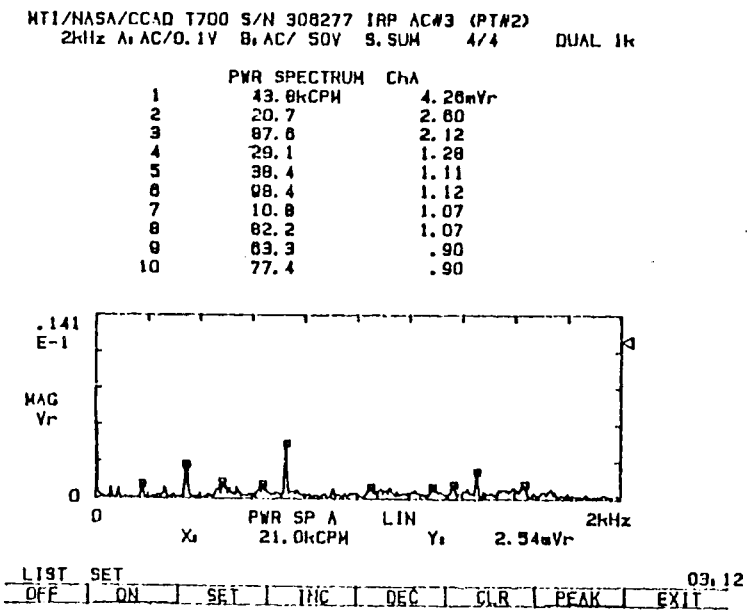

Figure 31 T700 Engine Serial No. 306277 (Power Turbine No. 2) Spectrum Plot at IRP

MTI/NASA/CCAD T700 S/N 906277 IRP AC#1 (PT#3)
2kHz A: AC/0.1V B: AC/ 50V S. SUM 4/4 DUAL 1k

	PWR SPECTRUM	ChA
1	57.0kCPM	12.18mVr
2	38.7	4.57
3	58.5	4.21
4	28.5	2.17
5	55.8	2.07
6	62.7	2.07
7	59.7	1.98
8	43.8	1.55
9	54.6	1.31
10	21.0	1.28

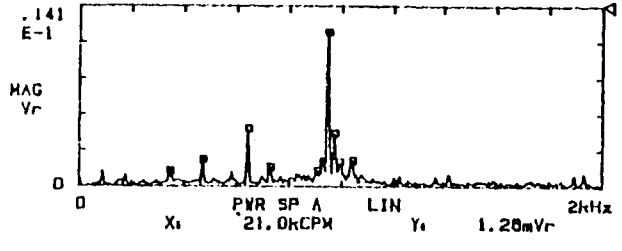

L

MTI/NASA/CCAD T700 S/N 306277 IRP AC#2 (PT#3)
2kHz A: AC/0.1V B: AC/ 50V S. SUM 4/4 DUAL 1k

	PWR SPECTRUM	ChA
1	87.6kCPM	2.81mVr
2	62.7	1.39
3	83.3	1.29
4	21.0	1.21
5	43.8	1.19
6	38.4	1.08
7	83.0	.98
8	5.4	.73
9	41.7	.74
10	29.4	.83

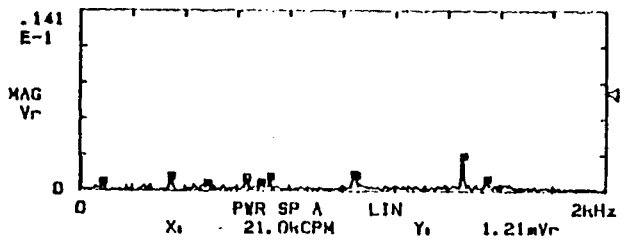

MTI/NASA/CCAD T700 S/N 306277 IRP AC#3 (PT#3)
2kHz A: AC/0.1V B: AC/ 50V S. SUM 4/4 DUAL 1k

	PWR SPECTRUM	ChA
1	87.6kCPM	10.21mVr
2	62.7	3.16
3	21.0	2.87
4	28.5	2.70
5	43.8	2.57
6	38.4	1.53
7	85.2	1.50
8	10.8	1.27
9	82.2	1.23
10	84.3	1.05

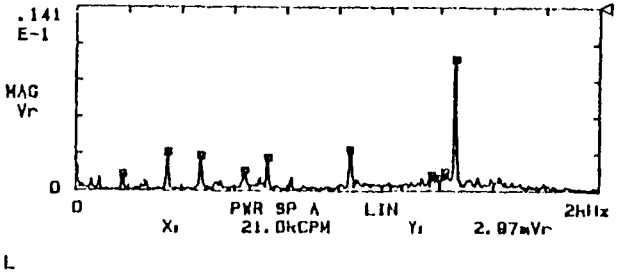

L

Figure 32 T700 Engine Serial No. 306277 (Power Turbine No. 3)
Power Spectrum at IRP

TABLE 15

T55 ENGINE DATA
94%/94% TEST POINT, SENSOR 1*

Power Turbine Serial No.	Np	N_G	$2N_G$ (millivolts)	2Np	40 krpm	$3N_G$	Other (Frequency → Amplitude)
M265499	18.5	23	10.5	7.5	5	5	3Np→5 mV
95250	18.7	22	4	5	16	20	
U00316	6.2	33	4	3	5	5	41K→13
265539	32.2	18	22	4	5	3	$2N_G$+Np→11
U00589	26.0	23	5	13	10	--	2Np+N_G→8
265604	32.9	68	7	17	8	--	Np+N_G→7, 2Np+N_G→7
268922	11.2	77	2	13	2	7	3Np→6
268541	5.2	30	13	9	8	--	41→12
265566	32.4	29	6	11	10	4	Np+N_G→8,
U00295	14.2	55	4	9	9	--	3Np→10
U00433	9.5	23	8	4	21	15	
265549	--	--	--	--	--	--	
M265682	2.5	18	--	--	--	--	
M261845	Peaks at 10,800, 14,400, 18,000 ... Every 60 Hz						
254954	6.5	52	5	7	11	9	3Np→12
U00259	22.5	21.5	9	7	18	8	3Np→7.5
265530	21.3	25	11	6	4	6	
261830	24.9	24	7	3	9	2	
268934	24.9	23	7	8	11	6	3Np→8, 41→13
U00212	24.1	41	18	6.5	3	26	

*Test points at % of maximum rated speed for power turbine/gas generator

TABLE 16

T55 ENGINE DATA
94%/94% TEST POINT, SENSOR 2*

Power Turbine Serial No.	Np	N_G	$2N_G$ (millivolts)	2Np	40 krpm	$3N_G$	Other (Frequency → Amplitude)
M265499	--	--	--	--	--	--	
95250	15.3	67	14	6	7	18	$3N_G$→18 mV
U00316	21.2	64	10	10	10	--	
265539	20.8	74	11	7	7	--	
U00589	54.6	55	5	10	9.5	7.5	
265604	40.5	36	13	9	3	4	N_p+N_G→15, $3N_p$→15 $2N_G+N_p$→21
268922	60.3	57.5	10	6	4	--	
268541	16.7	82	17	3	5	6	$2N_G+N_p$→6
265566	30.2	30	18	9	8	--	
U00295	11.2	48	12	7	6	--	11.6→20
U004333	20.8	87	7	6	5	7	
265549	29.4	57	7	5	5	--	$2N_G+N_p$→11
M265682	--	--	--	--	--	--	
M261845	26.1	41	--	--	--	--	
254954	16.1	32	11	7	12	--	
U00259	10.1	62	8	6	18	7	
265530	5.2	100	6	3	5.5	18	
261830	20.5	79	9	4	4	5	
268934	15.9	39	9	8	8	--	
U00212	2.2	100	4	3	3	33	

*Test points at % of maximum rated speed for power turbine/gas generator

TABLE 17

T55 ENGINE DATA
94%/94% TEST POINT, SENSOR 4*

Power Turbine Serial No.	Np	N_G	$2N_G$ (millivolts)	2Np	40 krpm	$3N_G$	Other (Frequency → Amplitude)
M265499	39	38	4	8	4	8	44.8K→10 mV
95250	27.3	86	11	3	--	22.5	$2N_G+Np$→25
U00316	32.9	65	9	6	10	--	$2N_G-Np$→22, 41K→19
265539	41.9	57	18	11	4	10	$3N_G$→10
U00589	--	--	--	--	--	--	
265604	93.2	53	2	10	3	--	11.2→21, $2N_G+Np$→22, $2Np+N_G$→16
268922	44.9	37	10	4	4	--	
268541	28.5	96	5	5	3	5	41→7, $2N_G+Np$→10
265566	69.8	64	13	4	5	--	$2N_G+Np$→12, $2Np+N_G$→11
U00295	74.2	58	3	9	2	9	$2Np+N_G$→16, $2N_G+Np$→13
U004333	24	19	3	4	5	--	
265549	25.2	87	6	3	7	10	
M265682	13.3	94	--	--	--	--	
M261845	25.6	30	--	--	--	--	
254954	29.4	94	17	3	3	7	$2N_g+Np$→11
U00259	6.0	70	7	9	--	16	$3N_G$→16
265530	13.5	100	7	3	--	20	$3N_G$→20
261830	73.7	37.5	--	--	--	--	
268934	72.2	39	16	4	6	14	$Np+N_G$→11, $2N_G+Np$→13
U00212	9.0	71	3	3	--	16	

*Test points at % of maximum rated speed for power turbine/gas generator

TABLE 18

T55 ENGINE DATA
93%/100% TEST POINT, SENSOR 1*

Power Turbine Serial No.	Np	N_G	$2N_G$ (millivolts)	2Np	40 krpm	$3N_G$	Other (Frequency → Amplitude)
M265499	35.1	21	10	12	4	4	$3N_P$→7 mV
95250	25	22	3	13	18	23	
U00316	9.2	35	4	2	8	--	
265539	45.0	21	26	9	9	--	
U00589	51.2	18	6	15	5	--	
265604	50	10	11	5	23	--	48.6K→24
268922	7	77	4	25	5	8	$3N_P$→13, $3N_G$→8
268541	7	26	10	2	13	12	$3N_G$→12
265566	40.7	30	8	7	11	--	
U00295	12.5	42	--	14	10	--	
U004333	14.8	22	8	10	20	16	
265549	--	--	--	--	--	--	
M265682	12.7	71	--	--	--	--	
M261845	4.3	3	--	--	--	--	10.8→33, 14.4→26, 18→43**
254954	15.5	49	5	10	14	8	
U00259	40.5	22	7	10.5	13	11	
265530	27.4	22	11	3	4	7	$3N_P$→9
261830	24.1	20	6	5.5	9	--	$2N_G+N_P$→8
268934	15	26	6	10	6	--	50.4K→9
U00212	21	46	20	5	2	28	$3N_G$→28

*Test points at % maximum rated speed for power turbine/gas generator
**10.8K cpm followed by decreasing amplitude peaks every 3600 cpm.

TABLE 19

T55 ENGINE DATA
93%/100% TEST POINT, SENSOR 2*

Power Turbine Serial No.	Np	N_G	$2N_G$ (millivolts)	2Np	40 krpm	$3N_G$	Other (Frequency → Amplitude)
M265499	44.6	35	3	3	5	--	
95250	39.5	66	14	4	--	13	
U00316	16.2	61	9	7	10	--	
265539	16.7	82	13	13	--	--	
U00589	60	51	7	8	9.5	--	
265604	79.5	40	4	12	6	--	
268922	56.6	45	4	9	3	--	
268541	14.7	83	17	3	5	7	
265566	47.3	22	16	11	8	5	3Np→7 mV
U00295	8	29.5	10	8	8	--	
U004333	27.2	92	5	3	3	12	
265549	44.9	58	5	5	5	5	$2N_G$+Np→7.5
M265682	12.7	71	--	--	--	--	
M261845	34.9	45	--	--	--	--	
254954	14.8	26	12	10	10	--	
U00259	11.2	65	7	4	15	--	
265530	17.3	102	4	3	--	13	
261830	11.5	61	9	8.5	5	--	
268934	12	37	12	7	10	--	
U00212	3.2	105	2	3.5	3	32	

*Test points at % maximum rated speed for power turbine/gas generator

TABLE 20

T55 ENGINE DATA
93%/100% TEST POINT, SENSOR 4*

Power Turbine Serial No.	Np	N_G	$2N_G$ (millivolts)	2Np	40 krpm	$3N_G$	Other (Frequency → Amplitude)
M265499	43	33	6	5	3	--	
95250	39.5	69	9	4	3.5	32	$2N_G+Np \rightarrow 21$ mV
U00316	21	55	11.5	7	10.5	6.5	
265539	60	58	22	3	3	7	$Np+N_G \rightarrow 18$
U00589	70	37	6	13	3	3	$Np+N_G \rightarrow 11$
265604	100	10	3	9	4	--	$3Np \rightarrow 29$
268922	51	39	7	8	3.5	5	
268541	61.5	77	9	4	3	7.5	
265566	95	46	5	11	3	6	$2Np+N_G \rightarrow 19$
U00295	89	26.5	7	6.5	4	3	
U004333	13	26	2	4	3	2	$3Np \rightarrow 4$
265549	36	70.5	5	4	8	4	
M265682	11.5	94	--	--	--	--	
M261845	45	52	--	--	--	--	
M254954	92	51	9	3.5	3	12	$2Np+N_G \rightarrow 14$, $2N_G+Np \rightarrow 15$
U00259	11	72	5	5	3	23	$22.5K \rightarrow 16$
265530	17	100	9	2	2	15	
261830	105	10	2	4	4	--	$3Np \rightarrow 25$
268934	95	27	13	10	6	8	$Np+N_G \rightarrow 12$, $2N_G+Np \rightarrow 17$
U00212	5	75	4.5	2	2	10	$3N_G \rightarrow 10$

*Test points at % of maximum rated speed for poer turbine/gas generator

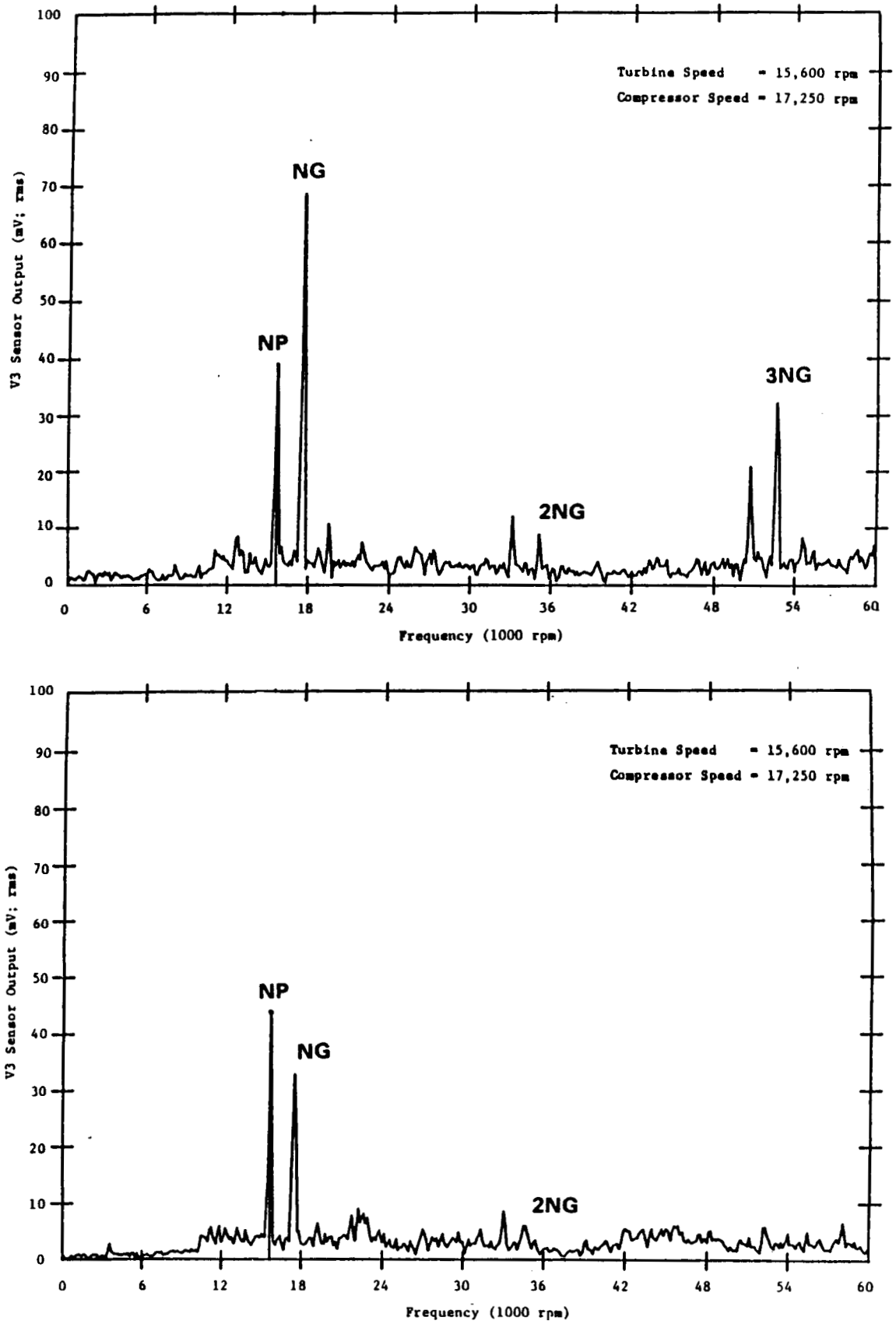

Figure 33 T55 Engine Vibration Spectrum Plots

5.3 T53 Engine Data

Previously recorded T53 engine test data were reviewed in a manner similar to that used for both the T700 and the T55 engines. FFT plots for twenty T53 engines were reviewed and the dominant frequencies were identified at one engine test condition, as shown in Tables 21 through 23. Figure 34 presents two representative FFT spectrum plots, which, when reviewed in conjunction with Tables 21 through 23, show that the dominant frequencies observed in the T53 engine are the power turbine and gas producer 1 and 2/rev components, which are indicative of rotor imbalance and misalignment or mechanical looseness. In addition, the water brake frequency at 6380 rpm was also commonly observed. As can be seen in Figure 34, the vibrations associated with the water brake (WB) can be quite large and may, therefore, cause engines to be rejected for high vibrations when not required. The reviewed T53 data were incorporated into the diagnostics manual presented as Appendix A.

TABLE 21

T53 ENGINE DATA
95%/97% TEST POINT, SENSOR 1*

Power Turbine Serial No.	Np	N_G (millivolts)	2Np	$2N_G$	Other (Frequency → Amplitude)
82C011	--	--	--	--	
4871	--	--	--	--	
LE21788	22.4	22	12	7.5	6.3→47 mV (followed by decreasing peaks)
M289659	38.5	15	--	--	6.3→40
1541	39.5	16	17	7	6.3→32
82C012	12	11	5	4	6.3→37, 5 to 8K→47
82C004	40	12	7	8	peaks from 6.3→12.6K cpm 6.3→28, highest 7.8→34
80K03P	29.5	35	12.5	8	6.3→43, 11→38, 12→37, 12.6→24
U00278	16.7	24	4	2	13K→35, 7.2K→36, 10.8→34, 6.3→30
C9M11244	32.4	11	4	2	6.3→33, 10.8→32, 12.5→29
9925	40.7	14	10	2	6.3→33
2484	57.6	10.5	3	5	6.3→33
P5132	4.9	15	10	9	6.3→27, 11K→26
96441	19.5	25	9	3	6.3→52, 6.3 to 12.6 group
12956	32.5	30	5	3.5	6.3→49.5 (followed by decreasing peaks up to ↶13K)
1896	5.1	4	7	2.5	6.3→3
5247	Sensor Failed on Tape				
8873	5.0	11	2	2	6.3→3, 3.6→13, 58K→6
1377	11.1	4	3	2	3.6→15, 6.3→4
5586	16.9	7	2	3	3.6→12, 6.3→24

*Test points at % of maximum rated speed for power turbine/gas generator

TABLE 22

T53 ENGINE DATA
95%/97% TEST POINT, SENSOR 2*

Power Turbine Serial No.	Np	N_G (millivolts)	2Np	$2N_G$	Other (Frequency → Amplitude)
82C011	--	--	--	--	
4871	--	--	--	--	
LE21788	34.6	31	4	8	6300→48, 7200→51 mV (followed by decreasing peaks up to15K, 33.8K→17
M289659	34.6	18	16	3	6.3→26
1541	47.1	13	29	3	6.3→32
82C012	94.2	30	36.5	10.5	
82C004	22.3	18	6	3	6.3→12.6K cpm peaks 6.3→12 highest 10.5K→31, 37.5K→36 (36-39K)
80K03P	45.8	23	12	9	35K→13, 6.3K→13
U00278	23.4	49	5	6	6.3K→39, 7.3K→36 numerous additional peaks up to 10.8K 20-30 mV. Group also @30→35K 12-19 mV. 6.3→59, 42.5→15 43.5→18
C9M11244	58.1	15	9	5	
9925	--	--	--	--	
2484	11.7	10	7.5	19	Peaks from 6.3 - 12.6K highest at 8500→47 6.3→27
P5132	20.5	34	25	3	6.3→31
96441	57.6	11	10	9	6.3K→50 (decreasing velocity to 12.6K) 14.1→37 35K→18

TABLE 22 (CONTINUED)

Power Turbine Serial No.	Np	N_G	2Np	$2N_G$	Other
12956	76.1	17	12	7	6.3K→57 (smaller peaks up to 18K) 36.8K→15
1896	22.5	12	30**	16.5	
5247	48.5	23	5	3	32.1K→52, 31.5→33, 32.4→42 (5-peak group) 6.3→6
8873	19	24	7	15	3.6→19, general high level between 43-48K cpm highest 48.2→17
1377	23.4	18.5	24***	13	3.6→18.5
5586	29.2	14	8	63	3.6→14, 6.3→5

*Test points at % of maximum rated speed for power turbine/gas generator
**Five peaks very close to 2Np, 15-30 mV, 6.3→4
***Multiple peak close to 2Np, 6.3→5

TABLE 23

T53 ENGINE DATA
95%/97% TEST POINT, SENSOR 3*

Power Turbine Serial No.	Np	N_G (millivolts)	2Np	$2N_G$	Other (Frequency → Amplitude)
82C011	--	--	--	--	
4871	--	--	--	--	
LE21788	--	--	--	--	
M289659	110	15	--	--	6.3→12
1541	81.5	6	10	7	6.3→41
82C012	--	--	--	--	
82C004	108	6	14	8	6.3→12
80K03P	97.1	8	9	9	6.3K→21 (fairly high level to 12.6K)
U00278	44.1	8	22	4	53.7→22, 56.4→16, 6.3→36
C9M11244	50.7	4	17	3	
9925	61.2	16	18	7	6.3→44, 53.7→21
2484	87.8	5	2	2	6.3K→31
P5132	26.2	4	9	7	6.3K→21
96441	--	--	--	--	
12956	89.3	6	12	4	6.3K→25, 14.3K→23
1896	85.4	4	28	--	6.3→4, 10.5, 12, 8
5247	25.1	10	11	15	6.3→13
8873	64.9	16	7	5	6.3→4, 58K→19, 50.5→18, 50→17, 15K→20
1377	46.1	6	11	10	50.5→16.5, 55.8→12, 6.3→6
5586	16.6	3	36	4	34.5→7, 6.3→5

*Test points at % or maximum rated speed for power turbine/gas generator

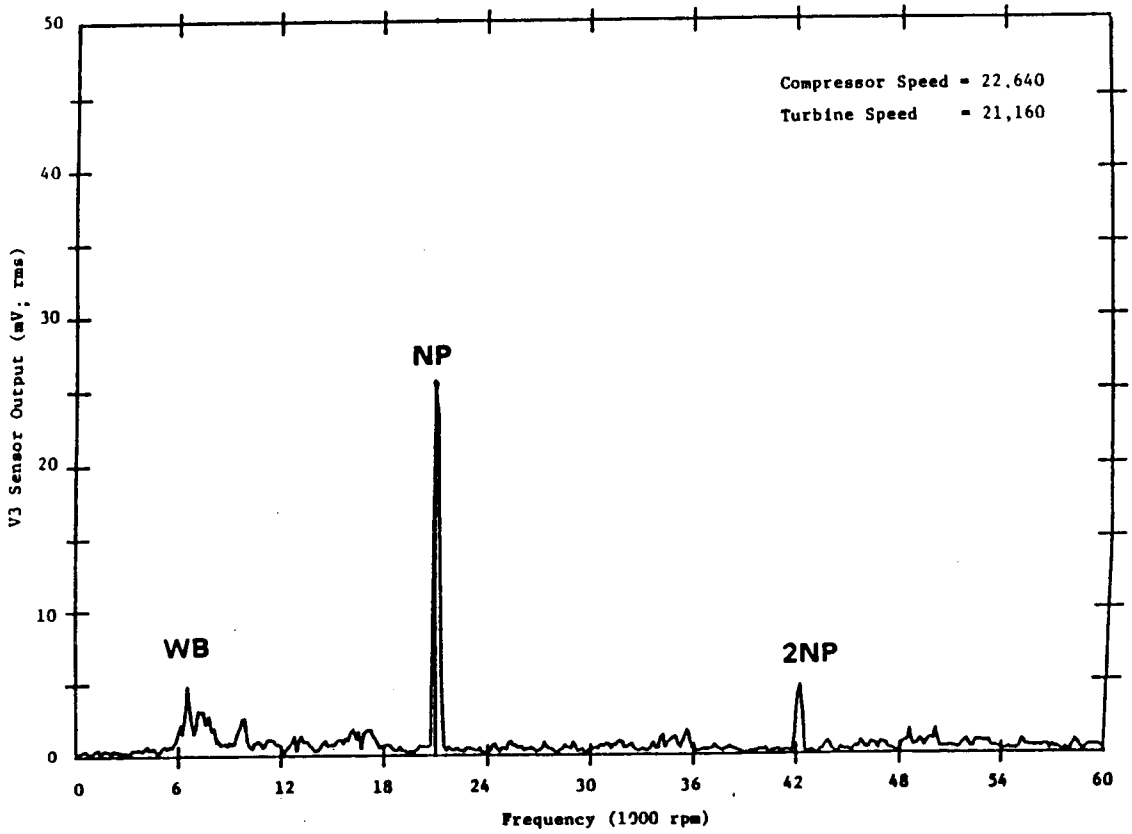

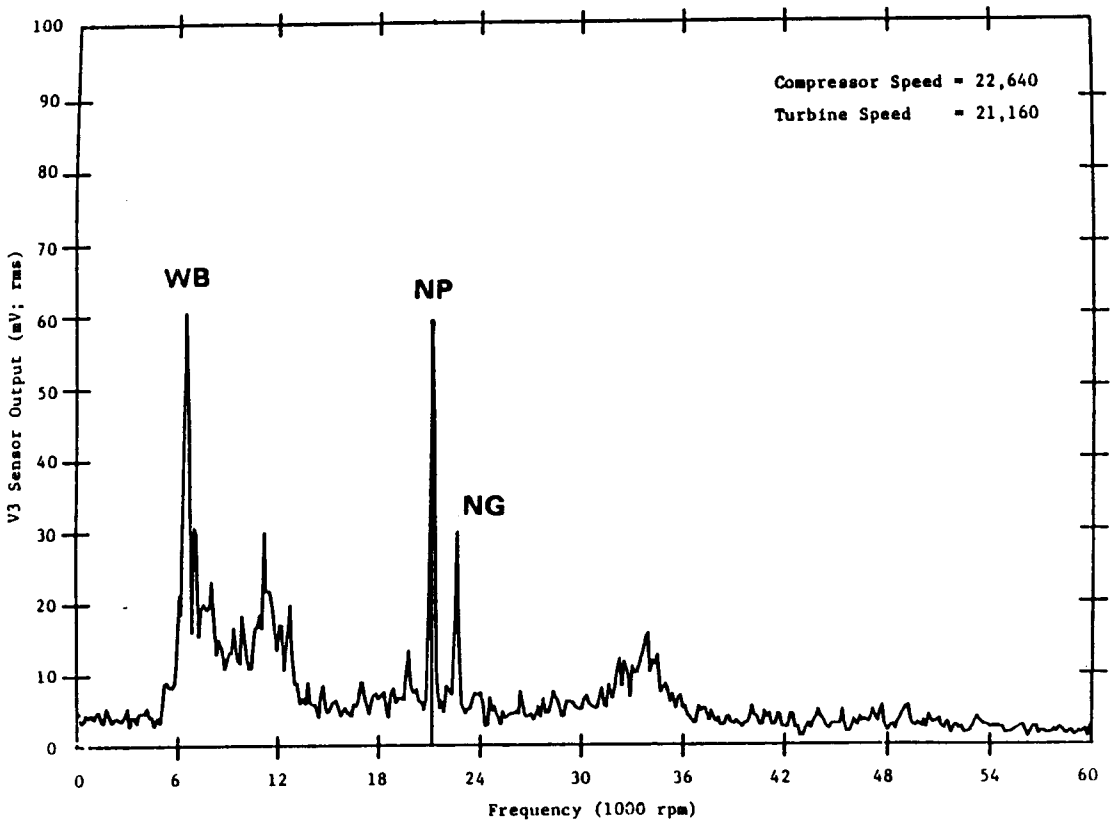

Figure 34 T53 Engine Vibration Spectrum Plots

6.0 DIAGNOSTIC GUIDELINES

To establish diagnostic guidelines for the T700, T53, and T55 engines, test cell vibration data were tape recorded and analyzed. The data analyzed included 12 T700, 20 T55, and 20 T53 engine tests. The vibration signal, as measured at CCAD, was analyzed using a real-time analyzer, also known as an FFT analyzer. This instrument separates the overall vibration signal into its individual components and generates a plot showing the amplitude of each component. Identification of specific frequency peaks that have larger than normal amplitudes for a given engine is the first step in determining the probable cause of the high vibration. The frequency can be related to a specific rotating component of the engine such as the accessory gearbox, power turbine, or gas generator. By comparing the amplitude at a discrete frequency to the average amplitude expected for that frequency for an acceptable engine, specific problems can be identified.

The diagnostic manual that summarizes the engine data analyzed is presented as Appendix A. To perform a diagnosis using the manual, the following steps are recommended:

1. Refer to the figure corresponding to the sensor and test point at which the engine requiring diagnosis was rejected.

2. Compare the predominant frequencies for the reject test point with the average levels for those frequencies. The range observed for each frequency peak over the engine tests is also provided to illustrate the degree of variability observed for each peak.

3. Match the frequency of any peak whose amplitude significantly exceeds the observed range with the probable fault.

7.0 CONCLUSIONS AND RECOMMENDATIONS

Based on the results of the efforts reported herein, the following conclusions and recommendations are made.

7.1 Conclusions

T700 power turbine rotors can be successfully high-speed balanced with improvements resulting in reduced vibrations and/or more circular orbits at the bearings. However, it was found that a high degree of accuracy is required when installing the correction weights in each of the available balance planes. It was also found that in order to achieve the 20,000-rpm operating speed, vibrations at that speed had to be traded off with vibrations at the lower balance speeds. Thus, while vibrations at 20,000 rpm could have been reduced further, to do so would have resulted in vibrations that were too high at the lower speeds to permit operation to 20,000 rpm. It was also shown that turbine rotors that had not been low-speed balanced in the overhaul process can be successfully high-speed balanced.

The analytical evaluation of T700 gas generator balancing feasibility indicates that benefits can be achieved through high-speed multiplane balancing methods. It was shown that component balancing may be eliminated and replaced with a single two-speed balance of the assembled gas generator. Balancing of the gas generator is not required at the full operating speed of the rotor but may be achieved through balancing at 8,000 and 22,000 rpm.

Engine test cell data for overhauled T700 engines were acquired on seven engines through a total of 12 engine test runs. These test data revealed that the T700 engine's primary vibration frequencies are related to the power turbine rotor, gas generator, and accessory gearbox speeds or multiples thereof. Furthermore, these data revealed that the two most responsive sensors for use in diagnostics are sensors 1 and 3. Sensor 1 is responsive to accessory gearbox related faults and sensor 3 is responsive to gas generator and power turbine faults. Based on the data review and discussions with CCAD personnel, it was also established that T700 engines are experiencing a very low reject rate. Finally, a diagnostic manual for T700/T53/T55 engines has been prepared for use by CCAD personnel.

7.2 Recommendations

Based on the results achieved under this program, it is recommended that:

- CCAD continue their present low-speed balancing procedures since engines are being overhauled and successfully accepted.

- A review of engine test cell vibration sensor location be conducted. This engine vibration survey is recommended based on the occurrence of a gas generator rub being experienced on an engine whose sensors showed acceptable vibration levels.

- An engine test cell vibration diagnostic knowledge-based system should be considered for CCAD because:
  - Current T700/T55/T53 engines, if rejected during acceptance testing, are returned to the rework line with no repair guidance.

- A rejected engine that is not properly diagnosed and then repaired may be rejected several times before proper corrective actions are taken. Mulitple rejects of a single engine are costly both in labor and fuel expenses.
- The value of a diagnostic capability has been demonstrated previously when high overall engine vibration readings were traced to a faulty test cell water brake.

APPENDIX A

DIAGNOSTIC GUIDELINES

A1.0 DIAGNOSTIC GUIDELINES

Modern overhaul facilities are required to meet demanding production schedules for turbine engines that must pass test cell performance tests. Engines that fail in the test cell are rejected and are reworked until acceptable performance is achieved. Currently, the efficient handling of rejects is seriously hampered due to the inadequate test cell data that are available to the test and engineering personnel who are called upon to determine the corrective actions. Often because of insufficient data, an engine is completely torn down and everything checked. On occasion, due to the experience of an individual, the problem is located and corrected simply and efficiently. For these cases, significant savings in turnaround time and manpower result.

Vibration rejects may be particularly difficult to handle efficiently due to the sampling of only overall vibration level from the test cell instrumentation. A study performed by MTI of recorded engine vibration data has shown that for all three engines evaluated (T700, T55 and T53), frequency spectrum analysis of the overall vibration signals can provide valuable data as to the specific engine problem. The purpose of this manual is to provide basic diagnostic criteria for T700, T53 and T55 engines based on analysis of the frequency spectrum of the overall vibration signal.

A1.1 Understanding Vibration Frequency Spectra

The vibration signal as measured can be analyzed by the use of a real-time analyzer (RTA), also known as an FFT analyzer. This instrument separates the overall vibration signal into its individual components and generates a plot of the amplitude of each component over the frequency range being analyzed. Identification of specific frequency peaks that have larger than normal amplitudes for a given engine is the first step in determining the probable source of the high vibration. The most common faults that can be determined by analysis of the vibration signal include imbalance, misalignment, and gear problems.

- Imbalance is a common source of machinery vibration and characterized by radial vibration of the shaft or casing in exact synchronization with rotor speed, as illustrated in Figure A-1*. With a complex piece of machinery, such as a turbine engine, imbalance of various components can be identified by matching the spectral data with known running speeds of each component.

- Misalignment of rotating elements can be indicated by a large second-order vibration component, as illustrated in Figure A-2. In general, parallel misalignment will show up as radial vibration at twice running frequency, whereas angular misalignment is indicated by axial vibration at twice running frequency.

- Gear Problems such as pitch line runout, mass imbalance, misalignment or faulty teeth are usually indicated by peaks at running frequency and

*For ease of readership, figures for this appendix are presented consecutively beginning on page 89.

gear mesh frequency (gear rpm × number of teeth) with ± gear rpm sidebands (smaller peaks flanking each of the gear-mesh-related peaks). The vibration will be predominantly radial for spur gears and axial for helical or herringbone gears.

There are, of course, other sources of vibration that can contribute to a rejected engine, such as defective rolling-element bearings, mechanical looseness of shaft parts, excessive bearing clearance, and coupling shifts. To identify specific symptoms for these faults, it is often necessary to perform fault implantation tests and/or include additional instrumentation.

A1.2 T700 Vibration Diagnostics

The T700 helicopter engine is a good example of a gas turbine that incorporates flexible rotor shafting. Developed by General Electric for the Blackhawk and the AAH, the T700 uses several high-technology elements to produce 1.1 MW from a 180-kg engine.

The five axial and one centrifugal stage compressor is driven by two air-cooled gas generator turbine stages to a maximum speed of 43,650 rpm. The low-speed power turbine has two uncooled stages operating at a constant 20,900 rpm. See Figure A-3 for engine cross section. The accessory gearbox operates at 0.64979 times the gas generator speed.

The T700 is assembled from a group of components in four basic modules:

- Accessory
- Cold section/compressor
- Hot section/turbine
- Power turbine.

Vibration data from 12 T700 engine test cell runs were recorded and analyzed (see Figures A-4 through A-15). Of the 12 test cell runs, some were reruns of engines with different power turbine modules. In total, 7 independent engines with 12 power turbines were studied. With this limited data sample, it is not possible to determine acceptance criteria for individual frequency components. This manual, however, can be used to establish probable faults for engines rejected for high vibration, provided the necessary data from spectrum analysis of the vibration signal are available. The engine module requiring rework can be identified by comparing the vibration spectrum of the rejected engine to the appropriate spectrum illustrated in this manual for the same test point and sensor. For instance, if a T700 engine is rejected for high vibration at the maximum continuous power (MCP) test point for sensor 3, then a vibration spectrum illustrating the content of this signal is required. Included in Section A1.2.1 of this manual is a spectrum plot that illustrates the observed levels of the significant frequencies for this test point for all 12 engines studied (Figure A-12). Presented is the average amplitude of each of the predominant frequencies, as well as the minimum and maximum amplitudes observed. Since each of the 12 engines studied passed the vibration test, detection of a frequency peak that is significantly higher than the average level observed indicates the probable fault location, such as accessory gearbox, power turbine, or gas generator. The table below each plot relates the peak frequency to a probable fault to the extent possible with the limited data.

A1.2.1. *Diagnostic Criteria*

The peak frequencies identified as significant contributors to overall engine vibration of the T700 engine are listed in Table A-1.

To perform a diagnosis, the following steps are recommended:

1. Refer to the figure corresponding to the sensor and test point at which the engine requiring diagnosis was rejected.

2. Compare the predominant frequencies for the reject test point with the average levels for those frequencies. The range observed for each frequency peak over the 12 engine tests is also provided to illustrate the degree of variability observed for each peak.

3. Match the frequency of any peak whose amplitude significantly exceeds the observed range with the probable fault.

A1.3 T55 Vibration Diagnostics

The T55 helicopter engines are shaft turbine engines each of which contains a two-stage power turbine and a two-stage turbine that drives a combination axial centrifugal compressor. The compressor rotor is driven by the gas generator turbine stages to a maximum speed of 18,400 rpm, while the power turbine is driven to a maximum speed of 16,000 rpm.

The intent of this section of the manual is to assist maintenance and test cell personnel in identifying a particular engine section requiring corrective action in the case of a vibration reject.

Vibration data from twenty T55 engine test cell runs were analyzed. With this limited data sample, it is not possible to determine acceptance criteria for individual frequency components. This manual, however, can be used to establish probable faults for engines rejected for high vibration, provided the necessary data from spectrum analysis of the vibration signal are available. The engine module requiring rework can be identified by comparing the vibration spectrum of the reject engine to the appropriate spectrum illustrated in this manual for the same test point and sensor. For instance, if a T55 engine is rejected for high vibration at the 94%/94% test point for sensor 3, then a vibration spectrum illustrating the content of this signal is required. Included in Section A1.3.1 of this manual is a spectrum plot that illustrates the observed levels of the significant frequencies for this test point for all engines studied. Presented is the average amplitude of each of the predominant frequencies, as well as the minimum and maximum amplitudes observed. Since each of the engines studied passed the vibration test, detection of a frequency peak that is significantly higher than the average level observed indicates the probable fault location, such as power turbine or gas generator. The table below each plot relates the peak frequency to a probable fault to the extent possible with the limited data.

TABLE A-1

FREQUENCIES OF SIGNIFICANT VIBRATION SPECTRUM PEAKS IN THE T700 ENGINE

	Nominal Value at Each Test Point			
Frequency	Ground Idle (GI)	900 SHP	Maximum Continuous Power (MCP)	Intermediate Rated Power (IRP)
Power Turbine (NP)	20,900 cpm	20,900 cpm	20,900 cpm	20,900 cpm
Gas Generator (NG)	30,378	41,760	42,950	43,650
Accessory Gearbox (AG)	19,739	27,135	27,908	28,363
2 x NP	18,580	41,800	41,800	41,800
2 x NG	60,756	83,520	85,900	87,300
2 x AG	39,478	54,270	55,816	56,726
0.89 NG	27,036	37,166	38,222	38,700

Vibration spectral data for all these sensors at all test points are presented in Figures A-4 through A-15. There are three figures at each test point, one for each of the engine's sensors. The figures that correspond to the test points are as follows:

Test Point	Figure Numbers
GI	A-4 through A-6
900 SHP	A-7 through A-9
MCP	A-10 through A-12
IRP	A-13 through A-15

A1.3.1 Diagnostic Criteria

The peak frequencies identified as significant contributors to overall engine vibration of the T55 engine are primarily related to the unbalance of the gas producer and power turbine as well as alignment.

Vibration spectral data for all these sensors at the 94%/94% and 93%/100% test points are presented in Figures A-16 through A-21. There are three figures at each test point, one for each of the engine's sensors. The figure that corresponds to each test point are:

Test Point	Figure Numbers
94%/94%	A-16 through A-18
93%/100%	A-19 through A-21

To perform a diagnosis, the following steps are recommended:

1. Refer to the figure corresponding to the sensor and test point at which the engine requiring diagnosis was rejected.

2. Compare the predominant frequencies for the reject test point with the average levels for those frequencies. The range observed for each frequency peak over the 12 engine tests is also provided to illustrate the degree of variability observed for each peak.

3. Match the frequency of any peak whose amplitude significantly exceeds the observed range with the probable fault.

A1.4 T53 Vibration Diagnostics

The T53 gas turbine engines are shaft turbine or turboprop engines each of which contains a two-stage, free-type power turbine and a two-stage turbine that drives a combination axial-centrifugal compressor. The five major sections of the engine are the inlet, accessory drive, compressor, diffuser and combustor, and power turbine and exhaust. The compressor rotor is driven by the gas generator turbine stages to a maximum speed of 25,150 rpm, while the power turbine rotor is driven to a maximum speed of 21,100 rpm.

The peak frequencies identified as significant contributors to overall engine vibration of the T53 engine are related to the unbalance of the gas producer and power turbine, as well as alignment.

Vibration spectra data for all test cell sensors at the 95%/97% test point are presented in Figures A-22 through A-24.

To perform a diagnosis, the following steps are recommended:

1. Refer to the figure corresponding to the sensor and test point at which the engine requiring diagnosis was rejected.

2. Compare the predominant frequencies for the reject test point with the average levels for those frequencies. The range observed for

each frequency peak over the 12 engine tests is also provided to illustrate the degree of variability observed for each peak.

3. Match the frequency of any peak whose amplitude significantly exceeds the observed range with the probable fault.

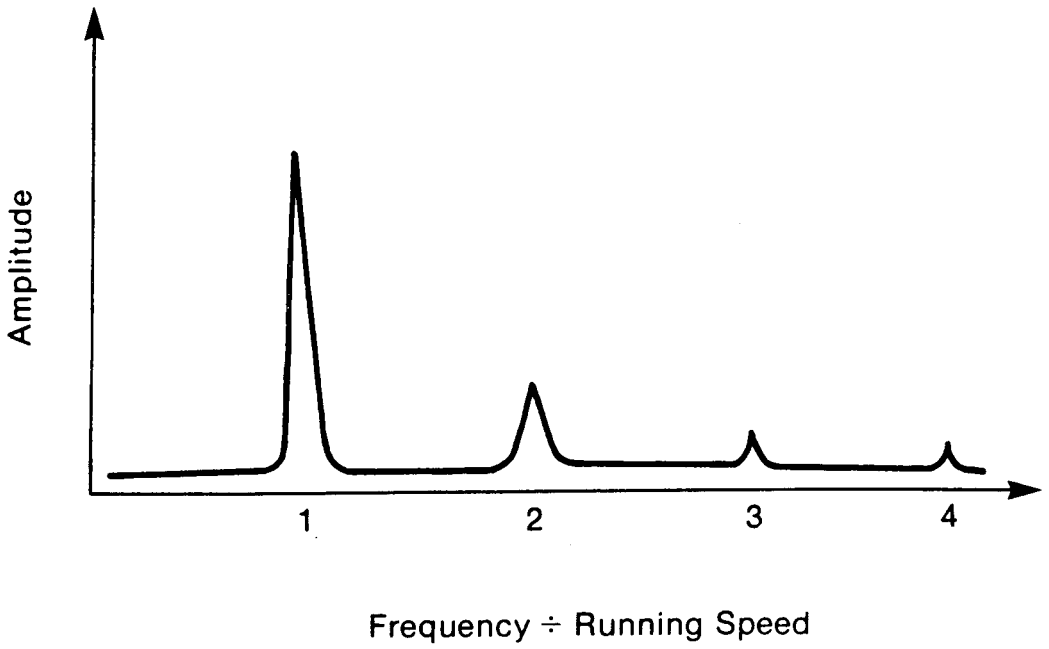

Figure A-1 Spectral Characteristics of Imbalance

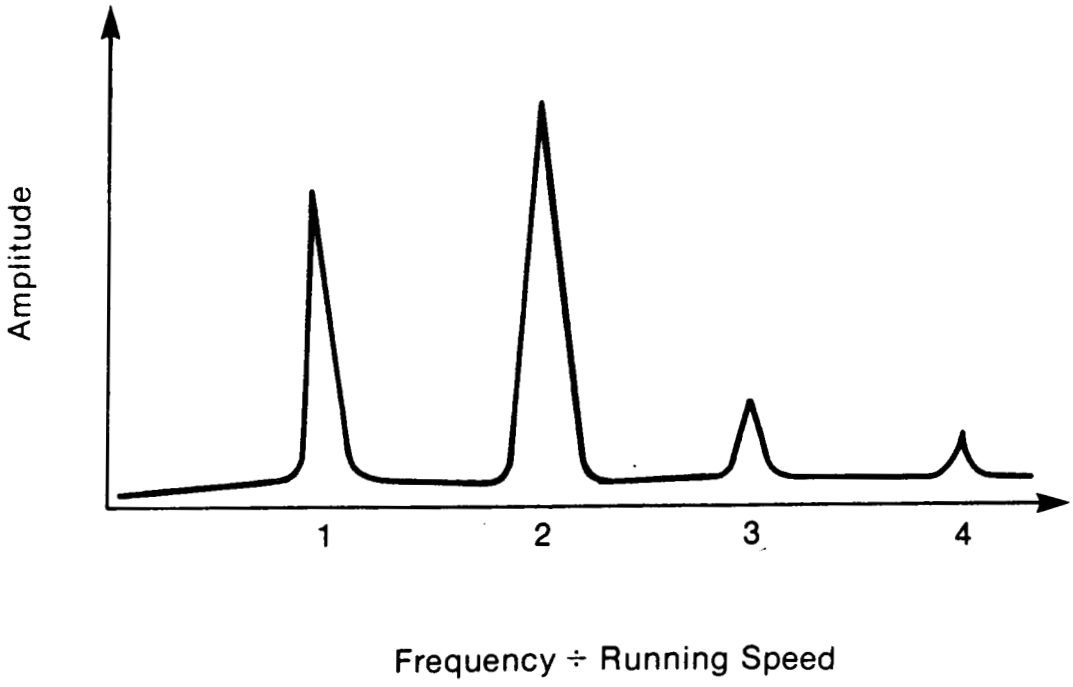

Figure A-2 Spectral Characteristics of Misalignment

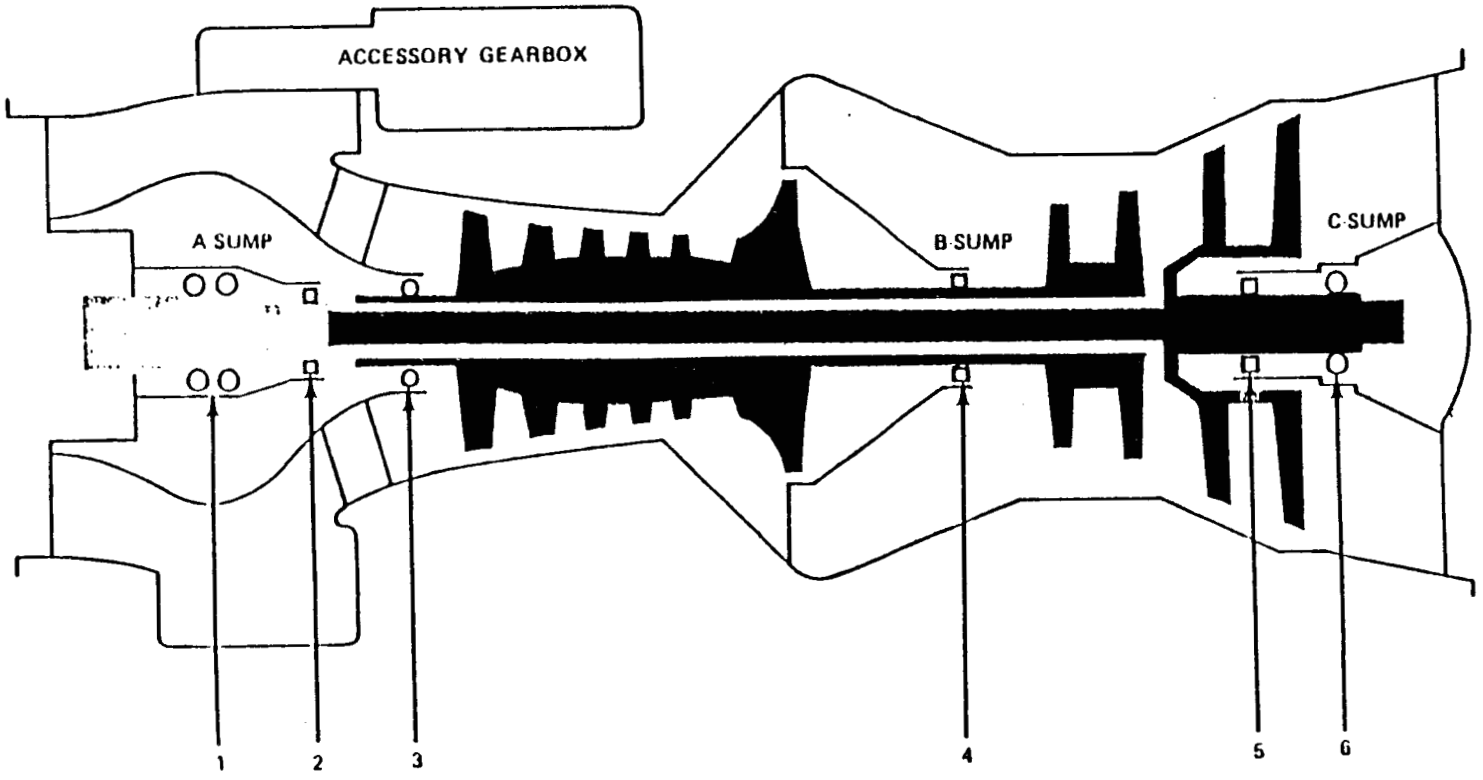

Figure A-3 T700 Main Bearings and Shafts

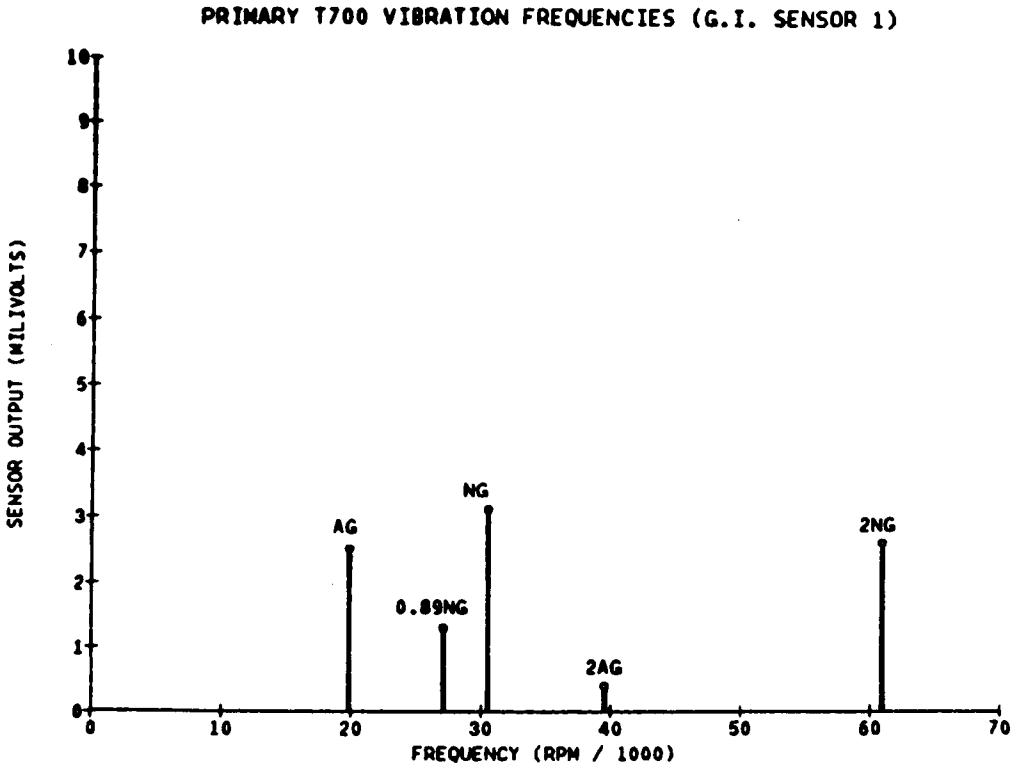

Peak	Frequency (cpm)	Amplitude (mV) Average	Min./Max.	Probable Fault
1	NG 30,378	3.1	0.5/5.4	Gas Generator Balance
2	2 NG 60,756	2.6	1.1/7.6	Gas Generator Alignment
3	AG 19,739	2.5	1.0/5.0	Accessory Gearbox Balance
4	2 AG 39,478	0.4	0.3/4.2	Accessory Gearbox Alignment
5	0.89 NG 27,036	1.3	0.3/4.2	

Figure A-4 Ground Idle Test Point, Sensor 1

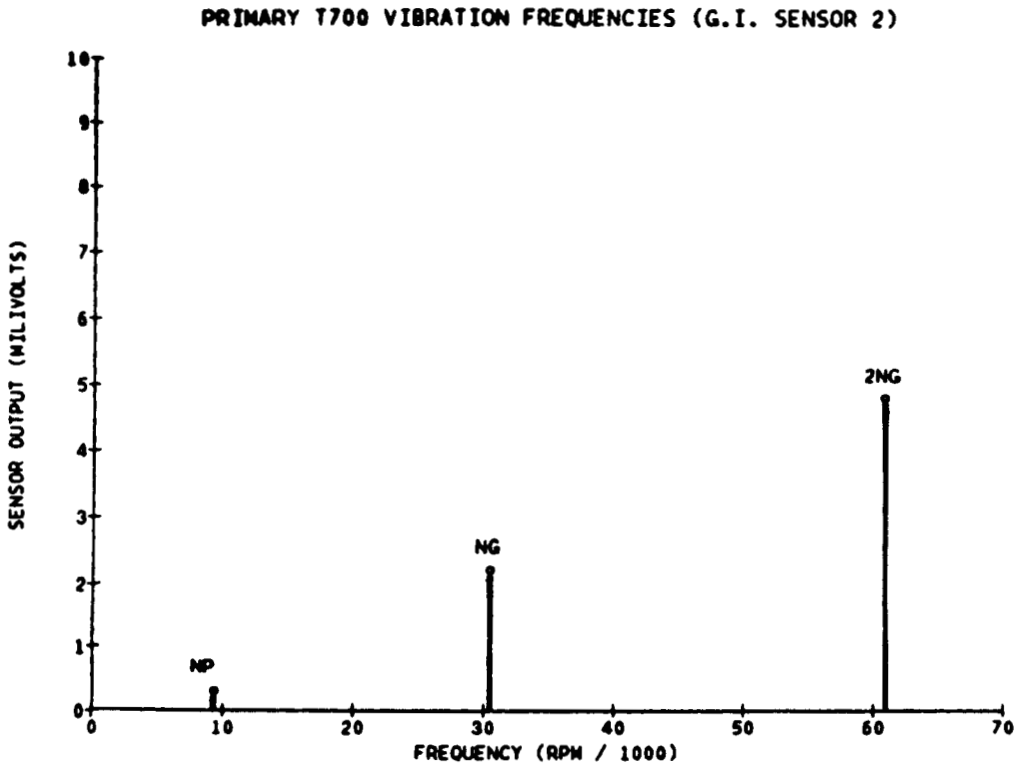

Peak	Frequency (cpm)	Amplitude (mV) Average	Min./Max.	Probable Fault
1	2 NG 60,756	4.8	0.2/12.7	Gas Generator Alignment
2	NG 30,378	2.2	0.2/8.2	Gas Generator Balance
3	NP* 9,290	0.3	0.1/0.7	Power Turbine Balance

*Power turbine speed.

Figure A-5 Ground Idle Test Point, Sensor 2

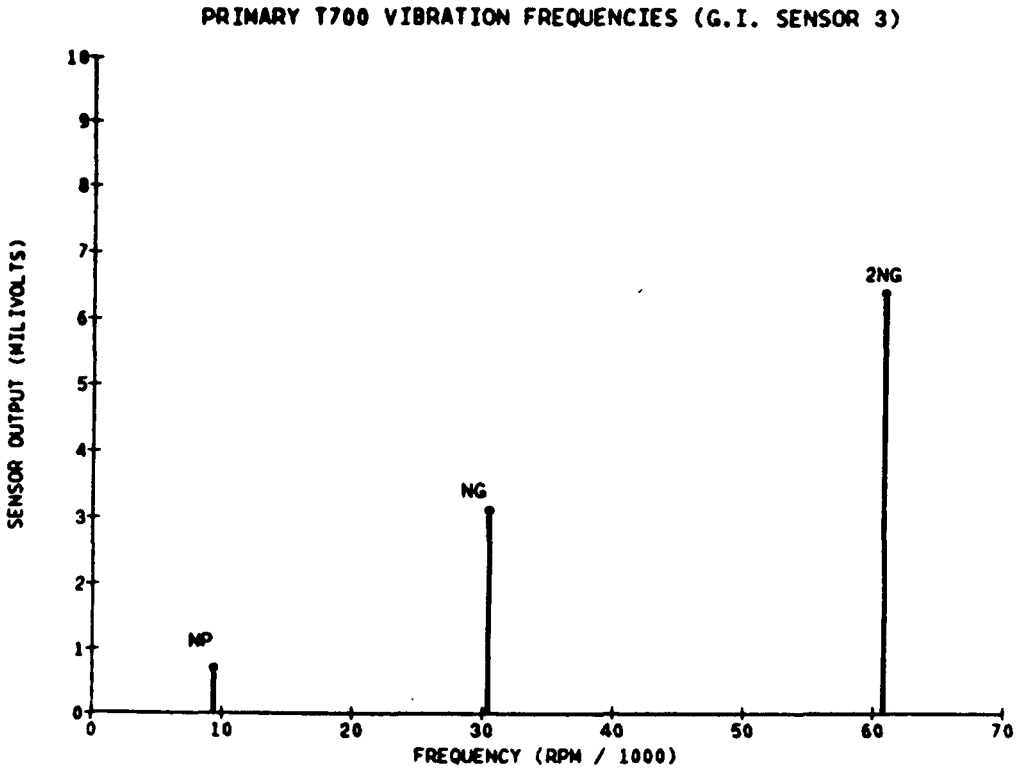

Peak	Frequency (cpm)	Amplitude (mV) Average	Min./Max.	Probable Fault
1	2 NG 60,756	6.4	0.2/12.6	Gas Generator Alignment
2	NG 30,378	3.1	0.9/7.6	Gas Generator Balance
3	NP 9,290	0.7	0.2/1.3	Power Turbine Balance

Figure A-6 Ground Idle Test Point, Sensor 3

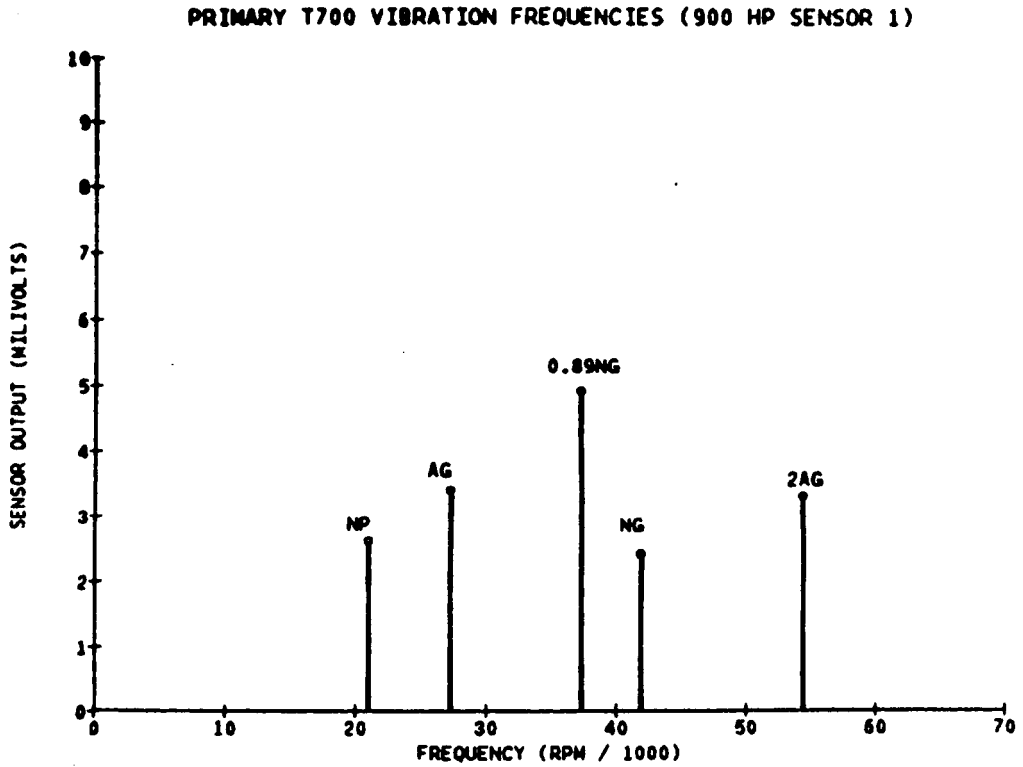

Peak	Frequency (cpm)	Amplitude (mV) Average	Min./Max.	Probable Fault
1	0.89 NG 37,166	4.9	1.4/12.6	
2	AG 27,135	3.4	0.8/10.9	Accessory Gearbox Balance
3	2 AG 54,270	3.3	1.1/7.6	Accessory Gearbox Alignment
4	NP 20,900	2.6	0.8/5.2	Power Turbine Balance
5	NG 41,760	2.4	0.4/10.7	Gas Generator Balance

Figure A-7 900 SHP Test Point, Sensor 1

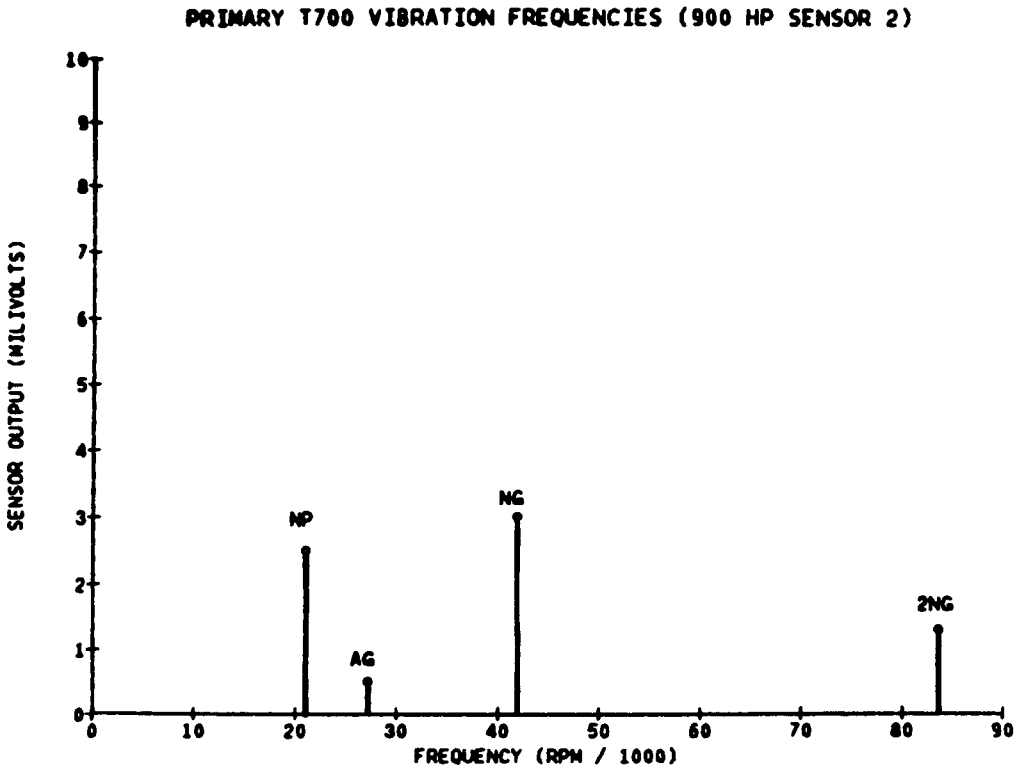

Peak	Frequency (cpm)	Amplitude (mV) Average	Min./Max.	Probable Fault
1	NG 41,760	3.0	0.6/4.7	Gas Generator Balance
2	NP 20,900	2.5	0.16/8.0	Power Turbine Balance
3	2 NG 83,520	1.3	0.1/3.2	Gas Generator Alignment
4	AG 27,135	0.5	0.1/2.8	Accessory Gearbox Balance

Figure A-8 900 SHP Test Point, Sensor 2

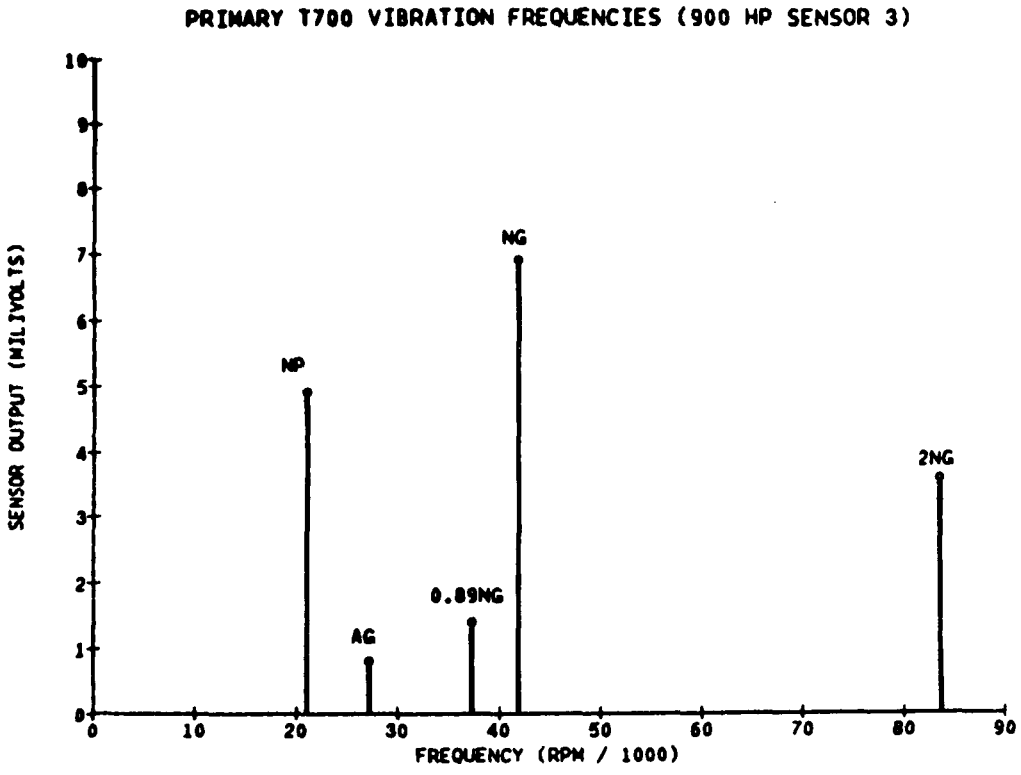

Peak	Frequency (cpm)	Amplitude (mV) Average	Min./Max.	Probable Fault
1	NG 41,760	6.9	2.0/17.0	Gas Generator Balance
2	NP 20,900	4.9	0.8/11.1	Power Turbine Balance
3	2 NG 83,520	3.6	1.1/7.7	Gas Generator Alignment
4	0.89 NG 37,166	1.5	0.89/3.4	
5	AG 27,135	0.8	0.1/2.8	Accessory Gearbox Balance

Figure A-9 900 SHP Test Point, Sensor 3

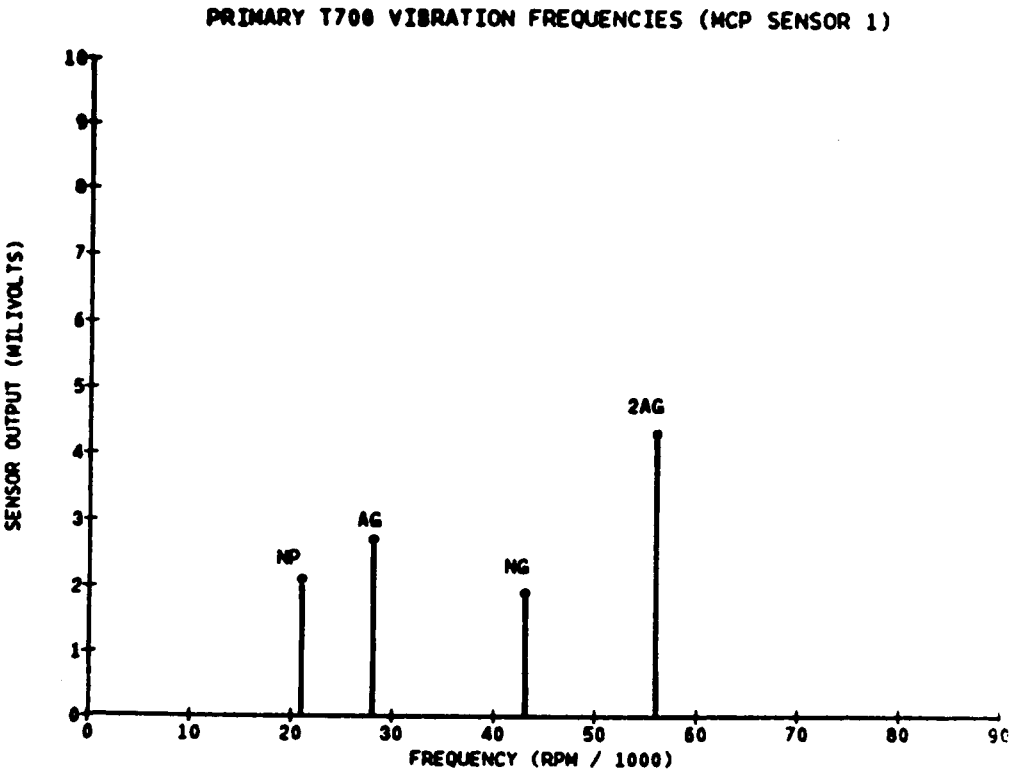

Peak	Frequency (cpm)	Amplitude (mV) Average	Min./Max.	Probable Fault
1	2 AG 55,816	4.3	1.0/9.1	Accessory Gearbox Alignment
2	AG 27,908	2.7	1.6/4.0	Accessory Gearbox Balance
3	NP 20,900	2.1	0.7/4.3	Power Turbine Balance
4	NG 42,950	1.9	0.6/7.8	Gas Generator Balance

Figure A-10 MCP Test Point, Sensor 1

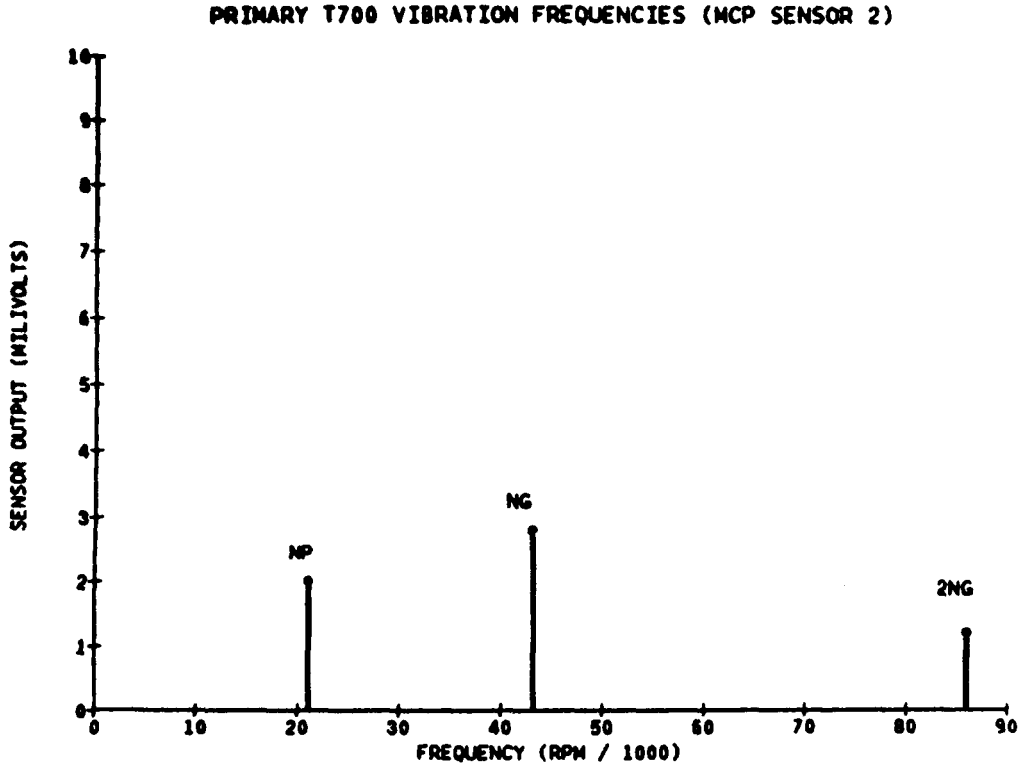

Peak	Frequency (cpm)	Amplitude (mV) Average	Min./Max.	Probable Fault
1	NG 42,950	2.8	0.7/6.3	Gas Generator Balance
2	NP 20,900	2.0	0.4/5.9	Power Turbine Balance
3	2 NG 85,900	1.2	0.2/4.3	Gas Generator Alignment

Figure A-11 MCP Test Point, Sensor 2

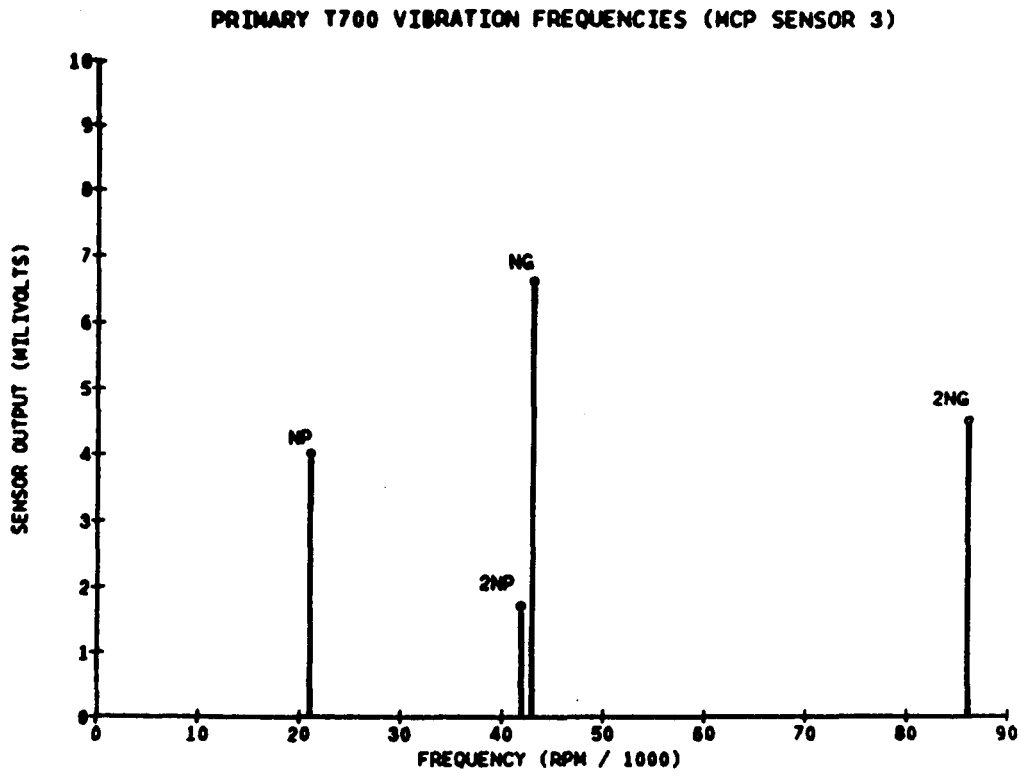

Peak	Frequency (cpm)	Amplitude (mV) Average	Min./Max.	Probable Fault
1	NG 42,950	6.6	1.4/16.5	Gas Generator Balance
2	2 NG 85,900	4.5	0.3/10.5	Gas Generator Alignment
3	NP 20,900	4.0	1.6/7.4	Power Turbine Balance
4	2 NP 41,800	1.7	0.2/6.6	Power Turbine Alignment

Figure A-12 MCP Test Point, Sensor 3

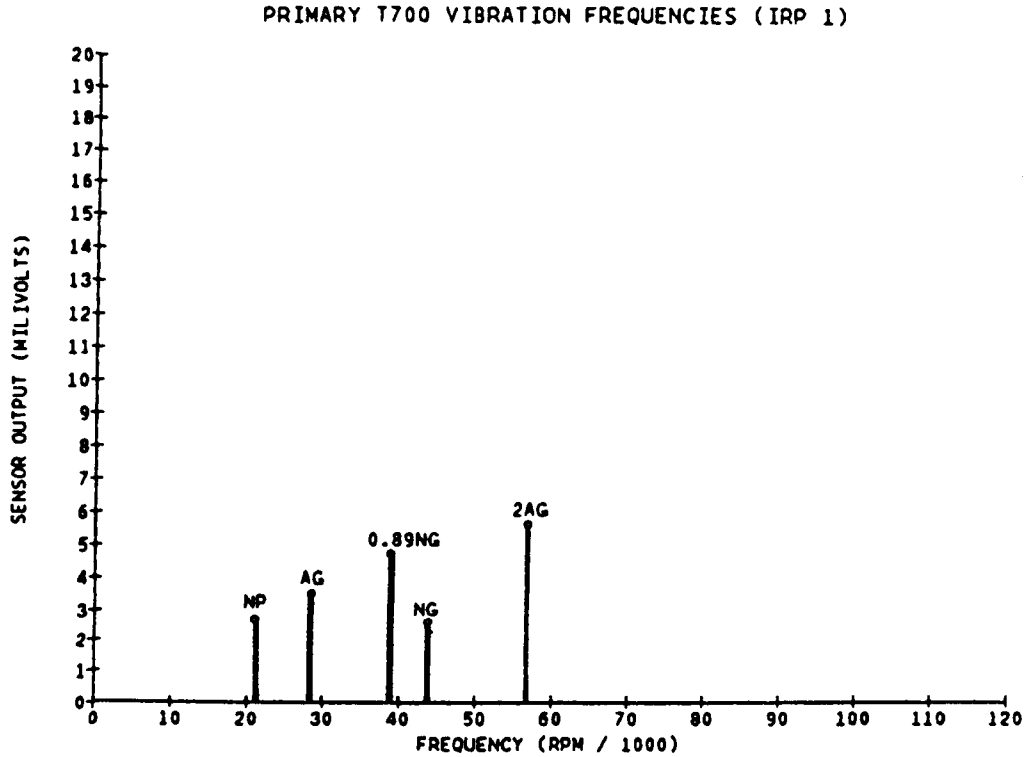

Peak	Frequency (cpm)	Amplitude (mV) Average	Min./Max.	Probable Fault
1	0.89 NG 38,700	4.7	0.8/10.3	
2*	2 AG 56,726	5.6	1.4/13.4	Accessory Gearbox Alignment
3	AG 28,363	3.5	1.4/6.6	Accessory Gearbox Balance
4	NP 20,900	2.7	0.8/7.2	Power Turbine Balance
5	NG 43,650	2.6	0.9/7.9	Gas Generator Balance

*Three engine runs studied, which used the same accessory gearbox, showed an unusually high peak at this frequency. On the third run of this engine, the gas generator rubbed. Amplitudes near the maximum observed should therefore be considered as indicative of a problem with the accessory gearbox.

Figure A-13 IRP Test Point, Sensor 1

C-2

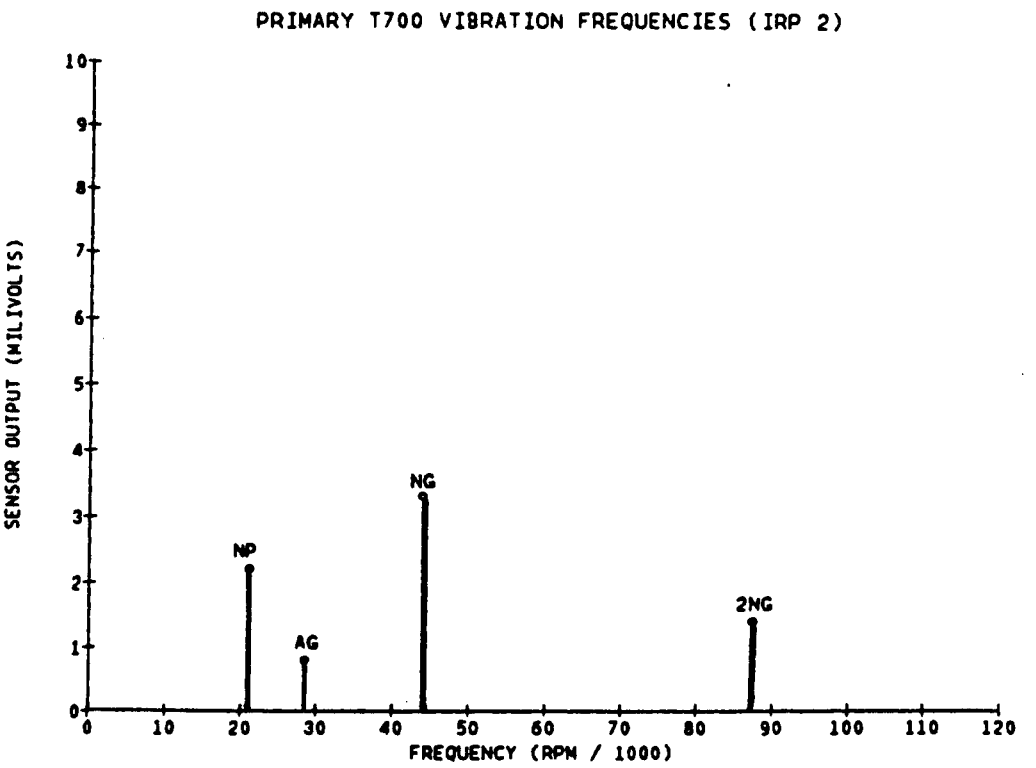

Peak	Frequency (cpm)	Amplitude (mV) Average	Min./Max.	Probable Fault
1	NG 43,650	3.3	1.3/6.0	Gas Generator Balance
2	NP 20,900	2.2	0.2/5.6	Power Turbine Balance
3	2 NG 87,300	1.4	0.2/5.0	Gas Generator Alignment
4	AG 28,363	0.8	0.2/4.2	Accessory Gearbox Balance

Figure A-14 IRP Test Point, Sensor 2

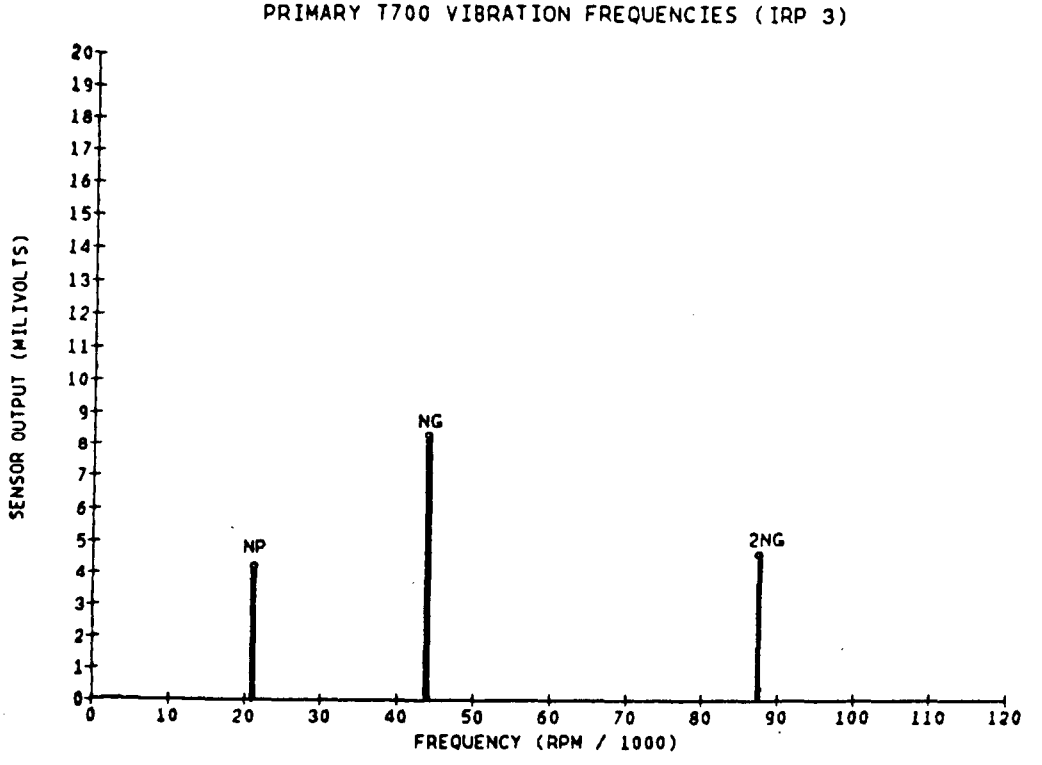

Peak	Frequency (cpm)	Amplitude (mV) Average	Min./Max.	Probable Fault
1	NG 43,650	8.3	2.2/13.3	Gas Generator Balance
2	2 NG 87,300	4.6	0.1/14.0	Gas Generator Alignment
3	NP 20,900	4.2	0.6-11.7	Power Turbine Balance

Figure A-15 IRP Test Point, Sensor 3

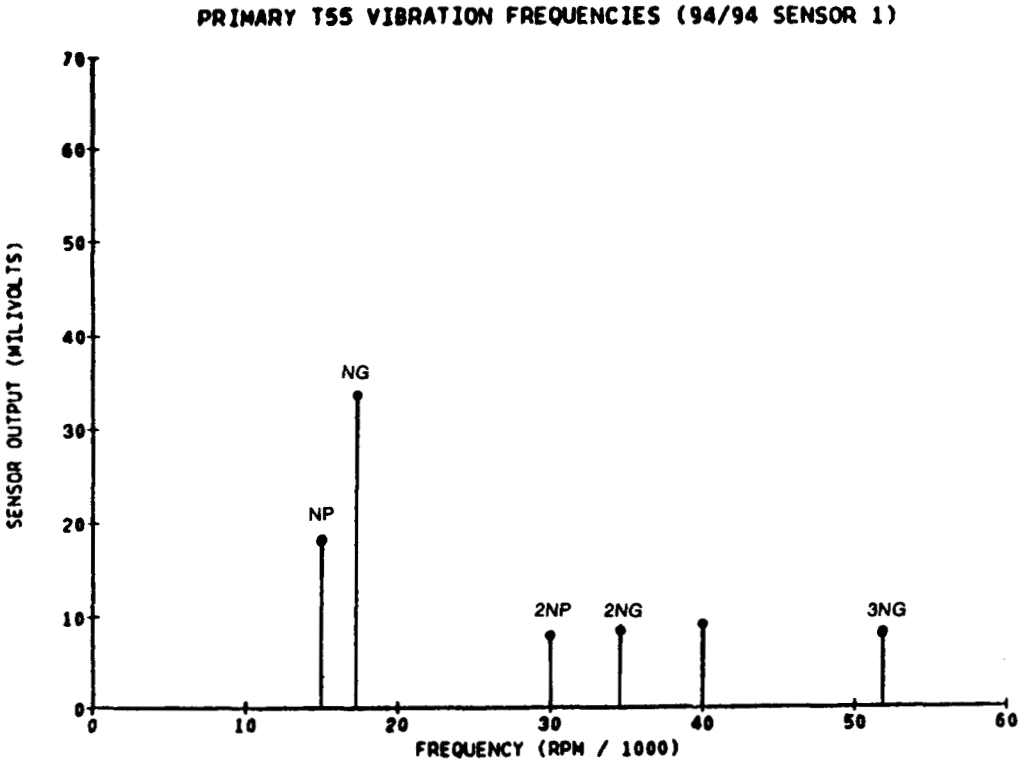

Peak	Frequency (cpm)	Amplitude (mV) Average	Min./Max.	Probable Fault
1	NG 17,300	33.6	18.0/77.0	Gas Generator Balance
2	NP 15,000	18.25	2.5/32.9	Power Turbine Balance
3	40,000	9.1	2.0/21.0	?
4	2 NG 34,600	8.4	2.0/22.0	Gas Generator Alignment
5	3 NG 51,900	8.2	2.0/26.0	Gas Generator; Loose Bearing/Support
6	2 NP 30,000	7.9	3.0/17.0	Power Turbine Alignment

Figure A-16 T55 94%/94% Test Point, Sensor 1

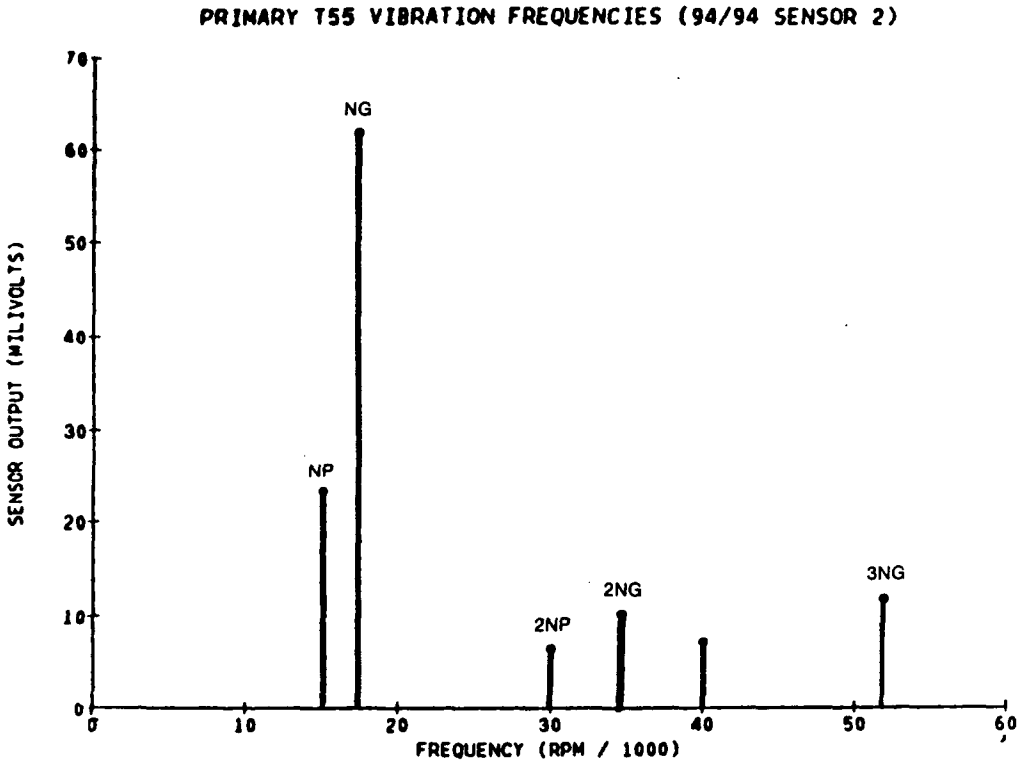

Peak	Frequency (cpm)	Amplitude (mV) Average	Min./Max.	Probable Fault
1	NG 17,300	61.7	30.0/100.0	Gas Generator Balance
2	NP 15,000	23.2	2.2/60.3	Power Turbine Balance
3	3 NG 51,900	11.7	4.0/33.0	Gas Generator; Loose Bearing/Support
4	2 NG 34,600	10.1	4.0/18.0	Gas Generator Alignment
5	40,000	7.1	3.0/18.0	?
6	2 NP 30,000	6.4	3.0/10.0	Power Turbine Alignment

Figure A-17 T55 94%/94% Test Point, Sensor 2

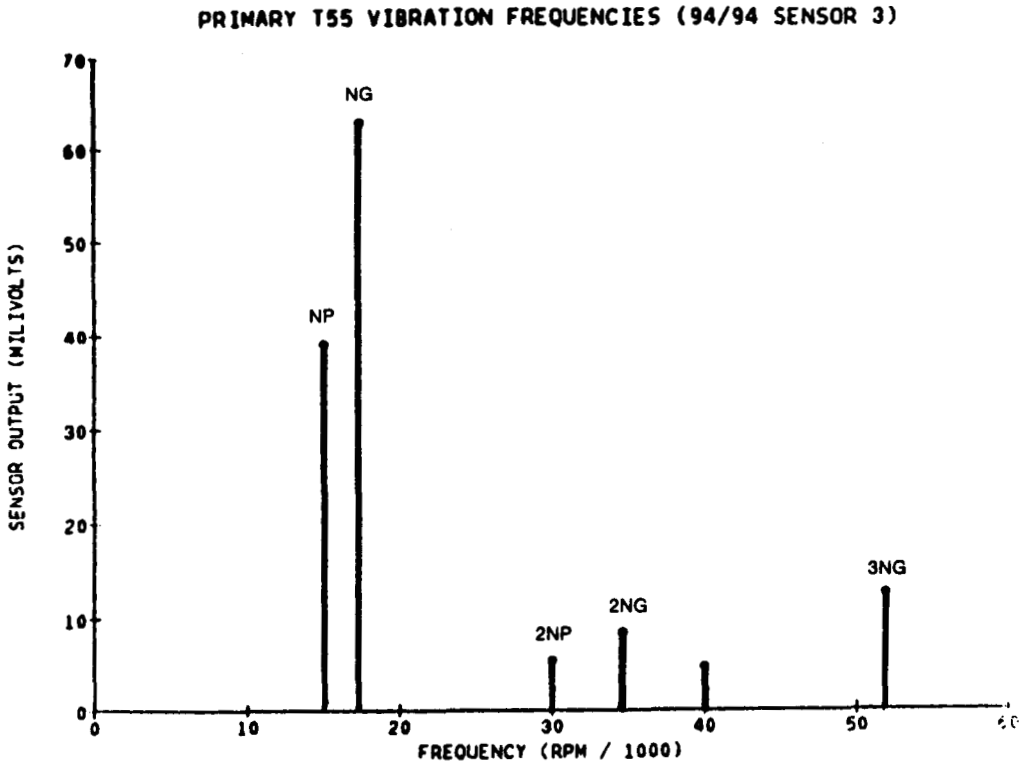

Peak	Frequency (cpm)	Amplitude (mV) Average	Min./Max.	Probable Fault
1	NG 17,300	62.9	19.0/100.0	Gas Generator Balance
2	NP 15,000	39.1	6.0/93.2	Power Turbine Balance
3	3 NG 51,900	12.5	3.0/22.5	Gas Generator; Loose Bearing/Support
4	2 NG 34,600	8.4	2.0/18.0	Gas Generator Alignment
5	2 NP 30,000	5.4	3.0/11.0	Power Turbine Alignment
6	40,000	4.7	2.0/10.0	?

Figure A-18 T55 94%/94% Test Point, Sensor 4

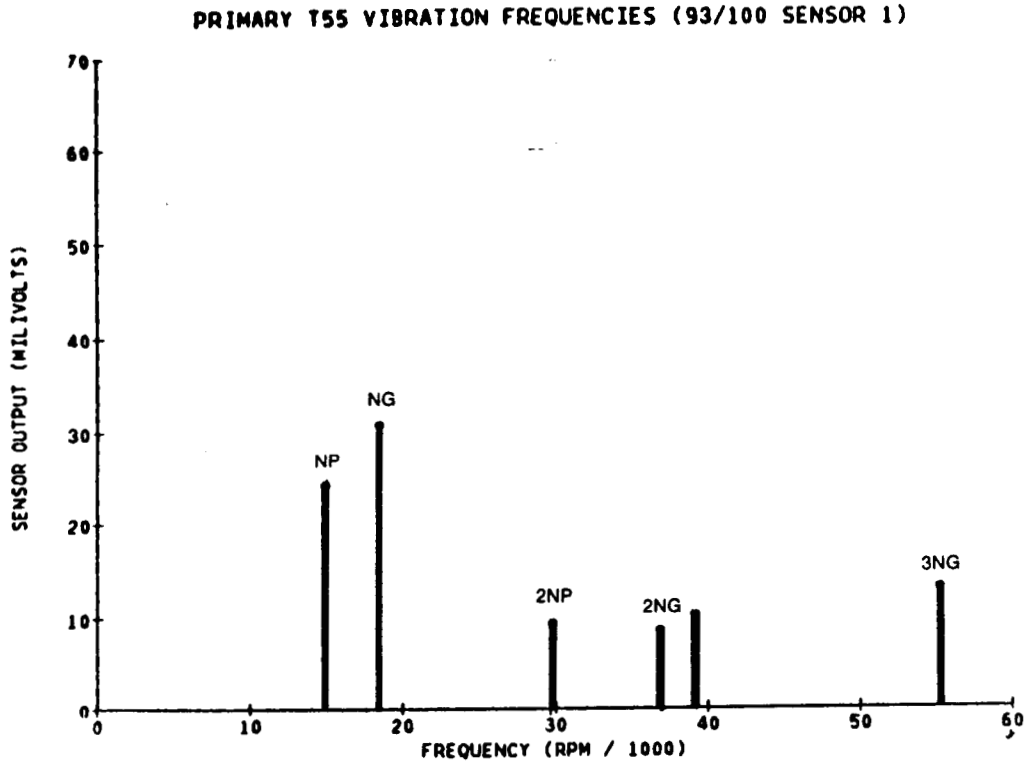

Peak	Frequency (cpm)	Amplitude (mV) Average	Min./Max.	Probable Fault
1	NG 18,400	30.7	3.0/77.0	Gas Generator Balance
2	NP 14,880	24.1	4.3/51.2	Power Turbine Balance
3	3 NG 55,200	13.0	4.0/28.0	Gas Generator; Loose Bearing/Support
4	39,100	10.2	2.0/23.0	?
5	2 NP 29,760	9.3	2.0/25.0	Power Turbine Alignment
6	2 NG 36,800	8.5	3.0/26.0	Gas Generator Alignment

Figure A-19 T55 93%/100% Test Point, Sensor 1

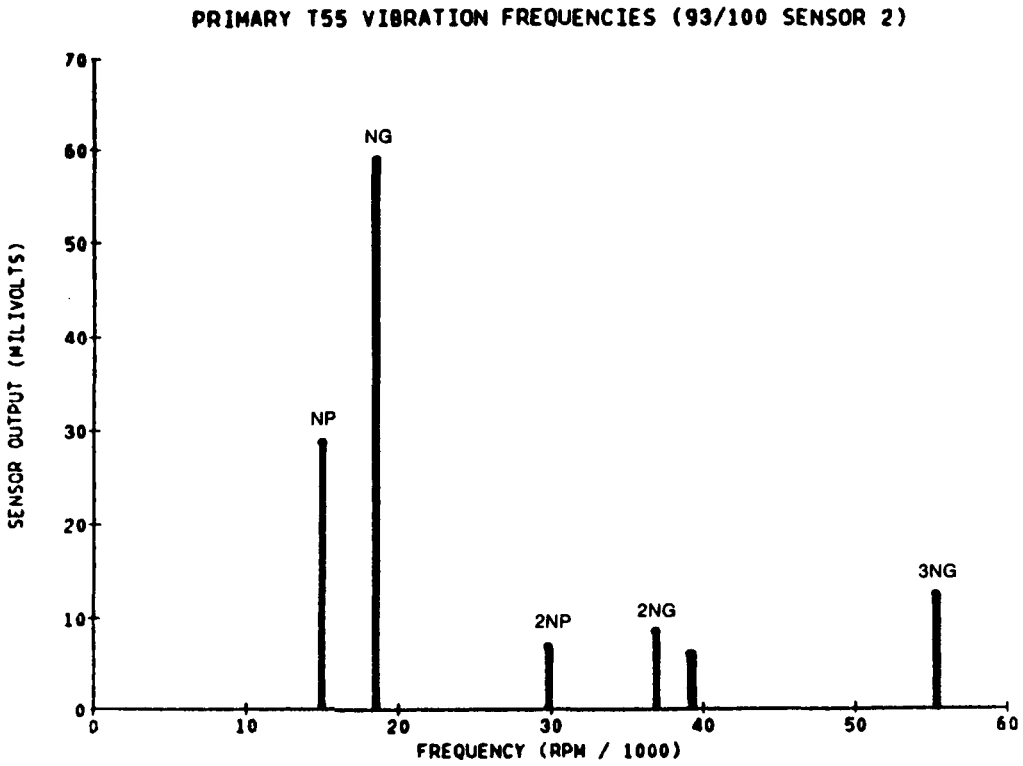

Peak	Frequency (cpm)	Amplitude (mV) Average	Min./Max.	Probable Fault
1	NG 18,400	58.8	22.0/105.0	Gas Generator Balance
2	NP 14,880	28.6	3.2/79.0	Power Turbine Balance
3	3 NG 55,200	12.4	5.0/32.0	Gas Generator; Loose Bearing/Support
4	2 NG 36,800	8.5	2.0/17.0	Gas Generator Alignment
5	2 NP 29,760	6.8	3.0/13.0	Power Turbine Alignment
6	39,100	6.0	3.0/15.0	?

Figure A-20 T55 93%/100% Test Point, Sensor 2

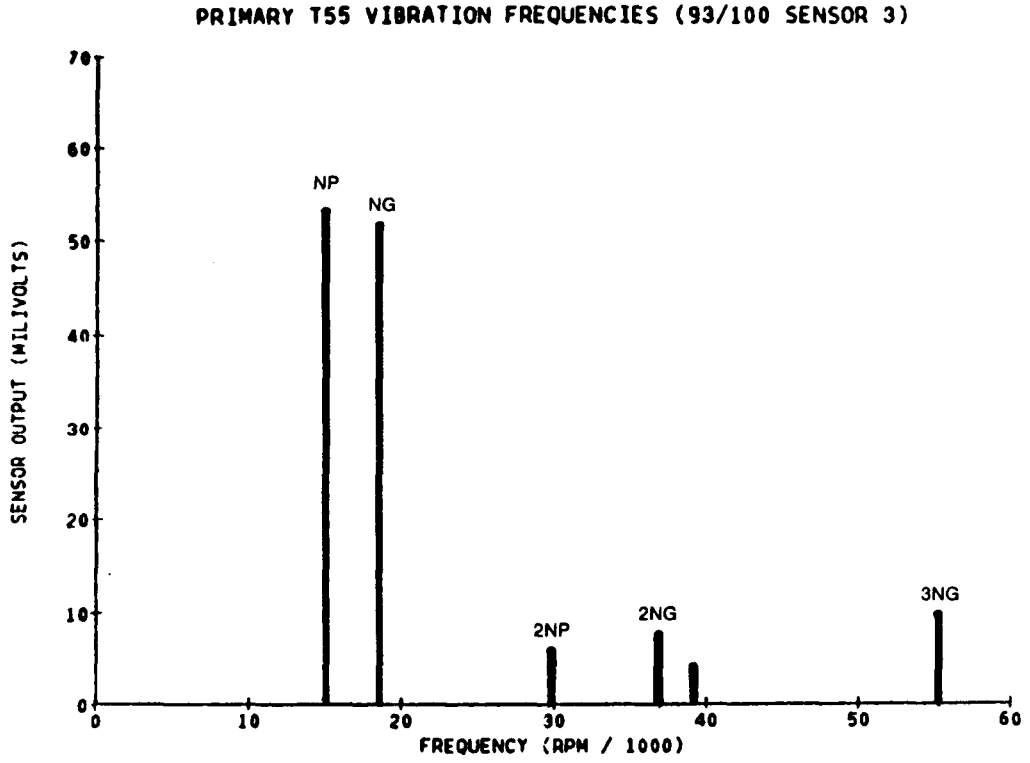

Peak	Frequency (cpm)	Amplitude (mV) Average	Min./Max.	Probable Fault
1	NP 14,880	53.0	5.0/105.0	Power Turbine Balance
2	NG 18,400	51.4	10/100.0	Gas Generator Balance
3	3 NG 55,200	9.6	2.0/32.0	Gas Generator; Loose Bearing/Support
4	2 NG 36,800	7.5	2.0/22.0	Gas Generator Alignment
5	2 NP 29,760	5.8	2.0/13.0	Power Turbine Alignment
6	39,100	4.0	1.0/10.5	?

Figure A-21 T55 93%/100% Test Point, Sensor 4

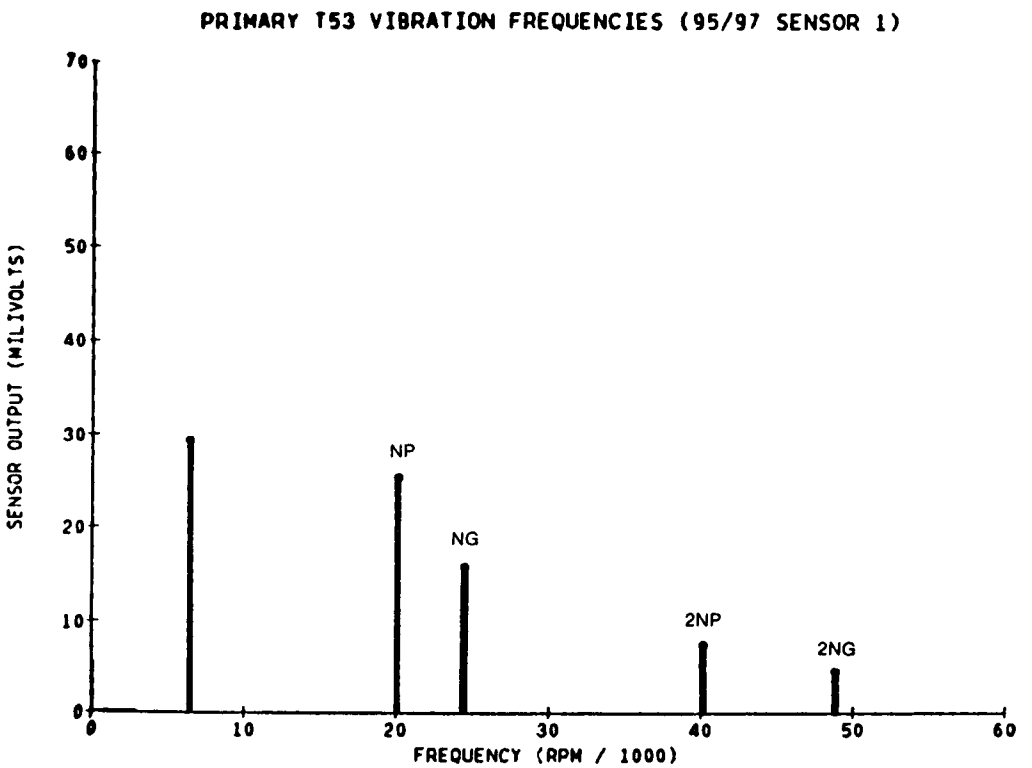

Peak	Frequency (cpm)	Amplitude (mV) Average	Min./Max.	Probable Fault
1	6,300	29.3	3.0/52.0	Water Brake
2	NP 20,045	25.3	5.0/57.6	Power Turbine Balance
3	NG 24,400	15.7	4.0/35.0	Gas Generator Balance
5	2 NP 40,090	7.4		Power Turbine Alignment
6	2 NG 48,800	4.5		Gas Generator Alignment

Figure A-22 T53 95%/97% Test Point, Sensor 1

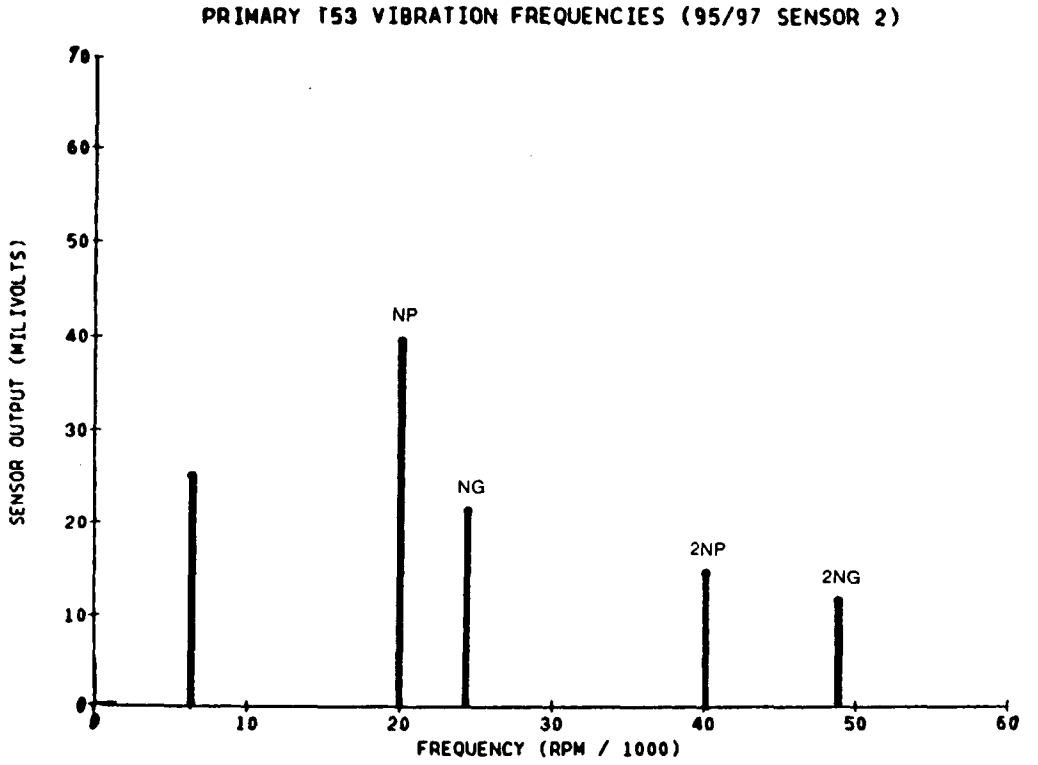

Peak	Frequency (cpm)	Amplitude (mV) Average	Min./Max.	Probable Fault
1	NP 20,045	39.4	11.7/94.2	Power Turbine Balance
2	6,300	25.1	3.0/59.0	Water Brake
3	NG 24,400	21.2	10.0/49.0	Gas Generator Balance
4	2 NP 40,090	14.5	4.0/36.5	Power Turbine Alignment
5	2 NG 48,800	11.5*	3/63 (19)	Gas Generator Alignment

*Average is reduced to 8.5 if the single 63-mV data point is discarded.

Figure A-23 T53 95%/97% Test Point, Sensor 2

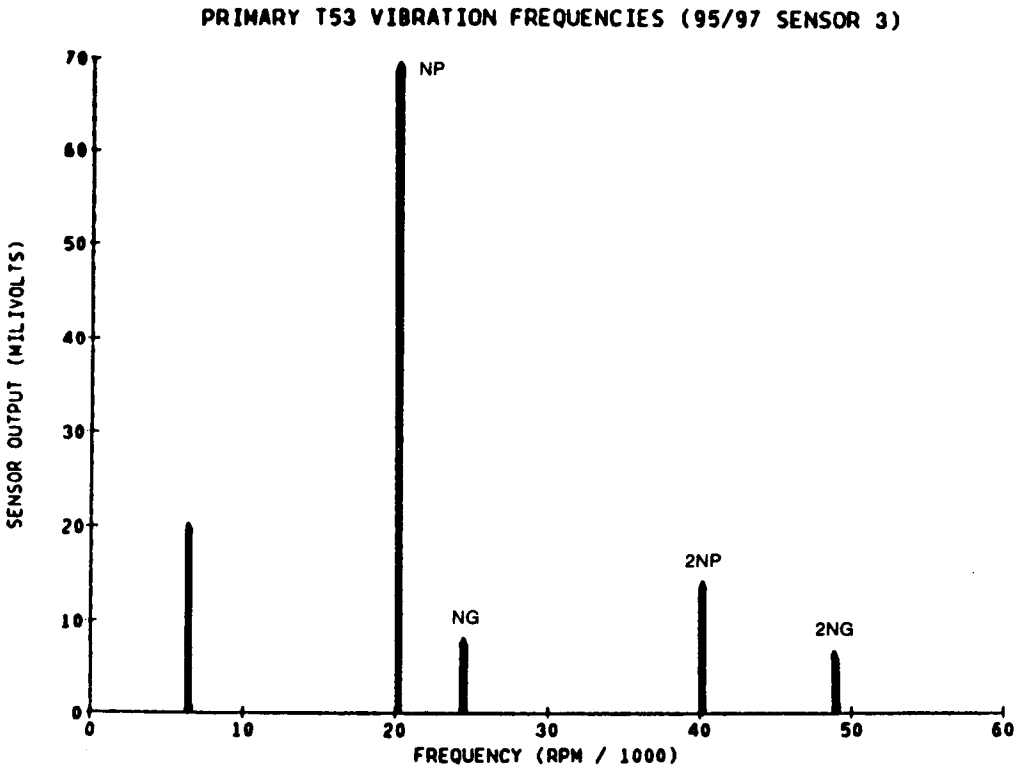

Peak	Frequency (cpm)	Amplitude (mV) Average	Min./Max.	Probable Fault
1	NP 20,045	69.1	16.6/112.0	Power Turbine Balance
2	6,300	19.9	4.0/46.0	Water Brake
3	2 NP 40,090	13.8	2.0/36.0	Power Turbine Alignment
4	NG 24,400	7.7	3.0/16.0	Gas Generator Balance
5	2 NG 48,800	6.3	2.0/15.0	Gas Generator Alignment

Figure A-24 T53 95%/97% Test Point, Sensor 3

NASA
National Aeronautics and Space Administration

Report Documentation Page

1. Report No.	2. Government Accession No.	3. Recipient's Catalog No.
NASA CR-180899 AVSCOM TR-88-C-007		

4. Title and Subtitle	5. Report Date
High-Speed Balancing Applied to the T700 Engine	March 1989
	6. Performing Organization Code

7. Author(s)	8. Performing Organization Report No.
J. Walton, C. Lee, and M. Martin	MTI 87TR56
	10. Work Unit No. 1L162209AH76 505-62-0K

9. Performing Organization Name and Address	11. Contract or Grant No.
Mechanical Technology Incorporated 968 Albany-Shaker Road Latham, New York 12110	NAS3-23929 and NAS3-24633

12. Sponsoring Agency Name and Address	13. Type of Report and Period Covered
Propulsion Directorate U.S. Army Aviation Research and Technology Activity—AVSCOM Cleveland, Ohio 44135-3127 and NASA Lewis Research Center Cleveland, Ohio 44135-3191	Contractor Report Final
	14. Sponsoring Agency Code

15. Supplementary Notes

Project Manager, David P. Fleming, Structures Division, NASA Lewis Research Center.

16. Abstract

This report covers the work performed under Contracts NAS3-23929 and NAS3-24633. MTI evaluated the feasibility of high-speed balancing for both the T700 power turbine rotor and the compressor rotor. Modifications were designed for the existing Corpus Christi Army Depot (CCAD) T53/T55 high-speed balancing system for balancing T700 power turbine rotors. Tests conducted under these contracts included a high-speed balancing evaluation for T700 power turbines in the Army/NASA drivetrain facility at MTI. The high-speed balancing tests demonstrated the reduction of vibration amplitudes at operating speed for both low-speed balanced and non-low-speed balanced T700 power turbines. In addition, vibration data from acceptance tests of T53, T55, and T700 engines were analyzed and a vibration diagnostic procedure developed.

17. Key Words (Suggested by Author(s))	18. Distribution Statement
High-speed balancing; Gas turbine engine vibration diagnostics; Shaft balancing; Gas turbine balancing; Turbine engine vibration analysis	Unclassified – Unlimited Subject Category 37

19. Security Classif. (of this report)	20. Security Classif. (of this page)	21. No of pages	22. Price*
Unclassified	Unclassified	110	A06

NASA FORM 1626 OCT 86

*For sale by the National Technical Information Service, Springfield, Virginia 22161